

QATAR UNIVERSITY

COLLEGE OF ENGINEERING

DEEP EUTECTIC SOLVENT FOR CO<sub>2</sub> CAPTURE: CHOLINIUM CHLORIDE WITH  
PHENYLACETIC ACID SYSTEM

BY

AMAL MOHAMMAD ALIYAN

A Thesis Submitted to the Faculty of the  
College of Engineering  
in Partial Fulfillment of  
the Requirements for the  
Degree of  
Masters of Science in Environmental Engineering

January 2017

© 2017. Amal Aliyan . All Rights Reserved.

## COMMITTEE EPAGE

The members of the Committee approve the Thesis of Amal Aliyan defended on  
21/12/2016.

Mert Atilhan  
Thesis/Dissertation Supervisor

Mustafa Nasser  
Committee Member

Ioannis Economou  
Committee Member

Abdelbaki Benamor  
Committee Member

Ahmad Sleiti  
Committee Member

Approved:

---

Khalifa Al-Khalifa, Dean, College of Engineering

## ABSTRACT

AMAL, MOHAMMAD, ALIYAN, Masters: January : [2017:]

Masters of Science in Environmental Engineering

Title: Deep Eutectic Solvent for CO<sub>2</sub> Capture: Cholinium Chloride with Phenylacetic Acid System

Supervisor of Thesis: Mert, Atilhan.

Global warming is one of the most pressing challenges that face societies these days. As a result, worldwide public attention has risen due to the serious greenhouse gas effect, which causes detrimental environmental effects such as climate change. Carbon dioxide emission is considered as one of the most significant greenhouse gases activity involved in climate change. In power plants, these gases especially carbon dioxide are emitted by fossil fuels; therefore, capturing it will reduce the greenhouse effect.

Increasing energy demand is triggering increased usage of fossil based fuels, which cause unprecedented toxic gaseous emissions to atmosphere. Release of these gases is harmful to environment, especially CO<sub>2</sub> as it increases the acidity and salinity of fresh and sea/ocean water sources. Due to increased global risk caused by the toxic emissions, several options have been considered in both political and academic platforms in order to find feasible and sustainable emission control models. CO<sub>2</sub> capture contributes to three fourths of the overall gaseous emissions capture activities and it has a cumulative negative cost side effect of 50% increase in electricity production in related industries. The choice of the suitable technology differs on the characteristics of the gas stream in which CO<sub>2</sub> will be captured. Such characteristic depends on the type of the dynamics of the process through which the fuel is processed and used.

Deep Eutectic Solvents (DESs) are a novel, advanced class of solvents, which maintain the most relevant characteristics of ionic liquids (ILs), but can be prepared using a more facile and inexpensive method. This alternative approach is based on producing eutectic mixtures of salts and hydrogen-bonding donors (HBDs).

The purpose behind this study is to examine a new system of DES system which is Choline chloride/ Phenylacetic acid (ChCl/PAA) for CO<sub>2</sub> capture. The CO<sub>2</sub> solubility as function of temperature and pressure, with other relevant physicochemical properties including density, conductivity, corrosion, surface tension, Fourier Transform Infrared (FTIR) and Thermogravimetric analysis (TGA) characterizations are reported to analyze DES system and its capability for capturing the CO<sub>2</sub>. Experimental studies of DES that reported in this work showed that this sort of eutectic solvents have appreciable performance of CO<sub>2</sub> at low corrosion effect in compared with monoethanolamine (MEA).

CO<sub>2</sub> absorption estimated by studying the behavior of the liquid –gas and interface properties. CO<sub>2</sub>/N<sub>2</sub> solubility values were determined using high magnetic sorption apparatus (MSA) of Rubotherm at temperature 298.15 up to 338.15 K and pressure up to 30 bars. It's conclude that the ChCl/PAA DES system with molar ratio of 1:2 absorbed 2.10 mmol/g of CO<sub>2</sub> at 308.15 K and 30 bar, with the same conditions ChCl/ Levulinic Acid system absorbed the same amount of CO<sub>2</sub>, while ChCl/ethylene glycol absorbed 3.1265 mmol/g of CO<sub>2</sub> at 303.15 K and 58.63 bars. The amount of absorption of ChCl/PAA increase to 3.35 mmol /g of CO<sub>2</sub> by increasing the molar ratio to 1:3 at the same temperature and pressure of the 1:2 molar ratio . In compared with amine based, solid amine sorbent, consisting of poly (ethylenimine) (PEI) absorbed 2.8 mol/kg of CO<sub>2</sub> at 353.15 K and partial pressures more than 10kPa (0.1 bar). Moreover, in compared

with the most known amine in industry MEA, DES (1:3) at 30 bars and 308 K absorbed 3.35 mmol/g CO<sub>2</sub> while MEA at 24 bars and 313 K absorbed 2.66 mmol/g CO<sub>2</sub>.

The non-toxic, low cost and the other advantages of reported eutectic solvent with favorable physical properties offers an environmentally promising alternative for effective CO<sub>2</sub> capture technological applications

## ACKNOWLEDGMENTS

Prima facea, I am grateful to the God for the good health and wellbeing that were necessary to complete this work.

I wish to express my sincere gratitude to my advisor Dr. Mert Atilhan for the continuous support of my master research, for his patience, motivation, and immense knowledge. His guidance helped me in all the time of research and writing of this thesis. I could not have imagined having a better advisor and mentor for my thesis study.

Besides my advisor, I would like also to express my thanks to the rest of people in the Chemical Engineering Department: Dr. Ruh Ullah Saleh Said for his great help, understandings and suggestions during the lab experiments. Dr. Tausif Altamash for his continuous encouragement and inspiration that helped me to pass through the hard days.

Last but not the least important, I owe more than thanks to my family members for the understanding and support they provided me through my entire life and in particular, I must acknowledge my husband, without whose love, financial support, encouragement and editing assistance, I would not have finished this thesis.

# TABLE OF CONTENTS

ACKNOWLEDGMENTS .....	vi
LIST OF FIGURES .....	x
LIST OF TABLES .....	xiii
LIST OF ACCRONYMS.....	xiv
1 . INTRODUCTION.....	1
1.1 Overall Carbon Dioxide Management .....	1
1.2 Current State of the CO <sub>2</sub> Management Processes .....	4
1.2.1 Capture Options .....	4
1.2.2 Capture Technologies .....	6
1.3 Corrosions Issues of Industry.....	18
1.4 Deep Eutectic Solvents (DES) .....	20
1.5 Research Question and Motivation .....	23
1.6 Research Objectives .....	23
1.7 Potential Beneficiaries.....	24
1.8 Limitations and Assumptions.....	24
2 . LITERATURE REVIEW .....	25
2.1 Physical Properties .....	25
2.1.1 Phase Behavior.....	25

2.1.2	Density .....	26
2.1.3	Viscosity .....	27
2.1.4	Conductivity.....	28
2.1.5	Polarity .....	29
2.1.6	Surface Tension .....	30
2.1.7	Contact Angle .....	31
2.1.8	Corrosion.....	33
2.2	Gas Separation and CO <sub>2</sub> Capture .....	35
2.3	DES and CO <sub>2</sub> System.....	37
3	MATERIALS AND METHODS .....	43
3.1	Materials Used in this Work.....	43
3.2	Methods.....	45
3.2.1	Fourier Transform Infrared Spectroscopy (FTIR) Characterization.....	45
3.2.2	Thermogravimetric Analysis (TGA).....	47
3.2.3	Corrosion Measurement and Data Analysis .....	51
3.2.4	Conductivity.....	54
3.2.5	Density .....	55
3.2.6	Contact Angle .....	56
3.2.7	CO <sub>2</sub> and N <sub>2</sub> Solubility Measurements.....	57
4	RESULTS AND DISCUSSIONS .....	60



4.1	FTIR of DESs.....	60
4.2	TGA of DESs.....	62
4.3	Corrosive Behavior of DESs.....	64
4.4	Conductivity of DESs.....	67
4.5	Density.....	68
4.6	CO <sub>2</sub> Solubility of DES.....	70
4.7	Contact Angle.....	77
5	. CONCLUSION AND FUTURE WORK.....	80
5.1	Conclusions.....	80
5.2	Future Work.....	82
6	. REFERENCES.....	85
7	. APPENDIX.....	104

## LIST OF FIGURES

Figure 1.1. Level of CO <sub>2</sub> emitted during 2015 .....	2
Figure 1.2. Schematic diagrams of the core technology of CCS which is CO <sub>2</sub> capture and it is classified as (a) post-combustion (b) pre-combustion (c) oxyfuel-combustion.....	5
Figure 1.3. Gas absorption membrane principle using hollow fiber membrane.....	7
Figure 1.4. Schematic diagram shows the CO <sub>2</sub> separation from other gases using a spiral wound membrane.....	8
Figure 1.5. Molecular structure of the activated carbon .....	10
Figure 1.6. Zeolite structure.....	12
Figure 1.7. MOF-5 structure and its topology. ....	13
Figure 1.8. Elementary reaction steps during CO <sub>2</sub> capture in aqueous MEA (a–d) and MEA regeneration (e–f).....	15
Figure 1.9. . List of common (a) halide salt used in preparing the DESs (b) HBD used in preparing DESs .....	22
Figure 2.1. Solid-liquid phase diagram for binary DES system .....	26
Figure 2.2. Contact angle of [C12MIM][NTf <sub>2</sub> ], [N4441][NTf <sub>2</sub> ] and [N1888][NTf <sub>2</sub> ] on TiN, CrN and ZrN. ....	32
Figure 2.3. Corrosion behavior of different amine based .....	33
Figure 2.4. Corrosion rate of single amines, piperazine activated amines, and amine/RTIL solutions at 353.15 K .....	35
Figure 2.5. Effect of pressure and temperature on CO <sub>2</sub> solubility in ChCl/ glycerol DES system .....	42
Figure 2.6. Isobaric CO <sub>2</sub> solubility in ChCl/LA kinetics: (a) 1 bar and (b) 30 bar.....	42

Figure 3.1. Glove box instrument. ....	44
Figure 3.2. ChCl/PAA DES system at (a) room temperature (b) 308.15 K (c) 321.15 K. ....	44
Figure 3.3. Infrared IR Spectroscopy Test Instrument. ....	45
Figure 3.4. Photo of FTIR platform.....	47
Figure 3.5. TGA instrument.....	48
Figure 3.6. Pyris program set up.....	49
Figure 3.7. TGA furnace and Sample container. ....	50
Figure 3.8. Pyris program set up. Balancing the empty container (a), balancing the sample (b), start measurement (c).....	50
Figure 3.9. Set up of corrosion test. ....	52
Figure 3.10. Linear Tafel behavior in the anodic and cathodic branches of the polarization curve. ....	53
Figure 3.11. Conductivity measurements instruments.....	54
Figure 3.12. Density meter instruments.....	55
Figure 3.13. KRÜSS drop analysis system.....	57
Figure 3.14. MSA instrument. ....	58
Figure 4.1. FTIR spectra of PAA.....	60
Figure 4.2. FTIR spectra of pure ChCl. ....	61
Figure 4.3. FTIR spectra of 1:2, 1:3 and 1:4 molar ratio of ChCl/PAA DES.....	62
Figure 4.4. TGA Curve for ChCl/PAA DES (1:2, 1:3 and 1:4).....	63
Figure 4.5. Corrosion resistance performance experiments for (a) ChCl:PAA(1:2 ), (b) ChCl:PAA (1:3) and (c) ChCl:PAA (1:4) DES system with and without CO <sub>2</sub> .....	66

Figure 4.6. Conductivity plot for ChCl/PAA DES (1:2, 1:3 and 1:4) at temperature range of 298.15 K to 340.15 K.....	68
Figure 4.7. Density of ChCl:PAA system with ratio of 1:2,1:3,1:4 and ChCl/Glycerol and Ethylene glycol.....	70
Figure 4.8. CO <sub>2</sub> solubility of ChCl/PAA DESs (a) 1:2 (b) 1:3 and (c) 1:4 molar ratio.....	74
Figure 4.9. N <sub>2</sub> solubility of ChCl/PAA DESs (a) 1:2 (b) 1:3 (c) 1:4 molar ratio. ....	75
Figure 4.10. Colum chart represent the absorption for the 3-different systems DES-2 (1:2), DES-3 (1:3), DES-4 (1:4). ....	76
Figure 4.11. Isobaric CO <sub>2</sub> solubility in ChCl/PAA kinetics: (a) 1 bar and (b) 30 bar.....	77
Figure 4.12. Contact Angles of ChCl/PAA (1:2) at different surfaces.....	79
Figure 7.1. Rubotherm® Magnetic Suspension Balance (MSB). Photos of the magnetic suspension assembly and the sample container basket.....	111
Figure 7.2. MSB overview. Photo of the measuring cell and the magnetic coupling housing...	111
Figure 7.3. Schematics of magnetic suspension sorption apparatus operating principle. (a) sample loaded to measuring basket in high pressure cell; (b) Measurement point 1 (MP1) - magnetic coupling is on and mass of the sample is measured; (c) Measurement point 2 (M(c) Measurement point 2 (MP2) – in-situ density of the adsorbed gas is measured. ....	112
Figure 7.4. Schematics of the gas dosing manifold system under (a) CO <sub>2</sub> measurement; (b) reference gas (He) measurement; (c) vacuum measurement. ....	113
Figure 7.5 .Magnetic suspension sorption apparatus screenshots at, (a) vacuum and, (b) under pressure measurement.....	114

## LIST OF TABLES

Table 2.1. Density of DES systems with ChCl based.....	27
Table 2.2. DES system with low viscosity .....	28
Table 2.3. Conductivity for selective DES system .....	29
Table 2.4. Polarity of ChCl/glycerol eutectic solvent at different molar ratio .....	30
Table 2.5. Surface tension of ChCl based DES . .....	31
Table 2.6. Contact angle of membrane .....	32
Table 2.7. Corrosion rate of amine based .....	34
Table 2.8. Solubility of CO <sub>2</sub> in various DES system.....	41
Table 4.1. Corrosion rate of DES systems and amine. ....	65
Table 4.2. Corrosion Test Experiments for DES mixtures of ChCl/PAA at different ratios.....	67
Table 4.3. Solubility of CO <sub>2</sub> in different systems. ....	76
Table 4.4. Contact angles for DES, membrane and IL systems. ....	78
Table 5.1. Different combinations of DESs from natural products .....	84

## LIST OF ACCRONYMS

[C12MIM][NTf]	1-Dodecyl-3-methylimidazolium bis(trifluoromethylsulfonyl)imide
CrN	Chromium nitride
CR	Corrosion current (mm/y)
DES	Deep eutectic solvents
D	Density (g/cm <sup>3</sup> )
EW	Equivalent weight (g/equivalent)
$i_{\text{corr}}$	Corrosion rate ( $\mu\text{A}/\text{cm}^2$ )
LTTMs	low transition temperature mixture
LA	Levulinic Acid
MEA	Monoethanolamine
MOFs	Metal Organic Frameworks
mS/cm	Millisiemens/centimeter
MP.S	Millipascal-second
[N4441][NTf2]	Tributylmethylammoniumbis(trifluoromethylsulfonyl)imide
[N1888][NTf2]	Methyltrioctylammoniumbis(trifluoromethylsulfonyl)imide
OPEC	Petroleum Exporting Countries
ppm	parts per millions

PAA	Phenylacetic acid
PP	polypropylene
X	Lewis base
Y	Brønsted acid
Z	number of Y molecules interacts with the anion

# 1 . INTRODUCTION

## 1.1 Overall Carbon Dioxide Management

Global warming is one of the biggest challenges that societies face these days. As a result, worldwide public attention has raised due to the serious greenhouse gases (GHGs) effect, which causes detrimental environmental problems<sup>1</sup>. In the politics and science fields the GHGs effects and global warming are considered as important issues<sup>2,3</sup>.

The main source of GHG emission is energy consumption<sup>4</sup>. The Organization of the Petroleum Exporting Countries (OPEC) reported that from 1970 to 2010 the energy consumption increased by 685%, whereas the carbon dioxide (CO<sub>2</sub>) emissions increased by 440% due to fossil fuels burning at the same time<sup>5</sup>. CO<sub>2</sub> emissions that emitted because of burning fossil fuel caused increased in global temperature<sup>6</sup>. The consumption of oil trend and emission of CO<sub>2</sub> of OPEC countries has serious implications by participate to global warming<sup>5</sup>. GHGs drive anthropogenic global warming, and CO<sub>2</sub> is considered as the main contributor. In compare with other GHGs gases, CO<sub>2</sub> display less global warming potential per mole, but it is the main one that exists in the atmosphere and it has longer atmospheric life.

Figure 1.1 shows the top twenty countries that released the maximum amount of CO<sub>2</sub> during 2015 based on their share of global energy-related CO<sub>2</sub> emissions<sup>7</sup>. The graph shows that, china comes at the top followed by the United States. The main source for CO<sub>2</sub> emissions are industrial plants and thermoelectric power plants (eg. Refineries and steel mills) which approximately contribute in 45 % of global warming. The emissions of CO<sub>2</sub> from combustion of fossil fuel are the most important source of anthropogenic carbon emissions, accounting for about 75% of global emissions since 1750<sup>8</sup>.



The amount of CO<sub>2</sub> that generated yearly by human activities is around 37 billion tons; therefore, climate change has become a global concern. Directly after CO<sub>2</sub> emission to the atmosphere, half of it either used by nature for photosynthesis or it's taken by ocean, while the remaining of CO<sub>2</sub> is left-over in the atmosphere. As a result the amount of CO<sub>2</sub> raised from 280 to 400 parts per millions (ppm) in the last 50 years<sup>9,10</sup>. The excess amount of CO<sub>2</sub> that dissolve in ocean cause several problems, its form carbonic acid and raised the level of acidity in water therefore, this amount of increasing can cause imbalance for marine life (nutrient levels). Moreover acidity of the water has the ability to dissolve the calcium-carbonate that used by marine life to produce coral reefs, and so it is destroying the marine habitat<sup>11</sup>.

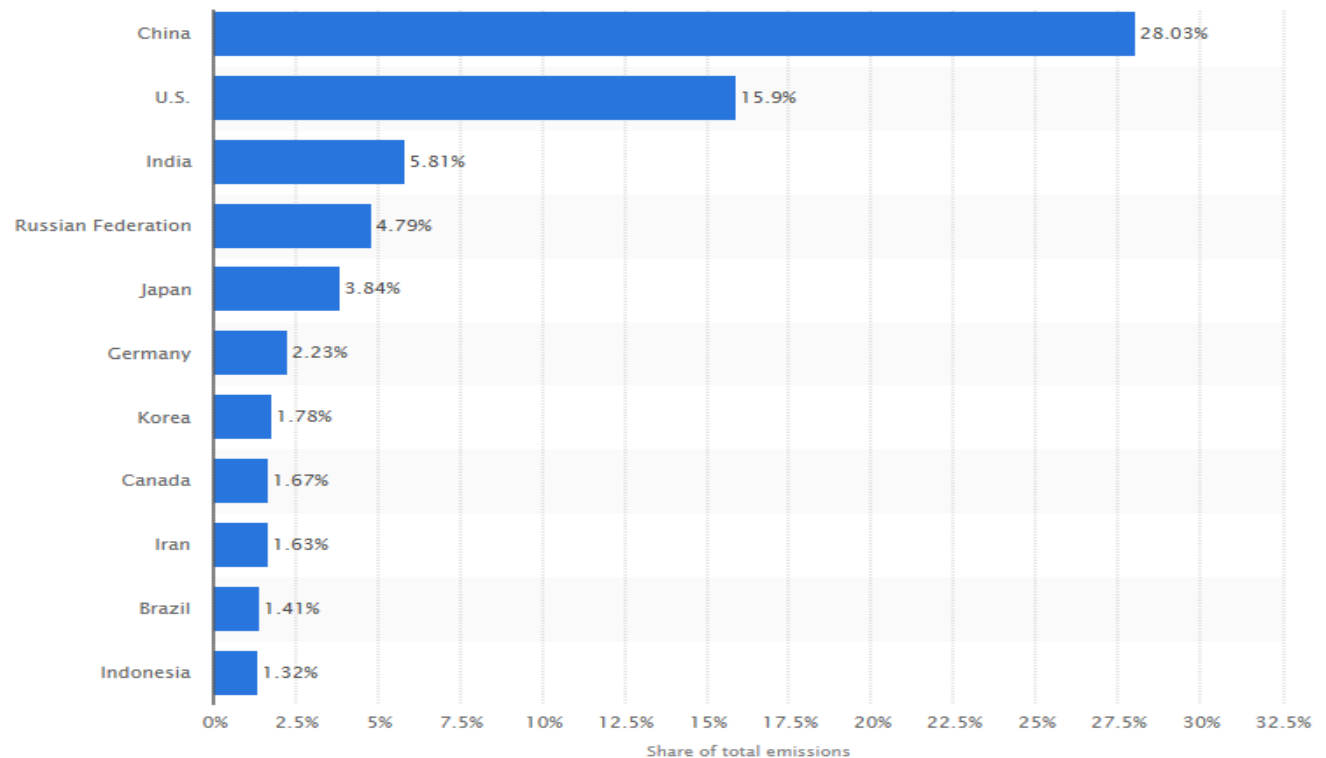


Figure 1.1. Level of CO<sub>2</sub> emitted during 2015<sup>7</sup>.

In order to control and reduce the emission of GHG especially CO<sub>2</sub> into the atmosphere, CO<sub>2</sub> capture from fossil fuel power plants is getting great attention. However, some economic, technological, environmental, and safety problems remain without solution with the capture system, such as increasing the efficiency of CO<sub>2</sub> capture, reducing process cost, and verifying environmental sustainability of CO<sub>2</sub> storage<sup>12</sup>. Post-combustion capture has an advantage over the other developed methods where it can be used to modify the existing power plant. The most established technology for the CO<sub>2</sub> post-combustion is the amine-based absorption due to its high affinity to CO<sub>2</sub><sup>13</sup> ,But this process is based on chemical separation method which requires using high energy to break down the chemical bound among the absorbent CO<sub>2</sub> and the absorbed in the solvent regeneration step<sup>14</sup>. Other promising processes are membranes, however the productivity as well as selectivity is missing in the presence of CO<sub>2</sub>. Therefore, developing new technologies to separate CO<sub>2</sub> is crucial to minimize energy consumption<sup>15</sup>.

Ionic liquids (ILs) are one of alternative solvents that get a great attention, duo to its properties that has possibility to tuning. However, several problems appear with using ILs ,such as high viscosity and cost, although these disadvantages should not be considered as reasons to negate ILs as possible capture for CO<sub>2</sub>, nevertheless some alternative have been recommended to preserve the design flexibility of ILs and at the same time avoid their problems , therefore Deep eutectic solvents (DESs) are the most promising alternative to overcome ILs<sup>16</sup>.

Consequently, the purpose behind this work is to study new system of DES which has not reported before, named choline chloride/ Phenylacetic acid (ChCl/PAA) and its appropriateness to capture CO<sub>2</sub>. So, full characterization for the new system was carried in order to analyze their strength and weaknesses for the aim of capturing CO<sub>2</sub>, for the purpose of design or to have information about the structure and behavior of fluid a physicochemical characterization of

ChCl/PAA was carried. Finally, at different temperature and pressure up to 30 bars CO<sub>2</sub> absorption was studied.

## 1.2 Current State of the CO<sub>2</sub> Management Processes

### 1.2.1 Capture Options

Due to sharp increase in the level of CO<sub>2</sub> in the past years, develop new technologies to reduce the emission of CO<sub>2</sub> become a critical need. Scientists and researchers believed that the main technology for this target is CO<sub>2</sub> Capture and Storage (CCS) to reduce these emissions. These technologies simply base on capturing CO<sub>2</sub> without emitting the emissions into the atmosphere. The main part of CCS technology is CO<sub>2</sub> capture where 70 to 80 % of the total cost is belongs to this part<sup>17</sup>. Based on the various configurations of the plant, the emissions of CO<sub>2</sub> from power plant can be classified by one of the following method (Figure 1.2):

**Post-combustion:** Before capturing CO<sub>2</sub>, fossil-fuel is converted to energy. Two challenges faced while using this technology; the main one is separating CO<sub>2</sub> with low concentration from nitrogen gas with high concentration; while the second challenges is flow of CO<sub>2</sub> is low<sup>18</sup>.

**Pre-Combustion:** Firstly, synthesis gas (syngas) produces from gasified coal of fossil fuel. Then the syngas prepares by water-gas shift in which carbon monoxide (CO) reacts with steam, and CO<sub>2</sub> with H<sub>2</sub> is formed after that CO<sub>2</sub> is removed<sup>19</sup>.

**Oxyfuel-Combustion:** In this system combustion fuel is inside a mixture of pure oxygen (O<sub>2</sub>) and CO<sub>2</sub> (recycled from the reactor exit). The purity of O<sub>2</sub> in the mixture is greater than 95%. This technology has a main attraction where it produces fuel gas that mainly contain water (H<sub>2</sub>O) and CO<sub>2</sub>. The H<sub>2</sub>O removed by condensation while CO<sub>2</sub> compressed for transport and storage<sup>20</sup>.

In short, for post-combustion capture chemical adsorption is the most popular separation approach, since it can practicably capture CO<sub>2</sub> at low concentration. For syngas that produce from gasification the most efficient capture technology is pre-combustion because the amount of CO<sub>2</sub> concentration in syngas is high. But, the capital cost for this type of method is larger in compare with a traditional pulverized coal combustion power plant. Possible separation techniques for pre-combustion capture are membrane separation and physical sorption. With Oxy-fuel combustion system the flue gas mostly having steam (H<sub>2</sub>O) and CO<sub>2</sub>, this due to that the combustion happened in N<sub>2</sub>-less environment<sup>21</sup>.

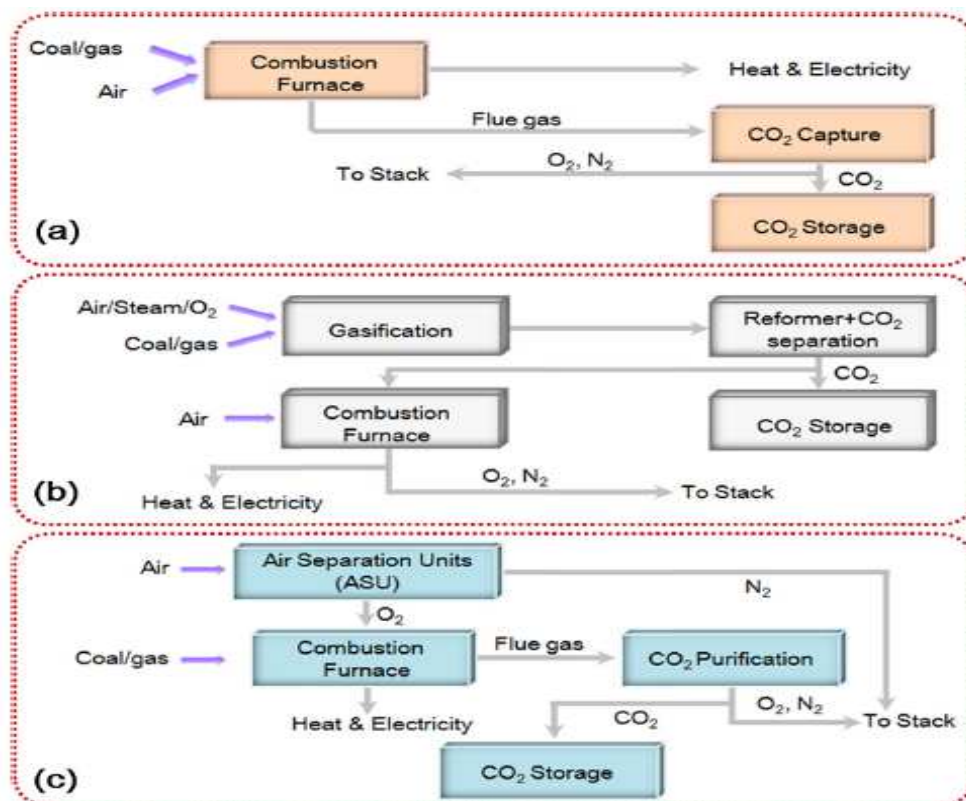


Figure 1.2. Schematic diagrams of the core technology of CCS which is CO<sub>2</sub> capture and it is classified as (a) post-combustion (b) pre-combustion (c) oxyfuel-combustion<sup>17</sup>.

## 1.2.2 Capture Technologies

### 1.2.2.1 Membrane

Membranes is relatively a novel concept for capture and separate some components from a gas stream, which can be used to separate CO<sub>2</sub> from flue gas in post-combustion system, in natural gas processing to remove CO<sub>2</sub> from the natural gas, in pre-combustion membrane can be used to separate CO<sub>2</sub> from hydrogen or to separate oxygen from nitrogen in oxy-fuel combustion system. Different mechanism can be used with membrane to separate substance (adsorption/diffusion, solution/diffusion, ionic transport and molecular sieve) and they are available in different types of material such as organic (polymeric), inorganic (metallic, zeolite, carbon or ceramic) porous or non-porous. The membrane process can be categorized as two types, gas absorption membrane and gas separation membrane<sup>22</sup>.

**Gas absorption membrane:** it's made of micro porous solid membrane, and used as contacting device between the liquid and gas flow (Figure 1.3). Figure 1.3 shows that in order to separate CO<sub>2</sub> from flue gas first, it diffused through the membrane then recovered by liquid absorbent by absorption. This process, due to high driving force, will gives higher removal rate than the other types. In this system at the beginning of autonomous control of liquid and gas flow cause flooding, foaming, channeling and minimum entrainment. More compact equipment used in this system in compared with other conventional membrane separator<sup>23</sup>.

**Gas separation membrane:** this type of membrane work base on principle of preferential permeation of mixture constituents through the pores of the membrane which lead to diffuse one component faster than the other trough the membrane (figure 1.4). Permeability and selectivity are the key of membrane operation and design parameters. In this method, a stream of gas containing

CO<sub>2</sub> enter at high pressure into the separator of membrane which consists of large number of hollow cylindrical membranes arranged in parallel. On the shell side of membrane separator the selectivity parameter of CO<sub>2</sub> recovered at reduced pressure<sup>23,24</sup>. Gas separation membrane is available in various type such as polymeric, ceramic or combination of both or mixed matrix membranes. In this process the separation depend on diffusivity or solubility of gas molecules in the membrane also it relied on the difference in partial pressure which is the driving force for gas separation

22.



Figure 1.3. Gas absorption membrane principle using hollow fiber membrane<sup>25</sup>.

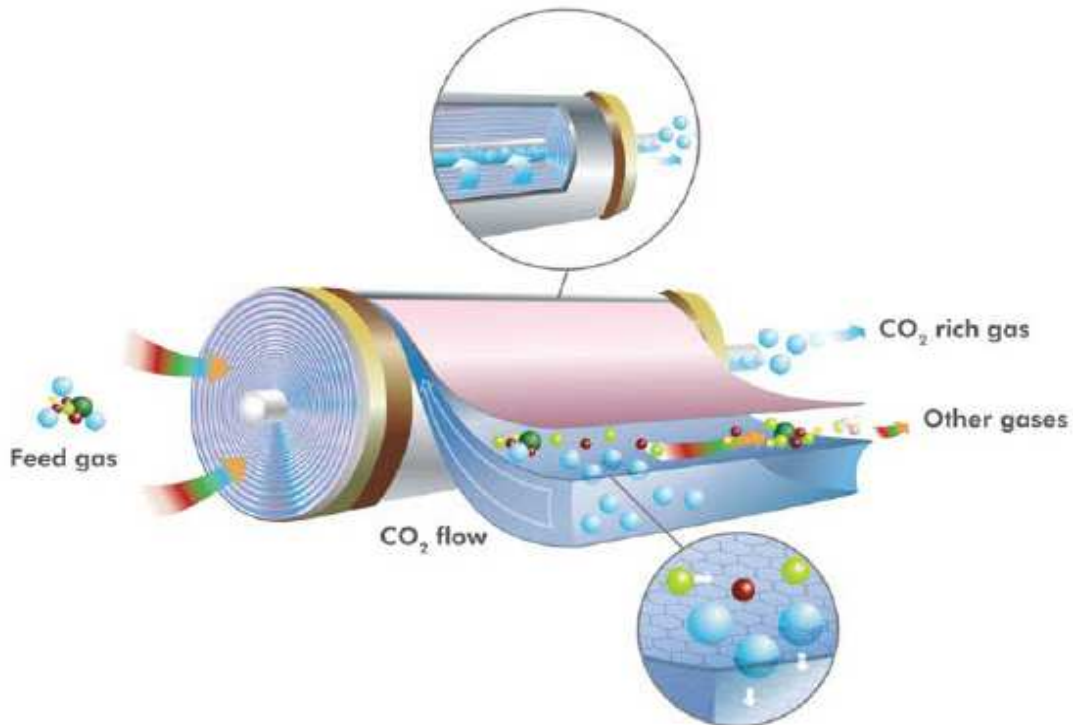


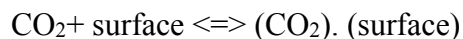
Figure 1.4. Schematic diagram shows the CO<sub>2</sub> separation from other gases using a spiral wound membrane<sup>25</sup>.

The advantage of membranes processes is even though when the initial design value is reduced by 10%, it has the ability to maintain the purity of the product, where this can be achieved either by increasing permeate pressure, minimize feed pressure or isolating modules from system. Moreover, membrane has low cost processes for gases separation and with reference to the factor of on-stream is really reliable. It is continuous method of separation and the shutdown can cause due to flow control components. The membrane system has instantaneous response time, also immediate results can be taken from corrective action. The start-up time that needed by the membrane process is extremely small. Uses of the membrane process can be limit due to number of losses that related with capturing CO<sub>2</sub> from flue gases. Whenever the concentration of CO<sub>2</sub> is

upper than 20% these system can be reflect high flexibility, while for concentration less than 20% is very low flexibility<sup>24</sup>. Low CO<sub>2</sub> concentration leads to minimize the driving force with a consequent reduction in the purity of the product and CO<sub>2</sub> recovery. Therefore it can be concluded that the main problem with this technology is related to low CO<sub>2</sub> in flue gases also pre-treatment such as cooling is required for high temperature application<sup>24,26</sup>.

### 1.2.2.2 Solid Adsorbents

Adsorption quality depends on the adsorbent surface (pore size, polarity and spacing) and the adsorbed particles (polarity, molecular weight and size). Adsorption is an exothermic process, so the adsorbents that used in adsorption can be regenerated by rising the temperature. Energy saving is an advantage that solid sorbents have over liquid solvent, this due to large amount of water which needed for repeatedly heated and cooled to regenerate the solvent solution is not required in solid sorbents. However, in compared these two-methods adsorption required lower energy and avoids shortcomings than absorption. In post-combustion method, adsorption is known to be attractive method for capturing CO<sub>2</sub> from flue gas, because of low energy requirements<sup>27</sup>. CO<sub>2</sub> emission from flue gas can be removed using different materials of solid physisorbents, such as zeolites, metal –organic frameworks (MOF), porous carbonaceous material and other. For CO<sub>2</sub> adsorption using activated carbon or zeolite, the mechanism for capturing CO<sub>2</sub> can be shown as follow<sup>28</sup>:



**Carbon-based adsorbents:** Adsorption capacity of CO<sub>2</sub> is very sensitive to surface group and textural properties of carbon-based adsorbents. Because the distributions of activated carbon pore size very from micro-pore to macro-pore, consequently, these materials are inappropriate for



selective adsorption of a specific gas. In general, pristine carbon-based adsorbents have weak affinities for CO<sub>2</sub> with adsorption heats of less than 25 kJ/mol. At 0.1 bar and 298.15 K activated carbon have CO<sub>2</sub> adsorption capacity about 5wt.%<sup>17</sup>.

Siriwardane et al.<sup>29</sup> investigate the adsorption isotherms of activated carbon, found that it is extremely reproducible and showing excellent reversibility of adsorption. Activated carbon at 298.15 K and 20 bar have equilibrium adsorption capacity around 8.5mol CO<sub>2</sub>/kg of sorbent (37.4wt%). Formation of close pack monolayer of CO<sub>2</sub> at saturation with activated carbon it is an indication of adsorption isotherm. Activated carbon at high pressure uses its whole surface to produce monolayer. Molecular structure of the activated carbon is shown in figure 1.5.

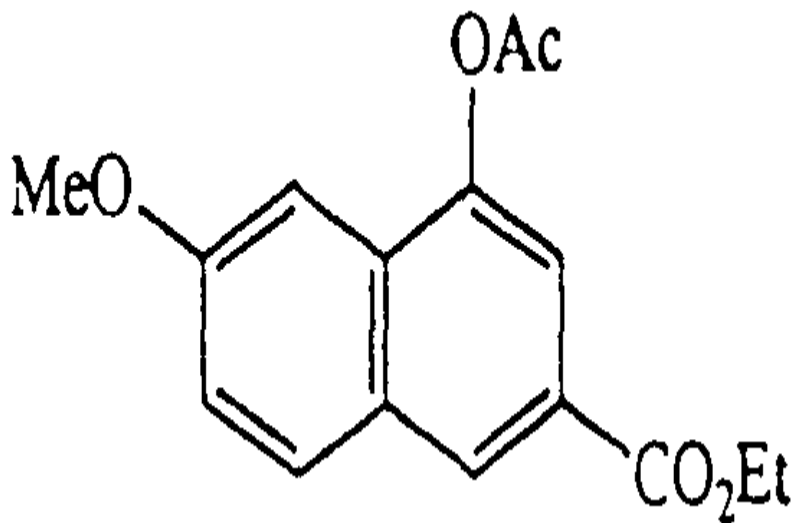


Figure 1.5. Molecular structure of the activated carbon<sup>30</sup>.

**Zeolite:** is member of aluminosilicate, where it belongs to microporous solids family named as molecular sieves. The name (molecular sieves) point out to its ability to arrange selectivity of

molecules, where it's mostly depend on a size of exclusion process, this because the molecular dimensions are very regular pore structure. Tunnels diameters determines the size of ionic species of molecular that can pass in the pores of a zeolite. This material exists naturally; however, they can be synthesized. It can be produced in a uniform, phase-pure state also desirable structure of zeolite where is not available in nature and can be manufacture<sup>31</sup>. Figure 1.6 shows the zeolite structure.

Siriwardane et al.<sup>32</sup> studied three natural zeolites, the major difference between them was the cation. They conducted volumetric gas adsorption of O<sub>2</sub>, CO<sub>2</sub> and N<sub>2</sub> at 298.15 K up to 20 bars. CO<sub>2</sub> adsorption showed better performance with all three types of the zeolites. The variations in adsorption of CO<sub>2</sub> capacity were related to changes in the nature of chemical at the surfaces, since average diameters of the pore are similar. At 2005 Siriwardane et al.<sup>33</sup> tested five manufactured zeolites, it was mentioned that if the sorbents were operated at moderated or higher temperature the CO<sub>2</sub> system capture would be more efficient. But zeolites capacities of CO<sub>2</sub> adsorption were lower at 393.15 K than at ambient temperature.

The main disadvantage with zeolites is when fluidized beds are used; the sorbent might be carried over due to attrition. Attrition rates for zeolites 13X and 5A were found to be 2.1 to 4 times higher than activated alumina or activated carbon. Therefore, sorbent maintenance costs would be higher. However the adsorption capacities of 13X and 5A were reported to be 2.35mmol/g (10.34wt%) and 2.23mmol/g (9.81wt%) and this indicated that zeolites have higher adsorption capacities than other sorbents tested ( 1.5 to 2.7 times higher )<sup>31</sup>.

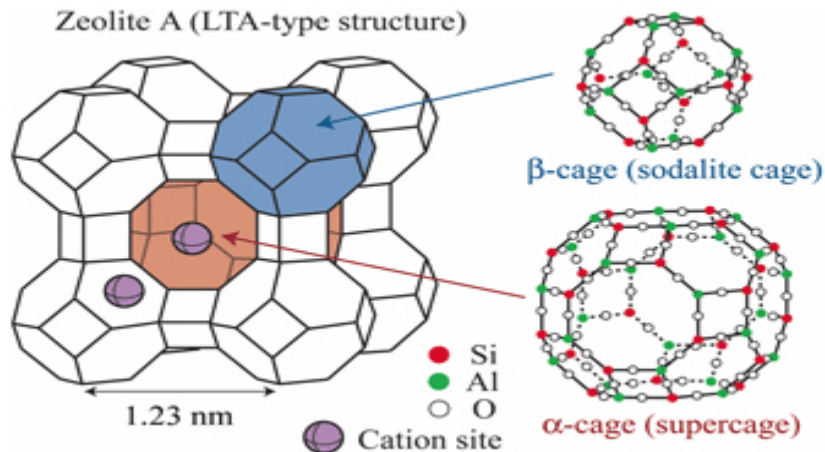


Figure 1.6. Zeolite structure<sup>34</sup>.

**Metal Organic Frameworks (MOFs):** They are crystalline compounds made of metal ion or clusters coordinated to organic molecules to produce one, two, or three dimensional structures that can be porous. These pores in some cases can be used to storage gases (eg. CO<sub>2</sub>)<sup>31</sup>. MOF structure and its topology is shown in figure 1.7.

Yaghi and Millward<sup>35</sup> studied the capacity of nine MOFs at room temperature for CO<sub>2</sub> storage. They found that MOF-177 which consist of zinc clusters and 1, 3, 5-benzenetribenzoate units have a capacity of 33.5mmol/g (147.4wt %), therefor its ability to adsorbed is much greater than any other porous material reported. Capacity of a container full of MOF-177 at pressure of 35 bar for capturing CO<sub>2</sub> is nine times more than a container without adsorbent, also it has around twice amount when the container filled with benchmark materials (zeolite 13X and activated carbon). While Arstad et al.<sup>31</sup> worked at low temperature adsorbent for CO<sub>2</sub> capture for selected MOF adsorbents. The best adsorbents reached by CO<sub>2</sub> capacity levels of 10wt% at atmospheric pressures of CO<sub>2</sub> and as high as 60 wt% at ~25 MPa CO<sub>2</sub> pressure and 25 C. The measured capacity had proportional relation with pore volume and surface area of the adsorbents. However, water

adsorption selectivity was greater than CO<sub>2</sub> because existing of water would minimize adsorption capacity of CO<sub>2</sub> in gas mixtures. Figueroa et al.<sup>31</sup> have pointed that appropriate characteristics for MOFs are low energy needed for regeneration, low cost, attrition resistance, tolerance to contaminants and good thermal stability.

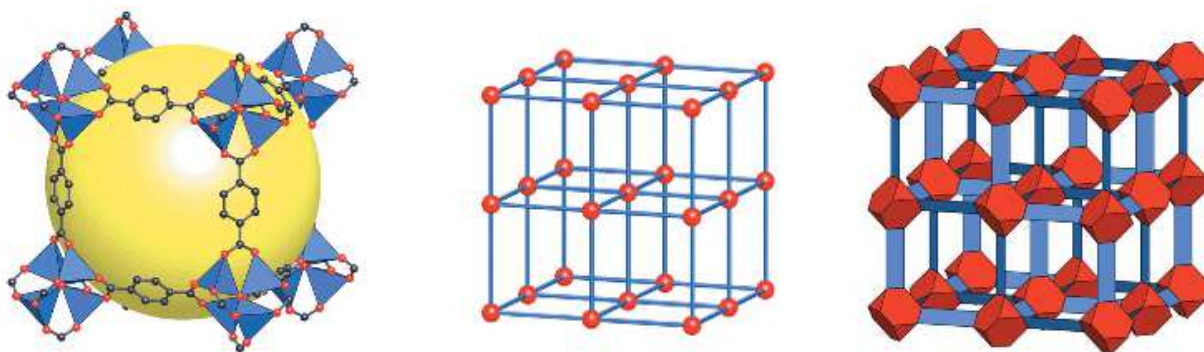


Figure 1.7. MOF-5 structure and its topology<sup>36</sup>.

### 1.2.2.3 Liquid Absorbents

Today in commercial use, most of the capture agents are based on liquid system either mixture, solutions in solvents (like water) or pure liquids. This means the system based on gas-liquid separation with the sorption mechanism and it's relied on many factor, however priority of the viscosity in the liquid phase is comes first. Regardless of the intermolecular interactions, usually the limiting step is mass transfer among the gas and liquid phase. In case, the mixture has low viscosity (good mixing) the process will be predominantly absorption into the bulk of the condensed phase, while for sorbents with high viscosity the mass transfer will be limited and the absorption will primarily on the surface<sup>37</sup>.

Nowadays the most common removal technology for CO<sub>2</sub> is absorption with amine-based absorbents. In this process, large gas flow can be considered as inherent problems; for example, exhaust resulting from fossil fuel fired power stations. The most common aqueous solution used to remove CO<sub>2</sub> and H<sub>2</sub>S (acid gas) from refinery, natural and synthesis gas is alkanolamines. Monoethanolamine (MEA) is the most popular aqueous has been used widely for this aim. Figure 1.8 represents the elementary reaction steps during CO<sub>2</sub> capture in aqueous MEA (a–d) and MEA regeneration (e–f).

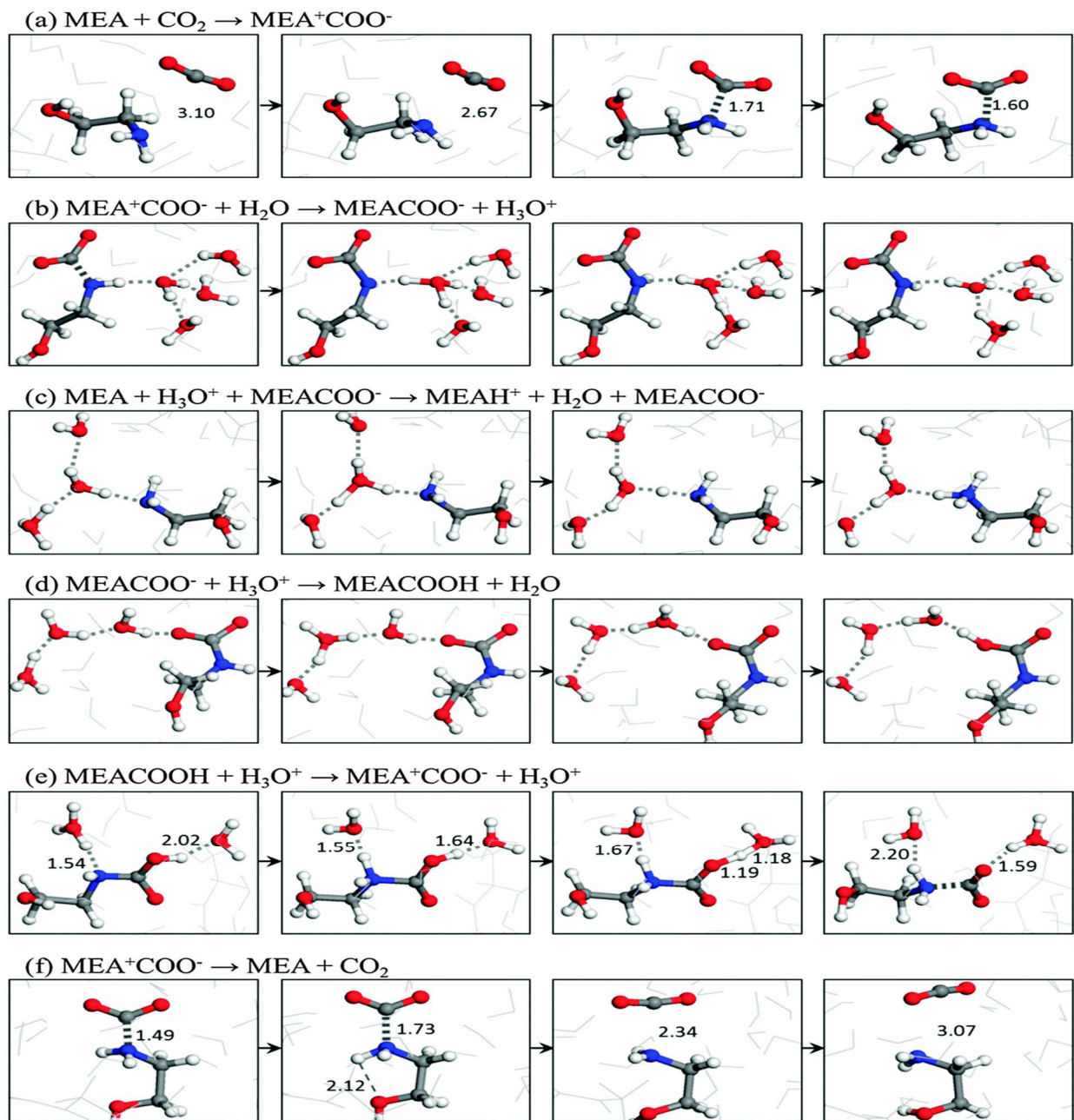


Figure 1.8. Elementary reaction steps during  $\text{CO}_2$  capture in aqueous MEA (a–d) and MEA regeneration (e–f)<sup>38</sup>.

Several qualitative values have been given for MEA sorption capacity, while quantitative data are rare. As an example, in one of the review paper the authors states that this process has a

high CO<sub>2</sub> adsorption capacity, but no numerical value was mentioned. Moreover, the authors do not mention if the process is pure MEA or aqueous solution. It has some advantages such as low solvent cost, high reactivity, low molecular weight and high absorbing capacity. In the other hand, it has high enthalpy which causes higher desorber energy consumption, producing stable carbamate and producing degradation products with COS or oxygen bearing gases. Furthermore this process does not have the ability to remove mercaptans, also due to high vapor pressure there is vaporization losses and finally alkanolamines are more corrosive than any other so with high concentration corrosion inhibitors are required<sup>37, 39,40</sup>.

In General amine – based is bulky processes which cause high energy consumption, large investment cost, unstable absorbents and they produce product which degrade that must be handled<sup>39</sup>. Even though there are numerous studies that proposed solutions for above problems<sup>41,42</sup> but the development of new CO<sub>2</sub> capture with better properties than amine-based has attract great attention in the literature elsewhere<sup>43,28, 44</sup>.

Green technology is considered as the key issues in the chemistry fields to preserve environment and to decrease the negative impact of human involvement. This technology facilitates the minimum use of non- hazardous chemical and environmentally acceptable solubilization techniques through controlling pressure, temperature and other physical properties to develop new green solvents. In the context of green technology, ionic liquids (ILs) have been considered as a good green solvent which can replace the current organic solvents<sup>45</sup>.

In the last decade ILs was one of the most popular solvents that commonly used to be studied than any other present topic<sup>46</sup>. IL was known as class of fluid that contain ions, which are liquid at temperature less than 100 °C, so base on this definition there was distinguish between IL and molten salts, because molten salts melts at higher temperature. This definition was the first

description that used for chloroaluminate based ionic fluids, but now days ILs known as solvents which generally contain solely of ions. There are two class of ILs, first and second generation. First generation at low temperature is fluid, because of formation of bulky chlorozincate or chloroaluminate ions at eutectic compositions of the mixture, while the second generation those that are completely composed of separated ions<sup>47</sup>.

ILs identified by Figueroa<sup>44</sup> to be long term targets that can be used for capture agents; but, recent studies suggest that these technologically important materials may prove commercially viable sooner than suggested. ILs become one of the most popular alternative solvents due to their low vapour pressure under ambient conditions<sup>48,37</sup>. As it mentioned ILs known as term that can be used for capturing, so they forward this interest to CO<sub>2</sub> capture. Although some problems notice from evidence, which are evaporation and decomposition loss of IL into the purified gas stream under elevated desorption temperatures<sup>49</sup>. However, in compared with amine solvents ILs have lower desorption temperatures<sup>37</sup>. Even though, in spite of the fact that ILs have all these benefits the literature has also deal with limitation and problems. Actually, several of papers and reports indicate the toxicity, poor biodegradability, unfavourable physical properties, for example high viscosity and high cost of production. Many of these problems can be avoided through appropriate selection or design considering the large amount of available ILs, therefore cheap, non-toxic, low viscous ILs can be found. Despite the possibility of finding appropriate candidates for several ILs technological applications, other methods are being developed to take advantage of ILs properties and avoiding their negative aspects<sup>10</sup>. Consequently, to overcome the problems related to ILs (eg. Toxicity and high price) a new generation of solvent has emerged at the beginning of the century which named Deep Eutectic Solvents (DESs)<sup>50</sup>. They formed from a eutectic mixture of Lewis or Brønsted acids and bases and they contain a different species of anion and cation<sup>47</sup>.



### 1.3 Corrosions Issues of Industry

The chemical corrosion is results of breaking down or distraction of metal through electrochemical reaction with their environmental. It is simply the tendency of the elemental metals to return to their natural more stable state as mineral oxides or carbonates. Therefore, corrosion of metals includes oxidation of the metal through oxidizing agents that exist in the nearby environmental and the concurrent reduction of these agents. Since corrosion is due to electrochemical reaction, so it has two type of reactions, oxidation and reduction reaction where both of them occurs simultaneously in the medium. The actual process of corrosion is the oxidation reaction, where in this part of reactions metal start to dissolve and metallic atoms loss electrons, therefore it converts to ions.

In order to maintain the system electrically natural, any released of electrons must be taken by oxidizing species adjacent to the metal. Indeed, once the species of oxidizing are available in the environmental they transfer from bulk solutions to surface of the meatal and then the process of corrosion is started. The driving force of this process which causes losses of the electron for the metal is potential differences.

Corrosion problems in the Worldwide CO<sub>2</sub> capture process occur in most frequent failures. Lots of industrial experiences showed that large quantities of CO<sub>2</sub> are being handled (eg. petrochemical industry or the oil and gas industry), nevertheless the process of capturing the CO<sub>2</sub> is one of the most important factor in this aspect. The acidity of the flue gas is due to impact of CO<sub>2</sub> on the equipment and existence of the oxidizing acid, Nitrous oxide (NO<sub>x</sub>) and Sulphur Oxide (SO<sub>x</sub>). Moreover, existence of free water made the flue gas to become corrosive to most parts of the installation's equipment<sup>51</sup>.

In alkanolamine plant the appropriate choice of materials used for capturing the CO<sub>2</sub> is determined based on the chemistry of the amine system, therefore carbon steel is the most common used for piping and equipment since it is an economical solution<sup>52</sup>. Kohl and Nielsen<sup>53</sup> reported that in such plant the carbon corrosion is due to high operating temperatures, lean/rich loading of amine (mole of acid gas/ mole of amine), ratio of CO<sub>2</sub> to hydrogen sulfide (H<sub>2</sub>S) in the acid gas, contaminants of solution (eg degradation of amine products and heat stable salts) and type of amine and its concentration.

Wet acid gas corrosion is encountered in all parts of the plant that made of carbon steel and they are in contact with aqueous phase where this phase have high concentration of acid gas such as CO<sub>2</sub>, H<sub>2</sub>S, and ammonia (NH<sub>3</sub>) and Hydrogen cyanide (HCN)<sup>54</sup>. The acid corrosion cause a reaction among iron (Fe) and hydrogen ion (H<sup>+</sup>) where is mainly depends on the pH. These gases will convert to acid gas in case the conditions of the environmental is wet, where leads to pitting in different parts of the installation. Under wet conditions, the rate of corrosion for carbon steel is between 1x10<sup>-3</sup> meter (m)/year (y) to 1.8x10<sup>-3</sup> m/y , where these variations observed particularly at the inlet to absorbers or coolers vessels in CO<sub>2</sub> compression systems<sup>52</sup>.

The economy of the plant can be directly affected by chronic corrosion because it causes production losses, reduction in life time of the equipment, unplanned downtime and injury or even death<sup>53</sup>. In terms of production losses the unplanned downtime of plant can cost \$10,000 to \$30,000 per day<sup>55</sup>. Moreover, downtime can cause a large portion of expenditure necessary for restoring the corroded systems and for treatments initiated to mitigate the corrosion<sup>56</sup>. According to Gerus et al<sup>57</sup> millions of dollars are yearly paid for this purpose. Corrosion also have indirect impact on the plant's economy by limiting the ranges of operating of the process. In general, excessive corrosion

cause to reduce the flexibility in varying the operating conditions. Corrosivity can be increased if the process operated beyond the typical conditions<sup>55</sup>.

#### **1.4 Deep Eutectic Solvents (DES)**

Relatively high costs of ILs synthesis is one of the main problem that avoid the widespread usage of it in industry, because the synthesis process of IL is costly due to expansive chemical requirements and the procedure of purification takes long time. Therefore, DESs emerged as low cost alternatives of ILs. By mixing two, three or even more components DESs can be formed. These compounds are ammonium halide salt known as hydrogen bond acceptor (HBA) mixed with hydrogen bond donor (HBD), they have melting point much lower than constituting component. The liquid state of DESs because of depression of melting point, whereby hydrogen bond interactions between an anion and a hydrogen bond donor are more energetically favored relative to the lattice energies of the pure constituents<sup>58,59</sup>. Usually, DESs are characterized by a very large depression of freezing point and at room temperatures (less than 423.15 K) they are liquid; while most of DESs are liquid between room temperature and 343.15 K. For some of the DESs it is hard to find the melting point, so obtaining glass transition temperature is required, thus these solvents know as low transition temperature mixture (LTTMs)<sup>10</sup>.

DESs and ILs solvents share many solvation properties<sup>60</sup>. Moreover, DESs have others advantages such as; low vapor pressure, non-toxic, biodegradable, does not react with water and low flammability. Therefore, with all this benefits DESs can be considers as environmental-friendly solvents. As it mentioned, DES are alternatives to IL in many application like, biodiesel purification<sup>61</sup>, bio- electrochemistry<sup>62, 63</sup>, pharmaceuticals<sup>64</sup>, catalysis<sup>65</sup>, CO<sub>2</sub> adsorption<sup>66</sup>.

DESs development has short history. Abbott et al<sup>67</sup>. in 2001 studied for different types of quaternary ammonium salts were heated with ZnCl<sub>2</sub> then the freezing point of the new liquids

measured. The lowering melting point (296.15-298.15 K) was found, when choline chloride (ChCl) used as the ammonium salt. In few years later in 2003, Abbott et al.<sup>68</sup> was the first who investigated DESs, which were a mixture of ChCl with urea in 1:2 molar ratio. Although numerous salts have been suggested for developing DES, ChCl is the most known based of DESs, due to its low cost, biodegradability, low toxicity, and biocompatibility. Moreover, it consider as essential nutrient since it might be extracted from biomass<sup>10</sup>. DES system can be described by equation 1.



Where;

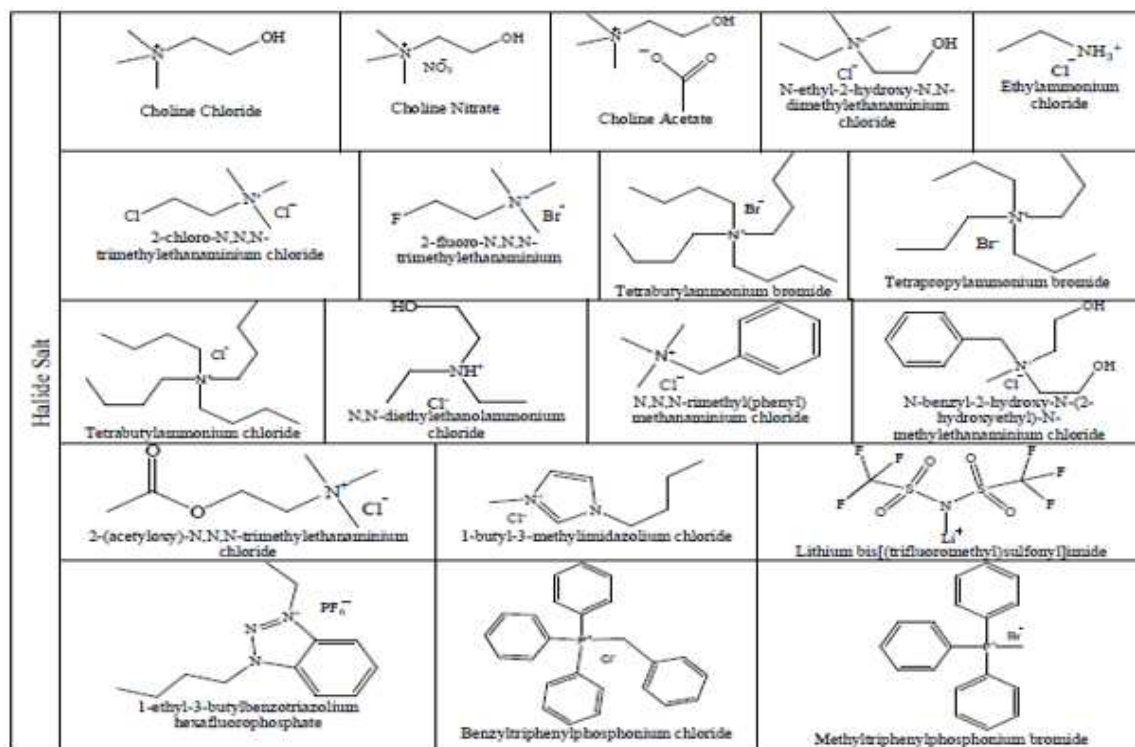
Cat<sup>+</sup>: present any ammonium, sulfonium or phosphonium

X: Lewis base, generally a halide anion

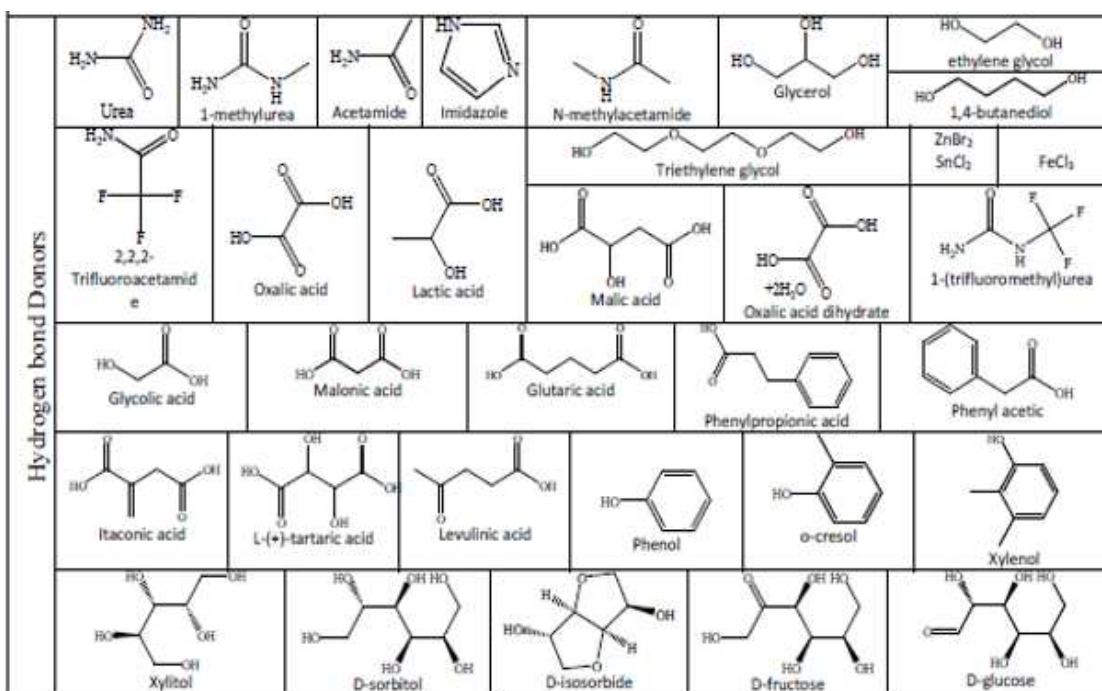
Y: Brønsted acid

Z= number of Y molecules interact with the anion

Most of the researches have concentrated on quaternary ammonium and imidazolium cations with particular emphasis being placed on more practical systems using choline chloride, [ChCl, HOC<sub>2</sub>H<sub>4</sub>N<sup>+</sup>(CH<sub>3</sub>)<sub>3</sub>Cl<sup>-</sup>]<sup>47</sup>. Figure 1.9 summarized the most common halide salts and HBD used in preparing deep eutectic solvents<sup>10</sup>.



(a)



(b)

Figure 1.9. List of common (a) halide salt used in preparing the DESs (b) HBD used in preparing DESs<sup>10</sup>.

## 1.5 Research Question and Motivation

Having discussed the current state of the art technologies for CO<sub>2</sub> capture and mitigation techniques that are implemented in process industries and their limitations, we seek answers to following questions:

1. Would DES based new sorbents be able to exhibit CO<sub>2</sub> capture performance that can compete with the existing amine-based solvents?
2. How easily DES based solvents be regenerated?
3. Are DES based solvents reusable? Do they lose capacity with time?
4. Considering acid nature of CO<sub>2</sub>, what will be the corrosion effect of DES solvents on process equipment?

## 1.6 Research Objectives

The research implements a comprehensive evaluation according to the following specific objectives:

- 1- Examine the proposed new system that made of ChCl/PAA with three different molar ratios (1:2,1:3 and 1:4).
- 2- Full physicochemical characterization of ChCl/PAA in order to analyze their strength and weaknesses for the aim of capturing CO<sub>2</sub> therefore, FTIR, TGA, density, conductivity, corrosion and contact angle measurements will be carried.
- 3- Gas solubility in order to analyze its appropriateness to capture CO<sub>2</sub>

## 1.7 Potential Beneficiaries

The experimental design of this work is planned by considering the process conditions for CO<sub>2</sub> capture units located in oil and gas process industries as well as power generation sector. The wide pressure and temperature experimental design was selected due to screening the proposed materials at conditions that can be applicable for both pre- and post- combustion conditions. The utilization of these materials will be further investigated for CO<sub>2</sub> capture units and how they can replace the existing amine systems with minimum process and equipment modifications.

## 1.8 Limitations and Assumptions

The design of efficient gas sorbents relies on below main factors:

- Cost efficiency
- Sorption efficiency
- Societal impact
- Environmental constraints

DES based solvents can be used as alternative systems from the perspective of sorption efficiency and environmental aspects. However, one of the biggest limitations of the gas capture processes is the high viscosity and solid state of most of DESs at room temperature restricting their application as extraction solvents. Thus, search for more stable and liquid DES at lower temperatures is a must to excel in these materials. On the other hand, the cost of ionic liquids can also be considered as a limitation for DES materials due to the low production capacities of the ionic liquids.

These factors must be considered in a separate study through economic benchmarking analysis against the other cutting edge sorbents.

## 2 . LITERATURE REVIEW

The aim of this chapter is to review recent researches on different types of DESs system, and to analyze the present knowledge on gas separation using these materials. Studying the physical properties of DES provided information about the strengths and weaknesses of this sort of system and gives a direction for reported DES in this work.

### 2.1 Physical Properties

Detailed characterization of the solvent are necessary in industry for many purpose such as: simulation, process molding, design the contactor columns of gas-liquid for CO<sub>2</sub> regeneration and adsorption<sup>69,70</sup>. Based to Wei et al<sup>71</sup>. and Kumar et al<sup>71</sup>. these results are important ,since chemical reaction kinetics from CO<sub>2</sub> absorption rate experiments can be deduce<sup>72</sup> by using this data.

#### 2.1.1 Phase Behavior

By mixing suitable amount of HBA and HBD DES is produced. Almost all literature base on binary DES, which means from each component (HBA and HBD) only one type is used to form DES mixture<sup>73</sup>. Below solid-liquid phase diagram summarized the major characteristics for binary deep eutectic (figure 2.1).The minimum melting temperature ( $T_m$ ) in the diagram represents the single value of the eutectic composition<sup>10</sup>. For better understanding let consider ChCl and urea DES system which produced at 1:2 molar ratio,  $T_m$  for the system is 285.15 K<sup>68</sup>, while the melting point for pure ChCl is 575.15 K and pure urea is 407.15. The strong intermolecular interaction between HBA and HBD cause this depression of melting point. Melting point for the DES system can reach 473 K<sup>50</sup>, but those with ambient temperature are more attractive, for practical reason for



example; energy required for melting the DES at ambient temperature less than those with higher temperature<sup>10</sup>.

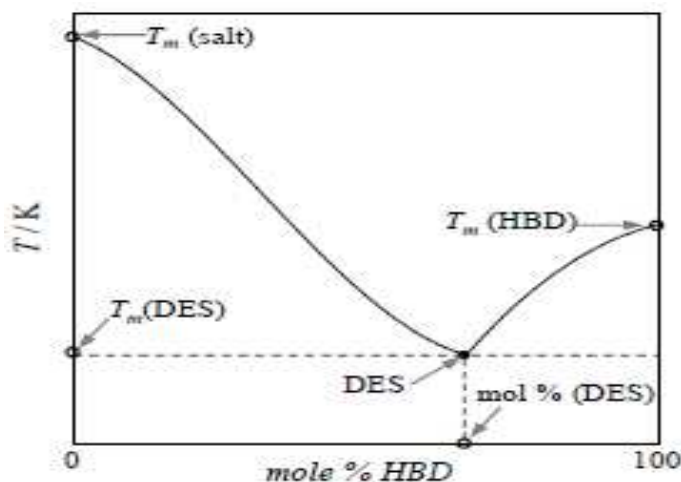


Figure 2.1. Solid-liquid phase diagram for binary DES system<sup>10</sup>.

### 2.1.2 Density

Density is one of the most important thermos-physical properties that have been studied for DESs. The majority, considered the density of the DES at the 298.15 K to be among 1 to 1.35 g/cm<sup>3</sup>. However, those with metallic salts like ZnCl<sub>2</sub> have larger densities (1.31 to 1.6 g/cm<sup>3</sup>)<sup>50</sup>. Table 2.1 summarized the literature that studied DESs system with ChCl based and their aqueous solutions. The densities of the system rely on temperature, molar ratio of HBA (ChCl) to HBD, pressure and water content. From the table, it is obvious that for ChCl/Urea DES system with same molar ratio there are around 4% differences between each source. These differences may be due to different experimental method, perpetration method, impurities of the samples. However, it is apparent that with increasing the temperature the density linearly decreased for all the systems that mention in the table and this can be true for all DESs with ChCl based where this reduction due to thermal expansion<sup>10,74</sup>.

Table 2.1. Density of DES systems with ChCl based<sup>10,74</sup>.

HBD	Molar Mixing Ratio	T (K)	$\rho$ (g/cm <sup>3</sup> )	Ref.
Urea	1:2	298.15	1.25	75
	1:2	298.15	1.212	76
	1:2	298.15	1.1979	77
	1:2	298.15	1.20	78
	1:2	313.15	1.24	79
	1:2	313.15	1.1893	79
	1:2	313.15	1.1887	80
Glycerol	1:1	298.15	1.1558	81
	1:2	298.15	1.1920	81
Malonic acid	1:1	303.15	1.0063	74
Lactic acid	1:2	298.15	1.1377	74

### 2.1.3 Viscosity

At room temperature, most of the DESs exhibit high viscosities usually as high as a 750 mPa.s. Which means the DESs is often represent a wide HB network among each component, therefore the high viscosity cause lower movement of free species within the DES. The viscosity of the DESs may be due to several means, ion size, small void volume of the DESs and electrostatic force or van der Waals interactions. Viscosity of DESs in general affected by water content, temperature and the chemical nature of the DESs (ammonium salts and HBDs type ,molar ratio of organic salt to HBD and etc.)<sup>82</sup>. High viscosity prevents many medical and industrial application, particularly for the aim of separation CO<sub>2</sub> and other gases and this due to excessively high pumping cost and poor mass and heat transfer, consequently the lower viscosity is more desirable (less than 500 mPa.s). Table 2.2 summarized some of DES systems that have low viscosity<sup>10</sup>.

Table 2.2. DES system with low viscosity<sup>10</sup>.

Salt	HBD	Molar ratio	T (K)	$\eta$ (mPa.s)	Ref.
ChCl	urea	1:2	303.15	449	83
ChCl	glycerol	1:2	303.15	246.79	84
ChCl	ethylene glycol	1:2	303.15	35	83
ChCl	glycolic acid	1:1	303.15	394.8	85
ChCl	levulinic acid	1:2	303.15	164.5	85
ChCl	phenol	1:3	303.15	35.17	86
ChCl	o-cresol	1:3	298.15	77.65	86

#### 2.1.4 Conductivity

This physical property has indirect relationship with viscosity, the higher the viscosity the lower the conductivity, therefore at the room temperature most of the DES system has very low conductivity, lower than 1 mS/cm, so this will cause problem for certain electrochemical applications. In order to predict the temperature effect on conductivity behavior of a DES Arrhenius equation can be used. Some of DES systems have high conductivity such as those containing ethylene glycol or imidazole with ChCl. As it mention , the molar ratio of the organic salt to HBD effect the viscosity, so it is clear that this parameter have a direct effect on the conductivity<sup>82,87,88</sup>. Table 2.3 shows the conductivity for some of DES system.

Table 2.3. Conductivity for selective DES system<sup>10</sup>.

Salt	HBD	Molar ratio	T (K)	$\kappa$ (mS $\times$ cm <sup>-1</sup> )	Ref
ChCl	Urea	1:2	313.15	0.199	<sup>79</sup>
ChCl	glycerol	1:2	298.15	1.300	<sup>89</sup>
ChCl	malonic acid	1:1	298.15	0.742	<sup>65</sup>
ChCl	Imidazole	3:7	333.15	12	<sup>82</sup>

### 2.1.5 Polarity

The key property for a fluid is polarity, since it characterizes the ability of the fluid for dissolving solutes. Regardless of this importance, the information about this property is almost null and this consider as remarkable problem, because DES has been suggested as environmentally friendly substitute to alternative to common volatile organic solvents<sup>10</sup>. Commonly, this property measure by solvents polarity scale,  $E_T$  (30), this refers to the electronic transition energy of a probe dye (Like Reichardt's Dye 30) in a solvent. Using UV-vis technology and Reichardt's Dye 30 the polarity of solvents can calculated by equation 2:

$$E_T(30)(\text{kcal mol}^{-1}) = h_{\text{CU max}}N_A = (2.8591 \times 10^{-3})U_{\text{max}}(\text{cm}^{-1}) = \frac{28591}{\lambda_{\text{max}}} \quad (2)$$

Table 2.4, summarized polarity of ChCl/glycerol system with different molar ratio using Reichardt's Dye method. Obviously, with increasing the ratio of the system the  $E_T$  (30) of the DES increases. Also with increasing the concentration of ChCl/glycerol system almost linear increase of  $E_T$  noticed <sup>82</sup>.

Table 2.4. Polarity of ChCl/glycerol eutectic solvent at different molar ratio <sup>82</sup>.

Salt	HBD	Molar Ratio	E <sub>T</sub> (30) (kcal mol <sup>-1</sup> )
	Glycerol		57.17
ChCl	Glycerol	1:3	57.96
ChCl	Glycerol	1:2	58.28
ChCl	Glycerol	1:1.5	58.21
ChCl	Glycerol	1:1	58.49

### 2.1.6 Surface Tension

Surface tension is property that indicates the cohesive forces among the molecules of a liquid that exist at the surface. Structure of the molecular is related to the surface tension, however no quantitative observation have been obtain<sup>90</sup>. Factors that can control the surface tension of DES with ChCl based are HBD type, molar ratio of HBA to HBD, temperature and water content. Table 2.5 shows some of ChCl based DES system with different HBD, the surface tension of malonic acid with ChCl based is higher than ChCl based with urea. For instance, at the same temperature (298.15 K) with molar ratio of 1:1 ChCl/malonic acid have surface tension of 65.7 mN/m while ChCl/urea system with molar ratio of 1:2 have surface tension of 52 mN/m. The surface tension and temperature has inverse relationship, with increasing one the other will decrease<sup>74</sup>.

Table 2.5. Surface tension of ChCl based DES <sup>74</sup>.

HBD	Ratio	T/K	$\gamma$ (mN/m)
Urea	1:2	298.15	52.0
Glycerol	1:2	298.15	56.0
Malonic acid	1:1	298.15	65.7
Lactic acid	1:2	298.15	48.0
Phenylacetic acid	1:2	298.15	41.9
Ethylene glycol	1:3	293.15	45.4

### 2.1.7 Contact Angle

In order to be able to characterize the degree of wettability or adhesion of liquid on solid surface, measurement of contact angle becomes an important tool. For membrane carbon capture technology wettability consider as one of the most important parameter, since it reduce the absorption performance of the membrane. The results of some of the literature on membrane wettability especially the contact angle is summarized in table 2.6. According to Lv et al. <sup>91</sup> contact angle of polypropylene (PP) membranes strongly decreased during immersion in absorbent solutions. Moreover, based on this study the contact angles of all the membranes were above 90°, therefore each one of studied membranes have hydrophobic surface.

Blanco et al. <sup>92</sup> investigated the contact angle of three bis(trifluoromethylsulfonyl)imide-based ionic liquids: 1-Dodecyl-3-methylimidazolium bis(trifluoromethylsulfonyl)imide [C<sub>12</sub>MIM][NTf<sub>2</sub>], tributylmethylammoniumbis(trifluoromethylsulfonyl)imide [N<sub>4441</sub>][NTf<sub>2</sub>] and methyltrioctylammoniumbis(trifluoromethylsulfonyl)imide [N<sub>1888</sub>][NTf<sub>2</sub>] on AISI 52100 steel and three coatings of Titanium nitride ,ceramic chromium nitride and zirconium nitride (TiN, CrN and

ZrN), the results are shown in Figure 2.2. In this study it was found that all the three surfaces showed hydrophobic behavior, where lower contact angle was due to lower surface tension. Furthermore, Lv et al.<sup>91</sup> found the same relationship between the contact angle and the surface tension for the membranes system.

Table 2.6. Contact angle of membrane<sup>93</sup>.

Membrane Type	Absorbent	Contact Angle	Ref.
PP hollow fiber	deionized water	CA: from 126.1° to 100°	91
	30 wt % MDEA solution	CA: from 121.6° to 90.8°	
	30 wt % MEA solution	CA: from 121.6° to ~92.5°	
	20 wt % DEA	CA: from 103.7° to 94.5°	94

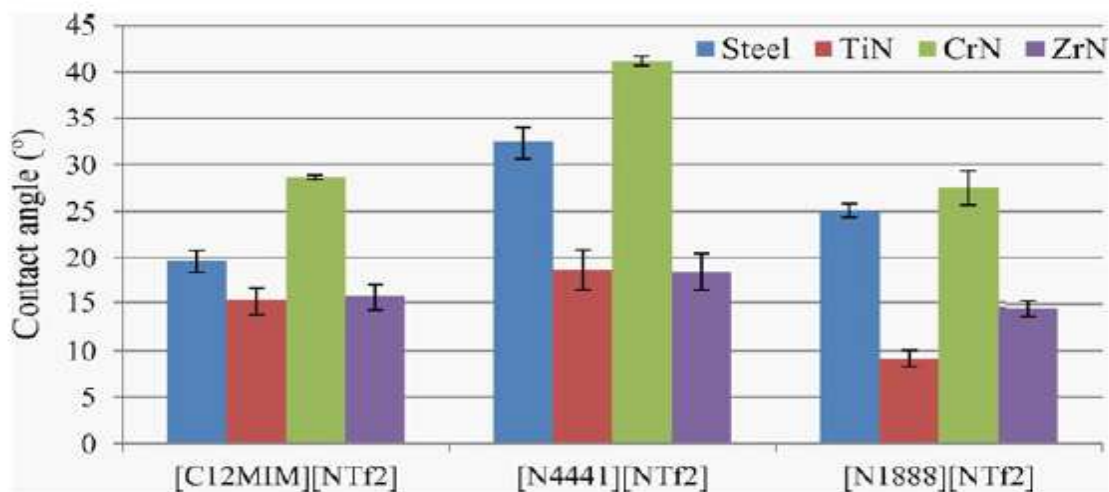


Figure 2.2. Contact angle of [C12MIM][NTf2], [N4441][NTf2] and [N1888][NTf2] on TiN, CrN and ZrN<sup>92</sup>.

### 2.1.8 Corrosion

One of the main problems related to the amine-based CO<sub>2</sub> capture is corrosion process materials which results in unexpected downtime, production loss and even major fatality. The cost of corrosion was rated to be 25 % of the maintenance cost for gas sweetening plants<sup>95</sup>.

Gunasekaran<sup>96</sup> studied the corrosion of carbon steel in a aqueous solution for Monoethanolamine (MEA), Methyldiethanolamine (MDEA), 2-Amino-2-methyl-1-propanol (AMP), Diethanolamine (DEA) and piperazine(PZ) amine based under CO<sub>2</sub> and temperature of 353.15 K. The corrosion rates of these systems are summarized in figure 2.3. According to Gunasekaran the corrosion rates of these five different system can be ordered as : MEA > AMP > DEA > PZ > MDEA, and this studied of corrosion rate has good agreement with Kohl and Nielsen<sup>53</sup> studied.

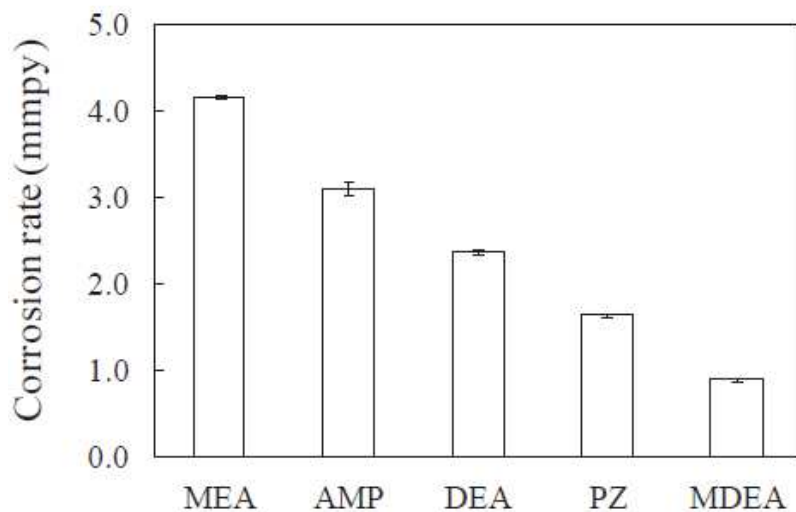


Figure 2.3. Corrosion behavior of different amine based<sup>96</sup>.



Aida<sup>95</sup> investigated the corrosion rate of carbon steel CS1018 in aqueous solution for MEA, DEA and MDEA (classic amine) at temperature of 353.15 K. The results were almost same as the previous. The results of Aida's studied on amine base are summarized in table 2.7. This study also includes the corrosion rate of activated amine (MEA/PZ, MEA/MDEA MDEA/ piperazine (PZ), MEA/MDEA/PZ and PZ) and amine/RTILs (MEA/1-butyl-3-methylimidazolium tetrafluoroborate [BMIM][BF<sub>4</sub>] and MEA/ 1-butyl-3-methylimidazolium trifluoromethanesulfonate [BMIM][Otf]). The results of 3 classification are summarized in figure 2.4. According to this study it's found that the corrosion rate of classic amine increased by increasing the CO<sub>2</sub> loading, also the corrosion rate increased based on the type of amine. The activated amines show less corrosivity in compared with classic amines where it's due to the structure of PZ. Moreover, in terms of less corrosivity and more CO<sub>2</sub> absorption capacity the mixtures of MEA/[BMIM][Otf] and MEA/PZ shows the better results.

Table 2.7. Corrosion rate of amine based<sup>95</sup>.

Amine type	Temperature (K)	Corrosion Rate (mm/y)
MEA		3.41
DEA	353.15	2.45
MDEA		1.25

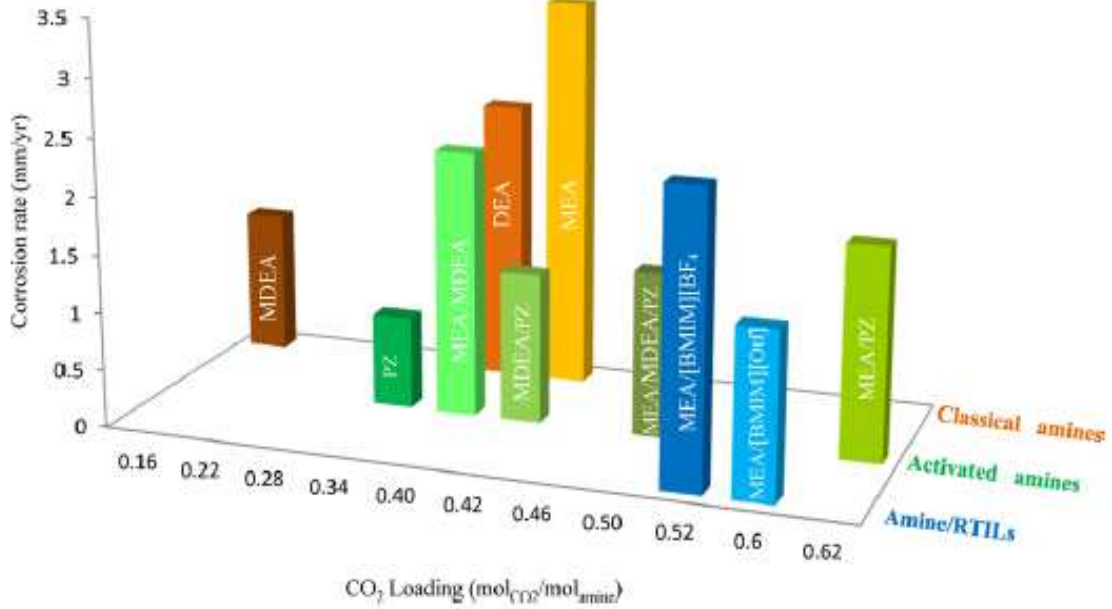


Figure 2.4. Corrosion rate of single amines, piperazine activated amines, and amine/RTIL solutions at 353.15 K<sup>95</sup>.

## 2.2 Gas Separation and CO<sub>2</sub> Capture

Around 3/4 of overall gaseous that emitted to the atmosphere capture by CO<sub>2</sub> capture technology. There are different technologies that recently used for capturing CO<sub>2</sub> such as adsorption, absorption, and cryogenic capture process and separation using membrane units. Characteristics of gas stream determine the best technology that have to be used for the purpose of capturing CO<sub>2</sub>. This characteristic is mainly relying on the sort of the dynamics of the process in which the fuel will be used or processes. Processes are based on chemical or physical separation method. Porous mediums' or solvents nature determined the nature of the separation system<sup>97</sup>.

The solvents that used for more than 70 years in CO<sub>2</sub> capture process is amine solvents based. It is chemical solvents that derivative from ammonia where the hydrogen (H<sub>2</sub>) atoms has

been changed by other groups such as alkyl or aryl therefore depend on the number of H<sub>2</sub> that have been changed by organic functional groups it classified as primary, secondary, and tertiary. The most often type of amines that are used are monoethanolamine (MEA), methyldiethanolamine (MDEA), piperazine (PIPA), di-ethanolamine (DEA) and etc. It is the most commonly acid gas removal used from early stages since it recovers almost 98% of CO<sub>2</sub> and the purity of product reach 99%<sup>10</sup>. However, there are several disadvantage of using amine solvents; for instance, loss of amine reagents, at desorption stage water transfer into gas stream, corrosive byproducts forms from chemical degradation, thru the regeneration the energy consumption is high and insufficient CO<sub>2</sub>/hydrogen sulfide capture capacity<sup>98</sup>.

To solve the amine problems both industry and academia has been researching to find the substitute solvents which are chemically stronger, high CO<sub>2</sub> affinity and with viable thermophysical properties. In last 20 years in the academia area ILs get incredible consideration and their ability to uptake the gas specially CO<sub>2</sub> was tested at different process conditions. The recent studies have shown that ILs are the promising alternative capture solvents for CO<sub>2</sub> and other gases like hydrogen sulfate (H<sub>2</sub>S) and sulfur dioxide (SO<sub>2</sub>)<sup>99,100,101,102</sup>. ILs has very low vapor pressure, this advantage gives them the opportunity to overcome the high volatility amine process<sup>10</sup>. Early studies with ILs showed that the affinity of SO<sub>2</sub> and CO<sub>2</sub> increase by cation and anion base on their select and their tunability to synthesize task-specific solvents that can physically interact with the gas<sup>102,103,104, 105</sup> to be absorbed through reversible binding. The first experimental study in 1999<sup>105</sup> showed that the nature of anion play the key role in solubility of CO<sub>2</sub> in the IL, this research followed by range of other studies<sup>106,107,108</sup> recommending the same concept. One of the study showed that the ILs with nitrate anion have less CO<sub>2</sub> solubility than ILs with bis(trifluoromethylsulfonyl)imide anion<sup>109</sup>. Later it was highlighted that minimal extent on the

cation or fluorination on the anion increase the solubility of CO<sub>2</sub> in ILs; but this fluorination has a trade-of negative side effect in actual processes<sup>110</sup>. In other hand, resent study showed that the solubility of CO<sub>2</sub> in ILs mostly controlled by entropic effects<sup>111</sup>. Removing CO<sub>2</sub> using ILs can be achieved by both pre and post combustion<sup>112</sup>,but however ,post-combustion gas capture and separation has the issue of low capacity<sup>113</sup>.Among all properties mentioned ,still ILs haven't been so far proven to be alternative materials for large-scale industrial scrubbing agent because of many reasons; for example, high synthesis cost<sup>114</sup>, toxicity<sup>115</sup> and low capacity<sup>113</sup>.Despite their fascinating functionalities, these materials still need huge capital investments for bulk productions<sup>10</sup>.Also other properties such as moisture and non-biodegradable make this solvent questionable for industrial application. Therefore to solve these problematic aspects of ILs and utilize their chemical flexibility, new techniques has been emerged which called DESs<sup>89,10</sup>.

### **2.3 DES and CO<sub>2</sub> System**

Different material and techniques over the past years have been developed to replace the amine base for the purpose of capturing CO<sub>2</sub>, such as DES and IL. Most of the ILs have the ability to dissolve CO<sub>2</sub>; DES system is similar to IL since it mainly contains ionic species and it has interesting solvent properties for high CO<sub>2</sub> dissolution. This combination between the green solvents (DES) and CO<sub>2</sub> has large potential for a diversity of chemical processes (gas separation and purification, catalysis, chemical fixation of CO<sub>2</sub> and etc.).

The effect of water in the DESs system can hinder the gas solubility performance, there are several published work on this issue that investigates the effect of the water content in a DES urea with 1:2, 1:2, 1:1, and 1:2 molar ratios respectively)<sup>116,117</sup>It has been shown that adding water to

DESs system causes significant drop in the solubility of CO<sub>2</sub>, representing that water can be used to regenerate the DES system. On the other hand, this indicated that the absorption of CO<sub>2</sub> in such solvents will be less if flue gas is wet basis that contains moisture.

Another study was conducted by Hsu et al<sup>120</sup> on mixing MEA (30%w/w) with the ChCh:urea (1:2 molar ratio) DES system. It was found that adding 30% (w/w) of aqueous MEA as 15% (w/w) to the aqueous DESs caused an increase about 4-fold in the solubility of CO<sub>2</sub> in compared with the original DES system. This method indicated promising results, however the disadvantages of MEA such as thermal degradation, high vapor pressure, ecological concerns<sup>121,122</sup> raised question about the applicability and sustainability of such method.

In literature it has been reported that the DES systems that are not amine functionalized can be regenerated with based on pressure swing methods<sup>16</sup>. Moreover, amine functionalized DES systems have posed a thermal requirement for regeneration<sup>10</sup>.

Most of the recent studies on DES and gas sorption focus on physisorption based gas sorption mechanisms at high pressures. However, despite thermal regeneration requirements, chemisorption with DESs has been proven to be an alternative to physisorption. The most popular example to this mechanism is utilization of ionic liquids such as 1-alkyl-3-methylimidazolium acetate<sup>116, 118</sup>. It is a known fact that anion dominates the interactions with the carbon dioxide through the Lewis acid-based interactions<sup>119</sup>. Nevertheless, the strength of the carbon dioxide solubility is not directly related with the strength of the carbon dioxide gas and anion interactions. However, latest observations showed that the basicity of the anion has an effect on stronger interactions with the C-2 proton on the imidazolium and an anion with high enough basicity has the potential to abstract the proton to produce an N-Heterocyclic carbene and acetic acid<sup>120</sup>. In a recent study it has been shown that the stability of the formed carbanes from 1-alkyl-3-

methylimizazolium acetate and instead of ion pair, carbene acetic acid complexes dominated the vapor of neat 1-ethyl-3-methylimidazolium acetate<sup>121</sup>. Thus it can be concluded that similar chemisorption mechanism of carbon dioxide via several other functionalized ionic liquids can be proposed for enhanced carbon dioxide uptake by including functional groups such as basic anions<sup>1, 2, 122</sup>, amine groups<sup>99, 123, 124, 125</sup>, pyrrolide anions<sup>126</sup>, or pyrazolide anions<sup>126</sup>. It would be advantageous to select the less viscous cases, thus the pyrrolide and pyrazolide anion cases shall be the special interest.

Most of the literature in this area (CO<sub>2</sub> solubility) focus more on the DES system with ChCl based<sup>82, 10</sup>. Lately, Li et al<sup>127</sup> determined the solubility of CO<sub>2</sub> using DES system made of ChCl with urea at different pressure, temperature and molar ratio. It's found that the solubility of CO<sub>2</sub> ( $X_{CO_2}$ ) in this system (ChCl/urea) depends on the following three factors:

1. Values of  $X_{CO_2}$  increased with increase the pressure of CO<sub>2</sub>, also at low pressure range this value was more sensitive to the pressure.
2. Values of  $X_{CO_2}$  decreased with increase in the temperature and this was true for all the pressure range.
3. The molar ratio of ChCl and urea has significant effect on the value of  $X_{CO_2}$ ; for example, at identical pressure and pressure the DES system of ChCl and urea at ratio of 1:2 exhibit higher  $X_{CO_2}$  values than molar ratio of 1:1.5 of 1:2.5.

DES system formed from ChCl and urea with molar ratio of 1:2 identified as reline and it have the lowest melting point. Reline describe as hygroscopic, because most of ChCl based DES always contain little amount of water and this may affect the HB interaction, therefore the chemical and physical properties of the system will modified<sup>128</sup>. For instance, densities of the DES system

made of ChCl and ethylene glycol at molar ratio of 1:2 reported to be decreased with increasing temperature and increased with increasing pressure in the range of 1 to 500 bars. This effect due to the dependency of HB on the temperature and also because of decrease in the molecular distance and free volume of the mixture<sup>129</sup>. Recently some finding shows that water in the DES act as anti-solvents which prevent the CO<sub>2</sub> absorption. At low pressure the hygroscopic behavior of DES remarkably affects in the solubility of CO<sub>2</sub>, and this cause limitation for those mixtures<sup>130</sup>.

Several studies<sup>16, 127, 131,132,133,134, 125,</sup> have investigated the effect of decrease and improvement in solubility of CO<sub>2</sub> with increasing pressure, temperature and present of water ( table 2.8). Based on Li et al.<sup>127</sup> study, increasing the molar ratio for ChCl/urea eutectic solvent from 1:1.5 to 1:2 and 1:2.5 does not show any effect on the CO<sub>2</sub> capture. However, the amount of dissolved CO<sub>2</sub> mole fraction in this system is 0.032 for molar ratio 1:2.5 at 333.15 K and 1.08 MPa and 0.309 for molar ratio 1:2 at 313.15 K and 12.5 MPa. According to table 2.8, it can be concluded that, DES system made of ChCl/ urea with ratio of 1:2 at 303.15 K and 60 bars shown the best performance to uptake CO<sub>2</sub> which measured to be 3.559 mmol/g. sulfonate ILs at 307 K and 80 bar it absorbed 4.52 mol/kg which means it uptake more than ChCl/urea eutectic system, however at atmospheric pressure and ambient temperature DES made of ChCl/ glycerol at ratio 1:1 has the highest CO<sub>2</sub> capture of 0.678 g/g in compare with mono-ethanol amine which it uptake 0.28 mol/mol of CO<sub>2</sub> at room temperature and 10 bar. Thus, this clearly indicates that, the DESs system can absorb more CO<sub>2</sub> than the toxic ILs based.

Table 2.8. Solubility of CO<sub>2</sub> in various DES system<sup>10</sup>.

IL	HBD	Molar ratio	Absorbent	Solubility	T/P (K/bar)	Ref.
ChCl	Urea	1:2	CO <sub>2</sub>	3.559 mmol/g	303.15/60	132
ChCl	ethylene glycol	1:2	CO <sub>2</sub>	3.1265 mmol/g	303.15/58.63	133
ChCl	ethanole amine	1:6	CO <sub>2</sub>	0.0749 mmol/g	298/10	135
methyltriphenylphosphonium bromide	ethanole amine	1:6	CO <sub>2</sub>	0.0716 mmol/g	298/10	135
ChCl	Urea+H <sub>2</sub> O	50wt%rel Chcl/Ur+ 50% H2O	CO <sub>2</sub>	0.111 mol/mol	313/7.8	130
ChCl	Urea+H <sub>2</sub> O	60wt% rel +40%H2O	CO <sub>2</sub>	0.103 mol/mol	313/8.06	130

The effect of pressure and temperature on CO<sub>2</sub> solubility for DES system with base of ChCl was investigated for range of 293.15 K to 323.15 K and pressure up to 30 bars was studied by Ruh et al<sup>16</sup> Figure 2.5 shows the results of CO<sub>2</sub> solubility in DES system made of ChCl and LA at 1:2 molar ratio at 5 different isotherm and up to 30 bars. The graph indicate that the solubility of the system linearly increased with pressure, but it decreases with increasing the temperature. Furthermore, the kinetics of the absorption in the ChCl/LA system has been studied. The amount of CO<sub>2</sub> absorptions with time and at both high and low pressures is shown in figure 2.6. For fully saturated DES solution at 1 bar it required time of 7 minutes in order to reach the equilibrium, while at 30 bars it required almost 12 minutes.



According to the promising results of ChCl/LA DES system in absorbing CO<sub>2</sub>, therefore this work is a complemented to the previous studied.

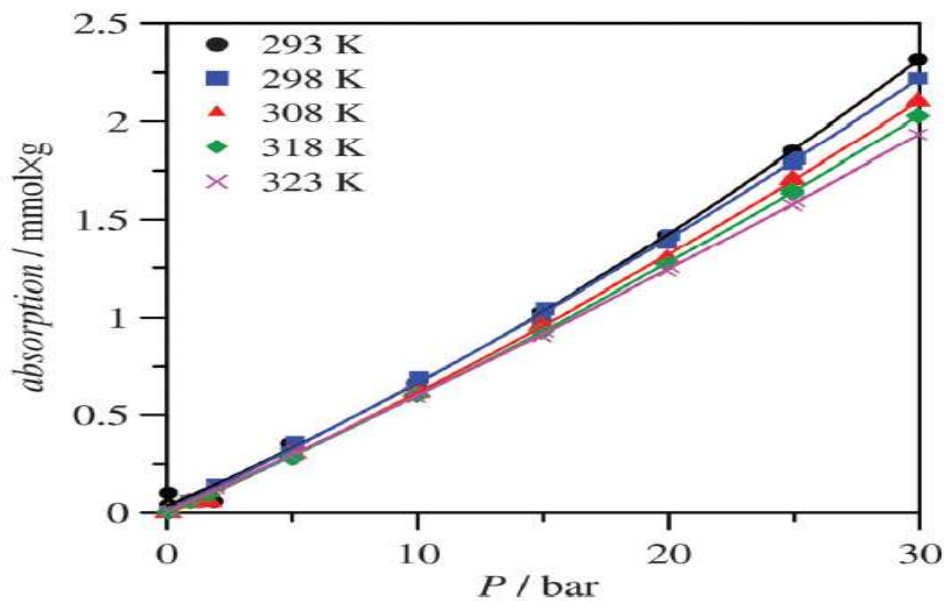


Figure 2.5. Effect of pressure and temperature on CO<sub>2</sub> solubility in ChCl/ glycerol DES system<sup>16</sup>.

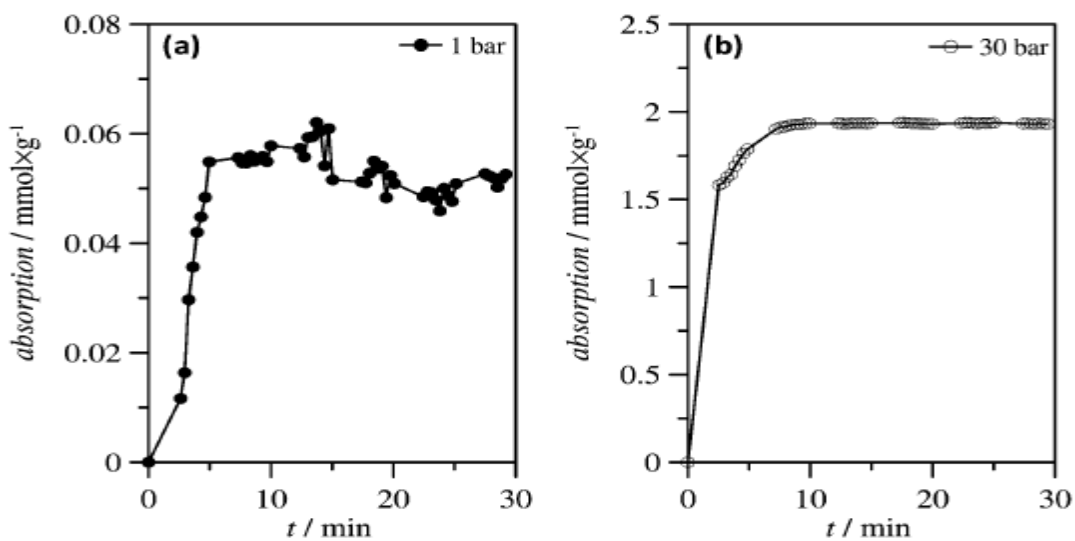


Figure 2.6. Isobaric CO<sub>2</sub> solubility in ChCl/LA kinetics: (a) 1 bar and (b) 30 bar<sup>16</sup>.

## 3 . MATERIALS AND METHODS

### 3.1 Materials Used in this Work

Materials that used for this work are ChCl, Phenylacetic acid (PAA), Nitrogen (N<sub>2</sub>) and CO<sub>2</sub>. The purpose of choosing ChCl and PAA because ChCl is the most common HBA used, since it is biodegradable, biocompatible where it's known as vitamin B<sub>4</sub> also both of them have low price, they are non- toxic and environmentally friendly, moreover no study has been published before focusing on suability of CO<sub>2</sub>/N<sub>2</sub> gas in this mixture.

The melting point of ChCl is 575.15 K with purity of 97.0% and PAA have melting point of 350.15 K with purity of 99.0% were purchased from iolitech and Sigma-Aldrich respectively. N<sub>2</sub> and CO<sub>2</sub> gasses with purity of 99.99% are purchased from Buzware Scientific Technical Gases, Qatar. PAA is used as it received, while ChCl dried for 24 hours in oven at 400.15 K. A mixture of 1:2, 1:3 and 1:4 molar ratio of ChCh/PAA prepared by mixing 35.014 g of ChCl and 68.64 g of PAA, 35.07 g of ChCl and 103.05 g of PAA, 35.01 g of ChCl and 136.11 of PAA respectively. In order to avoid the moisture that might end up in the final mixture, the three mixtures were prepared under glove box (figure 3.1). Since both chemicals are solid at room temperature, thus they were heated on a hot plate at 423.15 k and grinded in mortar to form liquid mixture, after that the mixture was stirred till clear and homogeneous DES achieved. The first ratio (1:2) was liquid at room temperature, while the other two ratios (1:3 and 1:4) were heated at temperature 308 K and 323 K respectively with continued mixing over stirred for one hour. An easy and uncomplicated procedures was taken to prepare the DESs where no solvent was added in order to melt the two chemicals, only heat was supplied to keep DES 1:3 and 1:4 on their liquid state for characterization because they are solid at room temperature, also no extra steps were included for purification.

Figure 3.2 shows the three different DESs system that prepared where only 1:2 is liquid at room this temperature (a) and the melting point for 1:3 ratio is 308.15 K (b) and 321.15 K for 1:4 ratio (c).



Figure 3.1. Glove box instrument.

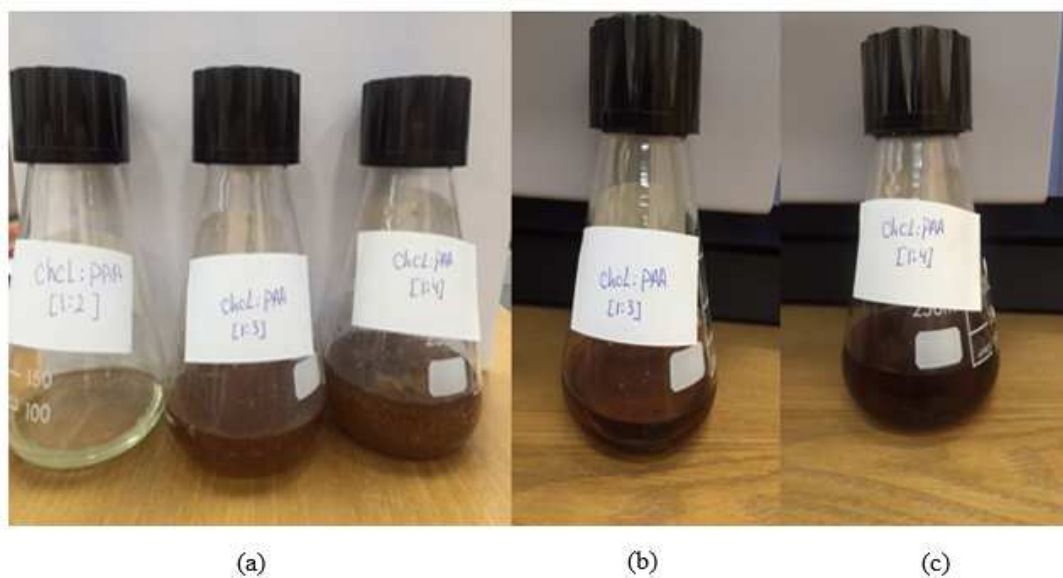


Figure 3.2. ChCl/PAA DES system at (a) room temperature (b) 308.15 K (c) 321.15 K.

## 3.2 Methods

### 3.2.1 Fourier Transform Infrared Spectroscopy (FTIR) Characterization

The most important functions of FTIR technology are to study the structure of compound and to analyze the degree of the compound purity, in other word to obtain information about complexation and interaction between prepared ChCl/PAA based DES systems. It is molecular versus atomic analysis where its look at molecules structure not individual atoms, it's a qualitative analysis. The devise has infrared light source, which is the base light of the energy. The sample is put in the light source and then absorbance of that sample is what is used to measure the bounds of the carbon atoms. FTIR used for several types of samples such as solid, liquid and others samples. FTIR instrument is shown in figure 3.3.



Figure 3.3. Infrared IR Spectroscopy Test Instrument.

The individual compound (ChCl and PAA) and the DES mixture for the three ratio were characterized by FTIR using Spectrum™ 400 Spectrometer (PerkinElmer,USA).The prepared samples were scanned several times in the range of 400-4000  $\text{cm}^{-1}$ . The Detailed method is as follow:

- 1- First start the OPUS software. No need to shut down the OPUS after use.
- 2- Before using the machine be sure that the sample platform (figure 3.4) is empty and free of materials, because a background scan is required,
- 3- If the platform is not clean use wipes and alcohol (ethanol is the best) to clean the lenses.
- 4- Back to the software click on :
  - a. Analysis.
  - b. Measurement.
  - c. Background scan.
  - d. At the bottom of the software a green bar will appear, so when the scan is completed, this bar will disappear.
- 5- For Liquid sample prepare a clean Pasteur pipette and pinch the bulb gently, only single drop will suffice because the droplet will separate.
- 6- Drop a single droplet of the sample on the platform and rotate the screw.
- 7- This time click on sample measurement in the software, the green bar will show up again when is disappear the spectrum will come into view. Figures 4.1, 4.2 and 4.3 show the spectrum of the materials that used in this work.
- 8- Finally clean the platform.

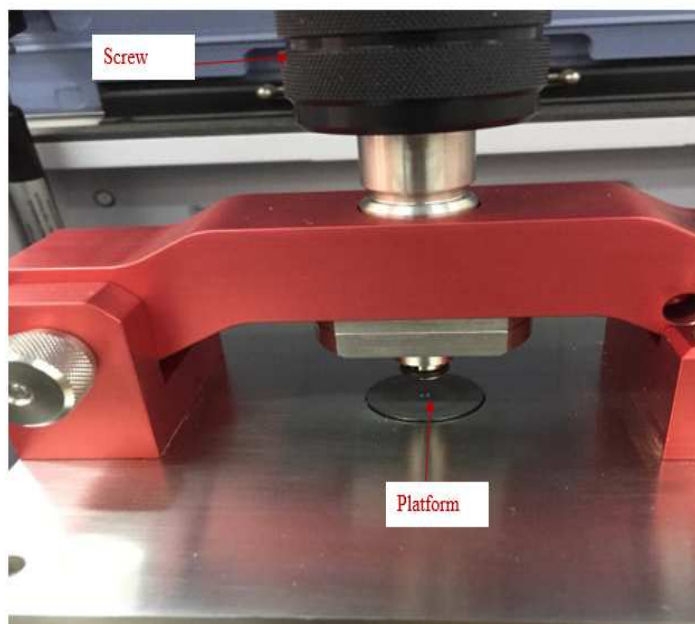


Figure 3.4. Photo of FTIR platform

### 3.2.2 Thermogravimetric Analysis (TGA)

TGA is a technique that frequently used in thermal analysis. It's mainly used to characterize the materials by measuring their change in mass as function of temperature and time. The properties and behavior that can be measure by TGA include composition, purity, decomposition reaction, decomposition temperature and absorbed moisture content. The principle of TGA is to measure the mass of a sample as it is heated, cooled or held at constant temperature in defined atmosphere. A TGA machine contain furnace and a highly sensitive balance, the device is shown in figure 3.5 where it is connected to the computer. In this work TGA used specifically to identify the temperature limitation of the absorbent. To put it differently, it used to check two essential temperatures, which are the decomposition temperature ( $T_d$ ) and onset temperature ( $T_{onset}$ ) for each molar ratio of prepared DES.

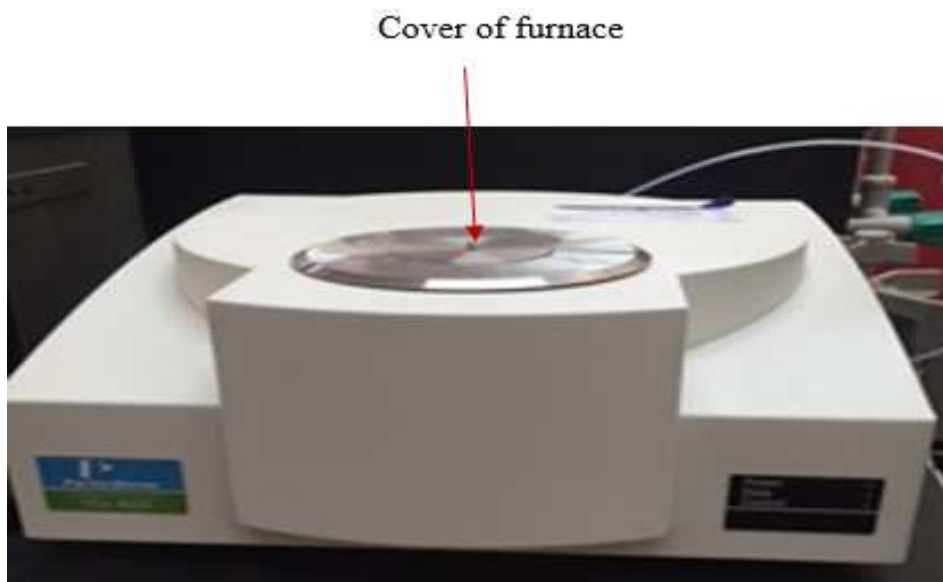


Figure 3.5.TGA instrument.

For this work PerkinElmer Pyris 6 TGA machine used for the samples characterization, to obtain the curve of weight loss with temperature. The DESs heated from 303.15 till 707.15 K at rate of  $5 \text{ K min}^{-1}$  under dried atmosphere using  $\text{N}_2$  gas. The procedure of using this device as follow:

1. First open Pyris program click on start Pyris then data analysis.
2. Method Editor Window will appear, therefore specify the sample name, operator and any comment regard to the sample then press Browse to save it.
3. From the same window click on (figure 3.6 ):
  - a. Initial state-to adjust initial temperature value (starting temperature value)
  - b. Program (in the same window) in order to set the heater and cooler program temperature.
4. Open the  $\text{N}_2$  gas (there is a  $\text{N}_2$  gas calendar next to the instrument).

5. Remove the cover of the furnace and insert the empty sample container (figure 3.7).
6. In the program click on balance symbol (figure 3.8(a)) to keep the Weight at 0. After that fill the container with the sample and put in the furnace again.
7. Click on sample balance (3.8(b))
8. The last step is to click on start measurement (figure 3.8(c)).

The measurements need almost two hours to give the exact plot. Figure 4.4 shows the TGA curve for the three ratios that used in this work.

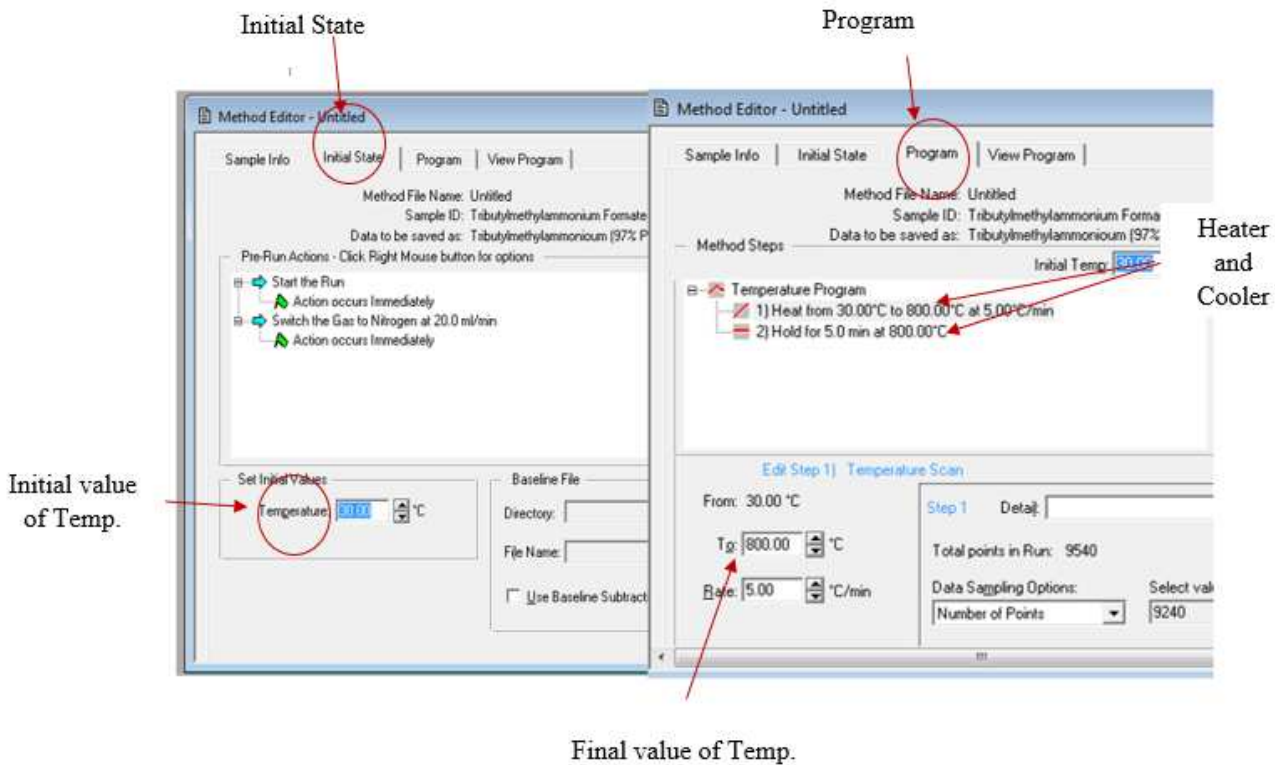


Figure 3.6. Pyris program set up.





Figure 3.7. TGA furnace and Sample container.

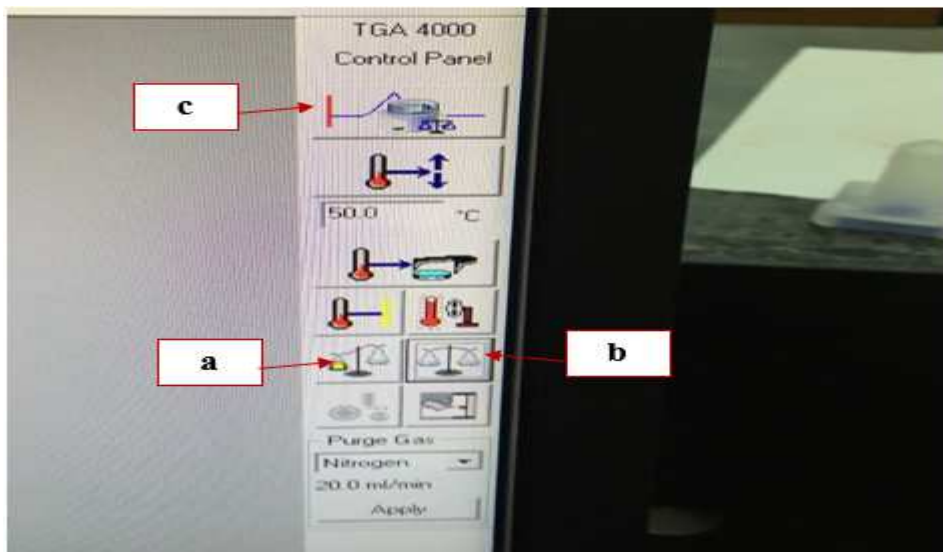


Figure 3.8. Pyris program set up. Balancing the empty container (a), balancing the sample (b), start measurement (c).

### 3.2.3 Corrosion Measurement and Data Analysis

#### 3.2.3.1 Experimental Procedure

The importunes of this measurements is to realize the corrosivity limitation of the prepared DES, since a serious danger can be occur because of corrosion, such as vessels corrosion , corrosion of metallic pipes and for other assemblies where they are in direct contact with material. Also this test provides information about the stability of metal from polarization values.

In order to carry the corrosion tests on the sample, ChCl/PAA DESs system should be at liquid state, therefore the tests were carried out at 298.15, 318.15 and 329.15 K for 1:2, 1:3 and 1:4 molar ratio respectively. For this test 20 mL from each DESs samples were used, with surface area of 0.785 cm<sup>2</sup> a circular specimen of low carbon steel was submerge into the liquid. Base on ASTM G1-03 standard the specimen was prepared. Wet grinding and polishing treatments were done using 320600 and 1200 paper of grit and SiC respectively. Additional cleaning was perform for the degassed specimen, first highly purified acetone and deionized water used then it dried using hot dry air. At the selected temperature the corrosion test was done in absent and present of CO<sub>2</sub> and the experiments of corrosion were performed following recently published methodology. The cell of the experiment was equipped with reference 30K Booster attached to a reference 3000 potentiostat / Galvanostate / ZRA, USA, standard calomel reference electrode, with graphite counter electrode and steel working electrode. The setup of the corrosion test is shown in figure 3.9.



Figure 3.9. Set up of corrosion test.

### 3.2.3.2 Tafel Extrapolation

In order to determine the electro-kinetic data (eg. corrosion rate and current) for the tested environments the Tafel extrapolation method was used. The data acquisition system was used in the range of  $\pm 250$  millivolts (mV) vs open circuit potential (OCP) and a scan rate of 0.0001 V/sec to generate the polarization curve. Tafel analysis is represented in figure 3.10. To execute this analysis the portion linear of the anodic and cathodic branches must be extrapolated till the two lines intersect in the middle. The current density of corrosion can be estimate by using this point (intersection point) where this density is corresponding to the corrosion potential. After obtaining the corrosion current, corrosion rate can be calculated using Equation (3)<sup>51</sup>:

$$CR = \frac{3.27 \times 10^{-3} i_{\text{corr}} \times EW}{D} \quad (3)$$

Where

CR: Corrosion current (mm/y)

$i_{\text{corr}}$ : Corrosion rate ( $\mu\text{A}/\text{cm}^2$ )

EW: Equivalent weight of the specimen (eg. Carbon steel 27.92 g/equivalent)

D: Density of the specimen (eg. Carbon steel 7.87  $\text{g}/\text{cm}^3$ )

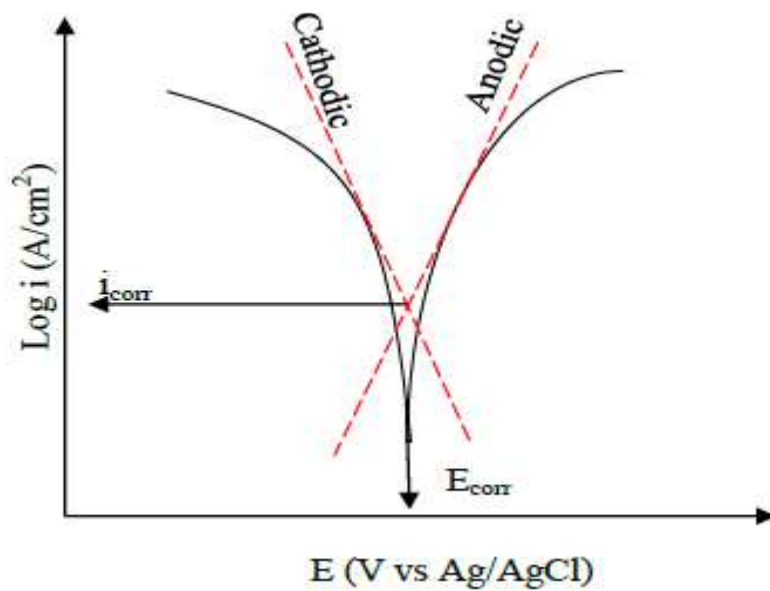


Figure 3.10. Linear Tafel behavior in the anodic and cathodic branches of the polarization curve<sup>51</sup>.

### 3.2.4 Conductivity

This test is important since it will evaluate ion mobility number of charged entity, where increasing the Van der Waals attraction force cause a reduction in the ion mobility. For conductivity measurement, also 20 mL of DESs samples were used and the measurements were conducted at different temperatures. The thermometer and the pro of 3200M Multi-Parameter Analyzer (Agilent Technologies, Inc., USA) with the accuracy  $\pm 5.2 \mu\text{scm}^{-1}$  was dipped into the samples. The device is shown in figure 3.11, the thermometer and pro are located behind the device. First switch on the device then click on the measurement button the instrument will read the conductivity at different temperature. Figure 4.6 was plotted using the data obtained from this device.



Figure 3.11. Conductivity measurements instruments.

### 3.2.5 Density

This measurement was performed, since density considered as one of the most important thermos-physical properties where this data can be used for simulation and modeling purpose. the densities measurements were performed at temperature range from 298.15 till 363 k. This measurement done by using an Anton Paar DMA 4500M densimeter, which uses the oscillating U-tube sensor principle. The accuracy for temperature and the density was  $\pm 0.05$  K and  $\pm 0.00005$  g m<sup>-3</sup> respectively. The instrument used for this experiment shown in figure 3.13. This devise has 2 main parts, operation and documentation. Figure 4.6 was provided using Anton Paar DMA 4500M densimeter where it shows the densities data for the different molar ratios that used in this work also the figure shows the data for ChCl/ Glycerol , ChCl/Ethylene glycol<sup>81</sup> and ChCl/LA<sup>131</sup>.



Figure 3.12. Density meter instruments.

### 3.2.6 Contact Angle

In order to be able to characterize the degree of wettability or adhesion of liquid on solid surface, measurement of contact angle becomes an important tool. Sessile drop method was used in order to obtain the contact angle measurements. For this measurement, only ChCl/PAA DES with ratio of 1:2 was characterized because the device can not characterize solid sample, and since only a signal drop will be use therefore using the heat for the solid sample is useless. Therefore DES 1:2 at room temperature was characterized using KRÜSS drop analysis system (Model: DSA25), Germany driven by software “Advance”. The instrument shown in figure 3.14 has the ability to record video and snapshot by installed microscope. The procedure to measure the contact angle is:

1. Chose the proper needle that is suitable for your sample.
2. Run the program of DROPimage Advanced
3. Pmlace the surface that chosen to measure the contact angel on it in the top of the chamber (ake sure it is flat).
4. Adjust the position of the needle so that the bottom of the needle appears about forth of a way down in the live window screen.
5. Adjust the baseline to be horizontal and about just below midpoint in the live window screen.
6. Carefully apply one drop of the sample onto the solid surface.
7. In the main bar click on measure then click on take picture.
8. Click on CA tools and then on contact angel to open the contact angel tool.
9. Adjust the green vertical line by simply clicking on the window screen to the lift of the drop. Make sure it is not touching the drop but that there is a small space between the line

and the drop. The yellow line should already be positioned to the right of the drop where it is not touching it on the wall of the application window.

10. In the contact angle window click on measure.

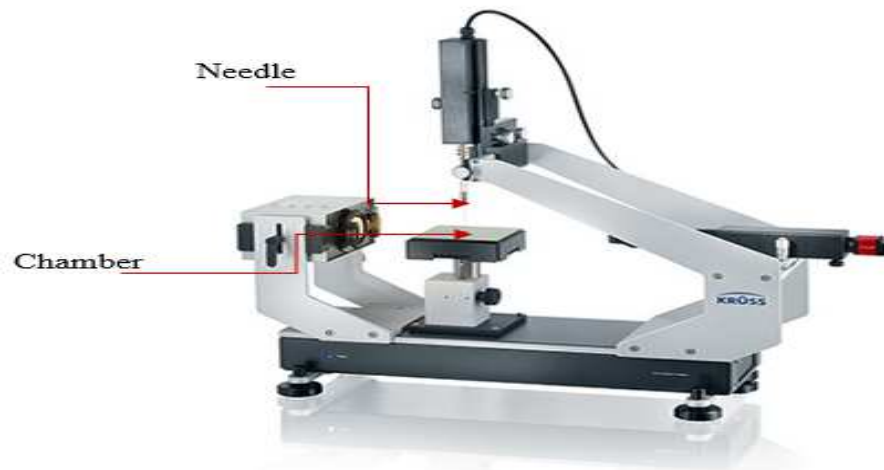


Figure 3.13. KRÜSS drop analysis system<sup>136</sup>.

### 3.2.7 CO<sub>2</sub> and N<sub>2</sub> Solubility Measurements

High magnetic sorption apparatus (MSA) of Rubotherm präzisions messtechnik GmbH, Germany used to obtain the solubility of CO<sub>2</sub> and N<sub>2</sub> gas. This apparatus (MSA) was demined up to 303 K and 350 bars. The MSA device has two main operation positions where they are different from each other. First step start with filling the cell of measurement with CO<sub>2</sub> or N<sub>2</sub> gases and then the MSA will start records the sample weight change that is inside in the sample container as the sample absorbed the high-pressure gas. The Next position is used to measure the in-situ density of the high-pressure gas, where this data needed to calculate the amount of gas that adsorbed by the sample. In this work, pressure up to 30 bars is used at three different isotherm<sup>131</sup>. The details of



the experimental findings of these measurements are provided in results and discussion section of this thesis and the detailed procedure is stated in the appendix. Figure 3.14 shows the devise that used for this purpose.



Figure 3.14. MSA instrument.

Operating principle, procedures, data correlation of the magnetic suspension force transmission and calibrations of overall instrument have been already explained in our previous works elsewhere<sup>131,137</sup> The density measurement works on Archimedes' buoyancy principle by utilizing a calibrated silicon sinker placed just above the sample basket in the pressure cell. A volume of 4.4474 cm<sup>3</sup> silicon sinker was used to measure at 20 °C with a 0.0015 cm<sup>3</sup> uncertainty and a density of 4508 kg m<sup>-3</sup> measured at 293.15 K with a 4kgm<sup>-3</sup> uncertainty. Pressure transducers

(Paroscientific, USA) have accuracy of 0.01% in full scale and they were connected to MSA to monitor experimental pressures with an uncertainty of  $\pm 0.05\%$  from vacuum to 350 bars. The temperature sensor that was used has an accuracy of  $\pm 0.5$  K and was provided by Minco PRT, USA.

## 4 . RESULTS AND DISCUSSIONS

### 4.1 FTIR of DESs

The purpose of using FTIR characterization was to obtain information about complexation and interaction between prepared ChCl/PAA based DES systems. This characterization has been done for pure ChCl, pure PAA and their mixture with different molar ratio as it shown figures 4.1 to 4.3 respectively. FTIR spectra of pure PAA (figure 4.1) is characterized by vibrational bands at around  $3032\text{ cm}^{-1}$ , which is indicate that hydroxyl group (OH) is present in this chemical, and absorbance band at  $1691\text{ cm}^{-1}$ , which shows the presence of ketone (C=O). While the absorption peaks appear at  $1076$  and  $1028\text{ cm}^{-1}$ , and this indicate presence of the benzene ring and the carbon-oxygen bond of the acid grouping. Therefore, the existence of this groups in the FTIR spectrum confirms that this chemical it's PAA.

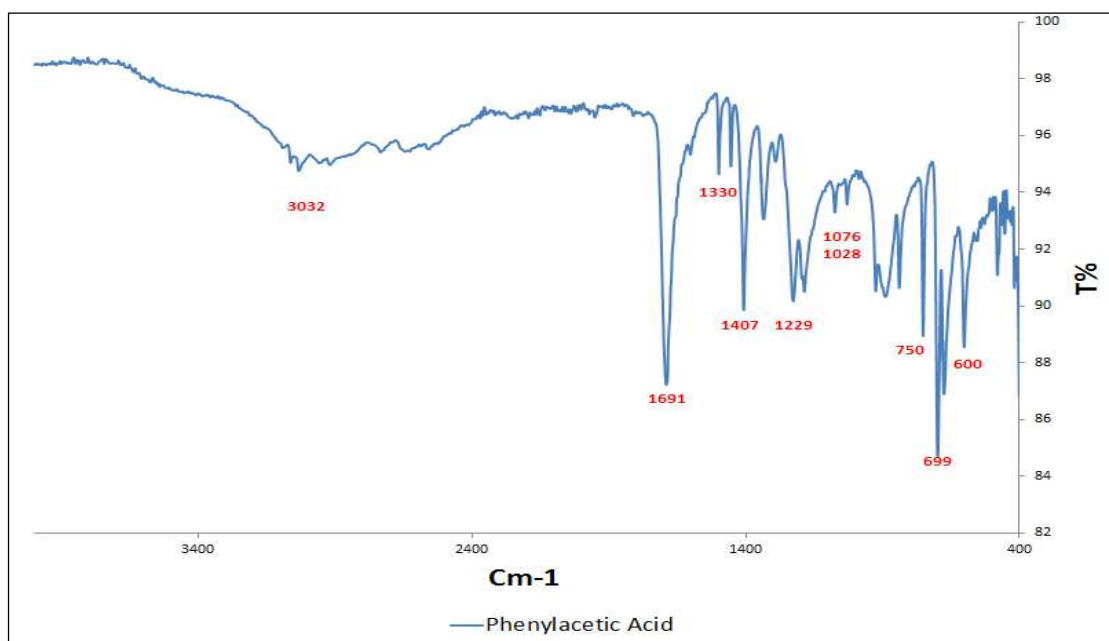


Figure 4.1. FTIR spectra of PAA.

The same analysis was carried for pure ChCl. The FTIR spectra of pure ChCl is shown in figure 4.2, it is characterized by a broad vibrational band that extends from 3500 to 3200  $\text{cm}^{-1}$  referring to the presence of hydroxyl (OH) or amino group (N-H), while those bands 3015-2882  $\text{cm}^{-1}$  and 1482-1417  $\text{cm}^{-1}$  refer to the presence of an alkyl group (C-H).

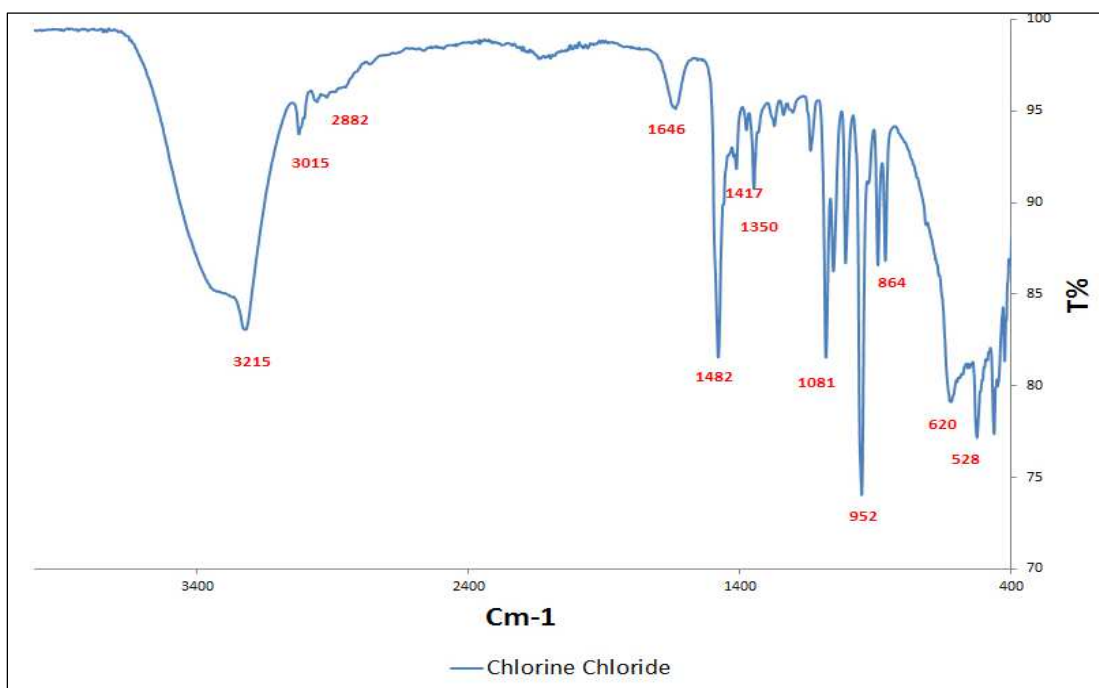


Figure 4.2. FTIR spectra of pure ChCl.

As it mentioned before, mixture of ChCl and PAA produce the reported DES system. This mixture with molar ratio of 1:2, 1:3 and 1:4 also characterized using FTIR as shown in figure 4.3. The vibrational bands at 3031-2891  $\text{cm}^{-1}$  and 1496-1370  $\text{cm}^{-1}$  indicate the presence of alkyl group (C-H). While vibrational bands at 1496-145  $\text{cm}^{-1}$ , 130  $\text{cm}^{-1}$  and 1230-1158  $\text{cm}^{-1}$  represent the aliphatic ketone group (C-O). Carbonyl group (C=O) is represented by 1720 $\text{cm}^{-1}$ . This spectrum

gives collective characteristics of ChCl and PAA, where it shows that during the reaction the hydrogen bond occur. Furthermore, the three-molar ratios of DESs systems showed almost similar and overlapped FTIR spectra. Comparing the functional group stretching bands of other works<sup>16,138,78</sup> with results of this work for ChCl/PAA DES FTIR spectra it showed good agreement.

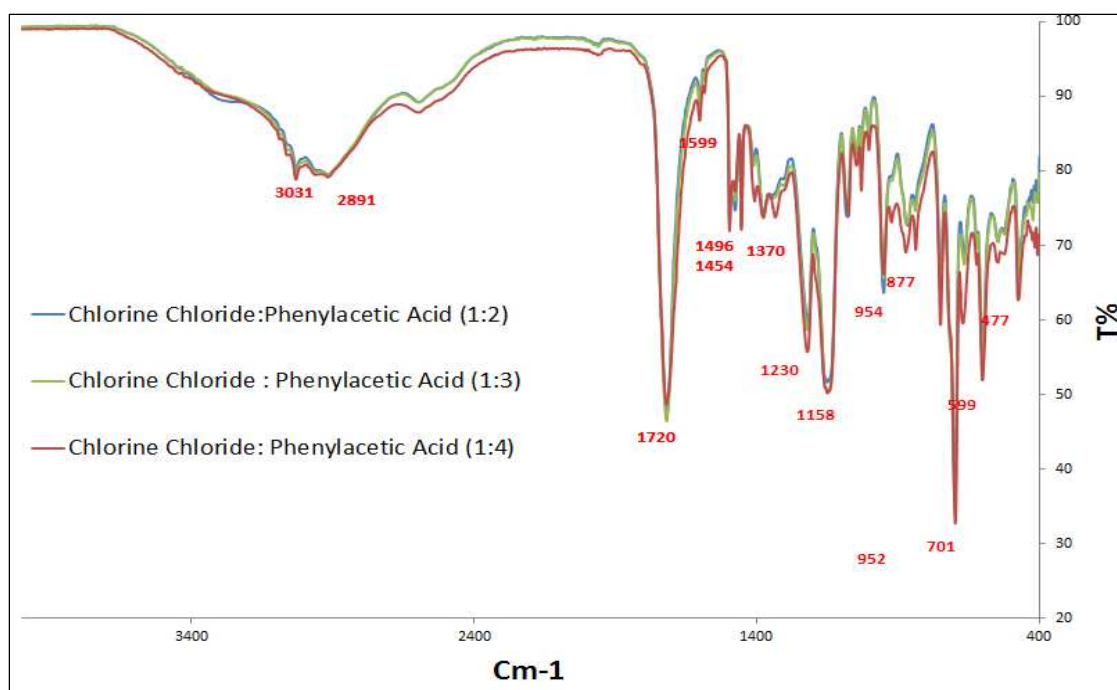


Figure 4.3. FTIR spectra of 1:2, 1:3 and 1:4 molar ratio of ChCl/PAA DES.

## 4.2 TGA of DESs

The aim behind using the TGA experiment was to check two essential temperatures, which are the decomposition temperature ( $T_d$ ) and onset temperature ( $T_{\text{onset}}$ ) for each molar ratio of synthesized DES; in other word to identify the temperature limitation of the absorbent. Figure 4.4 shows weight percent loss for each DES. The three systems of ChCl/PAA based have almost

similar  $T_{\text{onset}}$  where it is in the range of 373.15 K, while the  $T_d$  found to be closed to 473.15 K; but close observation indicate that the  $T_d$  of 1:2 molar ratio is 463.15 K whereas for 1:3 molar ratio is 473.15 and for 1:4 molar ratio is 468.15 K. Consequently, it is obvious that the DESs are stable if the temperature is less than 463.15 K because at higher temperature materials will start to decompose so is not advisable to use this material higher than 473.15 K. Moreover, from figure 4.4 it is clear that adding more PAA (acid ratio) did not have much change on the both temperatures ( $T_{\text{onset}}$  and  $T_d$ ). Therefore, the synthesized DESs are appropriate for post combustion  $\text{CO}_2$  capture process conditions.

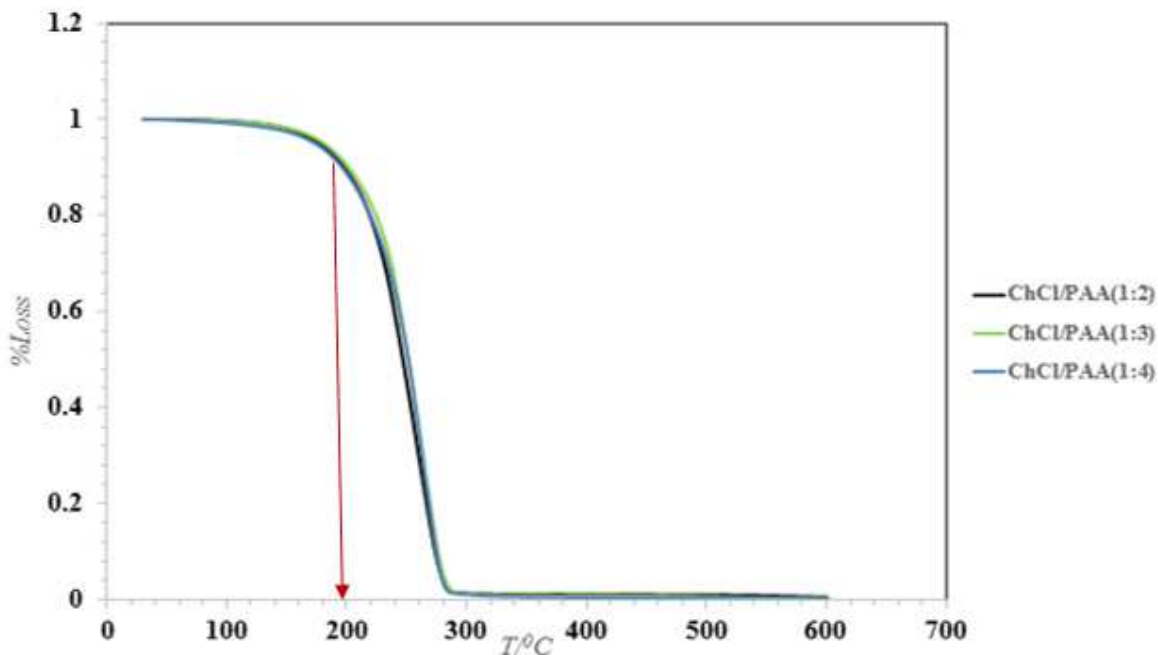


Figure 4.4. TGA Curve for ChCl/PAA DES (1:2, 1:3 and 1:4).

### 4.3 Corrosive Behavior of DESs

Before perform any materials (traditional or new) in industrial or commercial process it is important to know the properties of those materials such as chemical and physical properties. Therefore, it is necessary to check all the properties of the new DES (ChCl/PAA) one by one, also it is essential to understand the corrosivity limitation of this chemical, since a serious danger can be occur because of corrosion, such as corrosion for vessels, corrosion for metallic pipes and for other assemblies where they are in direct contact with the material. Polarization values gives information on the stability of the metal in the corrosive environment. The ChCh/PAA based DESs that have been prepared are targeted for capturing the CO<sub>2</sub> and since the corrosive rate increase by CO<sub>2</sub> saturated DESs, thus the experiments were carried with and without CO<sub>2</sub> saturated DESs. The temperatures for the test were selected based on the melting point of each molar ration in order to understand the behavior of corrosivity. Therefore, for the first molar ratio (1:2) where it is liquid at room temperature so it measured at 298.15 K , however the other ratios (1:3) and (1:4) are solid at room temperature so to bring them to the liquid condition and measure them they heated up to 318.15 and 329.15 K, respectively. The current density for the three molar ratios as a function of potential is shown in figure 4.5. At the mentioned temperatures, also carbon steel used to assess the corrosion behavior, the curves show the corrosion potentials for ChCl/PAA (1:2), (1:3) and (1:4) to be -0.633 (Figure 4.5 (a)), -0.511 (Figure 4.5(b)) and -0.521 (Figure 4.5(c)) volt where the values for corrosion rate were 0.0224, 0.118 and 0.278 mm/y respectively. For CO<sub>2</sub>, saturated DES, the corrosion rate found to be 0.044 (Figure 4.5 (a)), 0.267(Figure 4.5(b)), and 0.916 (Figure 4.5(c)) mm per year while the corrosion potentials appear -0.490, -0.493 and -0.488 volt with respect to above mentioned DESs. These informations also summarized in table 4.1. Comparison between the three DESs cannot be done since they have different melting point temperature.

However CO<sub>2</sub> loaded ChCl/PAA (1:2) of this work can be compared with other published data reported by Ullah et al<sup>16</sup> on ChCl/Levulinic acid (ChCl/Lev) with the same molar ratio (1:2) and monoethanolamine (MEA) system at temperature of 298.15 K. The corrosion rate for ChCl/Lev reported by Ullah et al was 0.027 mm /year and the potential -0.43 volts where it was 0.540 mm/year at potential -0.750 volts for MEA. From the results, it is obvious that the ChCl/PAA (1:2) reported in this work was not better than the other published data, however it has lower corrosion rate than the previous reported MEA loaded CO<sub>2</sub> samples. The literatures<sup>139</sup> shows that with increasing the concentration of CO<sub>2</sub> (acidity) or temperature, this lead to increase current density and thus increase the corrosion rate. In 2014 Abbott et al<sup>78</sup> published the corrosion behavior for four pure DES named as Glyceline, Ethaline, Reline and Oxaline with mild steel , the rate of corrosion were appear 0.0004, 0.00198, 0.002503 and 0.1764 mm per year, respectively. According to this study the DES can have very low corrosivity so the results encourage working more in this area. Table 4.1 summarized the corrosion rates of this work, previous work with ChCl/LA and the resent published data for the most common amine type.

Table 4.1. Corrosion rate of DES systems and amine.

Molar Ratio	T/K	Corrosion Rate /(mm/yr)	Amine type	T/K	Corrosion Rate /(mm/yr)	Ref
ChCl/PAA(1:2)	298	0.044	*MEA	353.15	3.41	*95
ChCl/PAA(1:3)	318	0.267	*DEA		2.45	
ChCl/PAA(1:4)	329	0.916	*MDEA		1.25	
**ChCl/LA(1:2)	298	0.027	**MEA	298	0.540	131



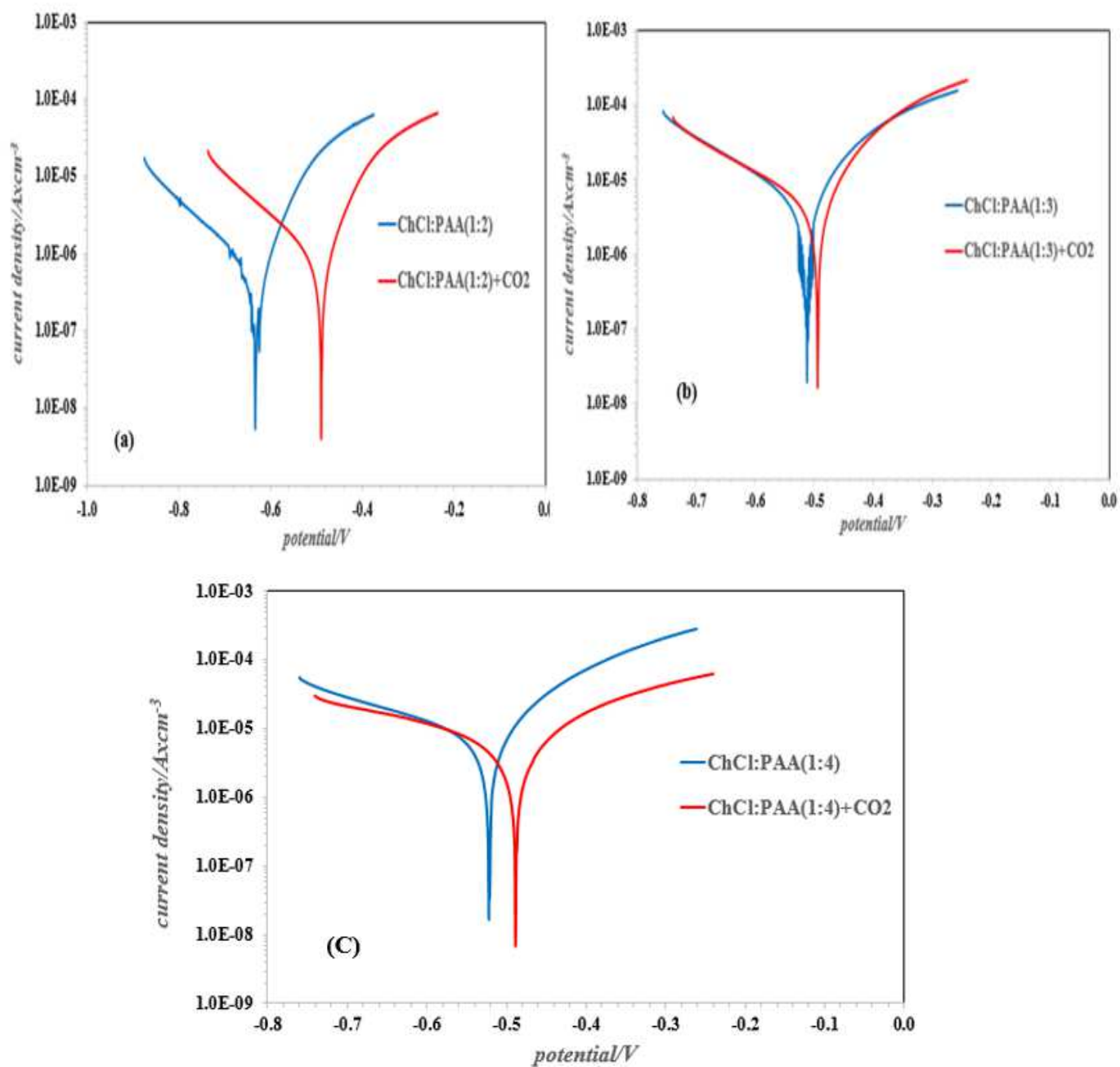


Figure 4.5. Corrosion resistance performance experiments for (a) ChCl:PAA(1:2), (b) ChCl:PAA(1:3) and (c) ChCl:PAA(1:4) DES system with and without  $\text{CO}_2$ .

Table 4.2. Corrosion Test Experiments for DES mixtures of ChCl/PAA at different ratios.

DES Ratio	(1:2)	(1:3)	(1:4)
CO <sub>2</sub> solubility	T/ K= 298.15, 303.15, 318.15	T/ K= 303.15, 318.15, 328.15	T/ K = 328.15, 329.15, 339.15
Corrosive tests	At 298.15	At 318.15	At 339.15
	Without CO <sub>2</sub>		
Potential (V)	-0.633	-0.511	-0.521
Corrosion rate (mm/yr)	0.0224	0.118	0.278
	With CO <sub>2</sub>		
Potential (V)	-0.490	-0.493	-0.488
Corrosion rate (mm/yr)	0.044	0.267	0.916

#### 4.4 Conductivity of DESs

The goal behind carrying the conductivity experiment is to evaluate ion mobility number of charged entity where increasing the Van der Waals attraction force cause a reduction in the ion mobility. Ion mobility will increase in case there is weak interaction and this is close to the viscosity temperature dependence behavior. Therefore, this means that increasing the conductivity lead to increasing the ion mobility, where the conductivity increases with temperature. The same outcomes were found in this work for the conductivity experiments when temperature range from 298.15 K to 340.1 K applied for the three DESs (1:2, 1:3 and 1:4) as it shown in figure 4.6. The results of conductivity for the molar ratio of 1:2, 1:3 and 1:4 at temperatures of 333.15, 340.15, and 330.15 K were 2470, 3560, and 2310  $\mu$  S/cm, respectively. The other values in the mentioned range for the three molar ratios they had the same trend line, and the acid concentration does not have much change in the conductivity results. In compared with Cholinium-amino acid based ionic liquids at different temperatures the DESs in this work have very high conductivity, moreover in

other publication the conductivity of Oxalic acid-Trimethylglycine DES was 5.1 mS / cm, at temperature 303.15 K<sup>140,141,90</sup>.

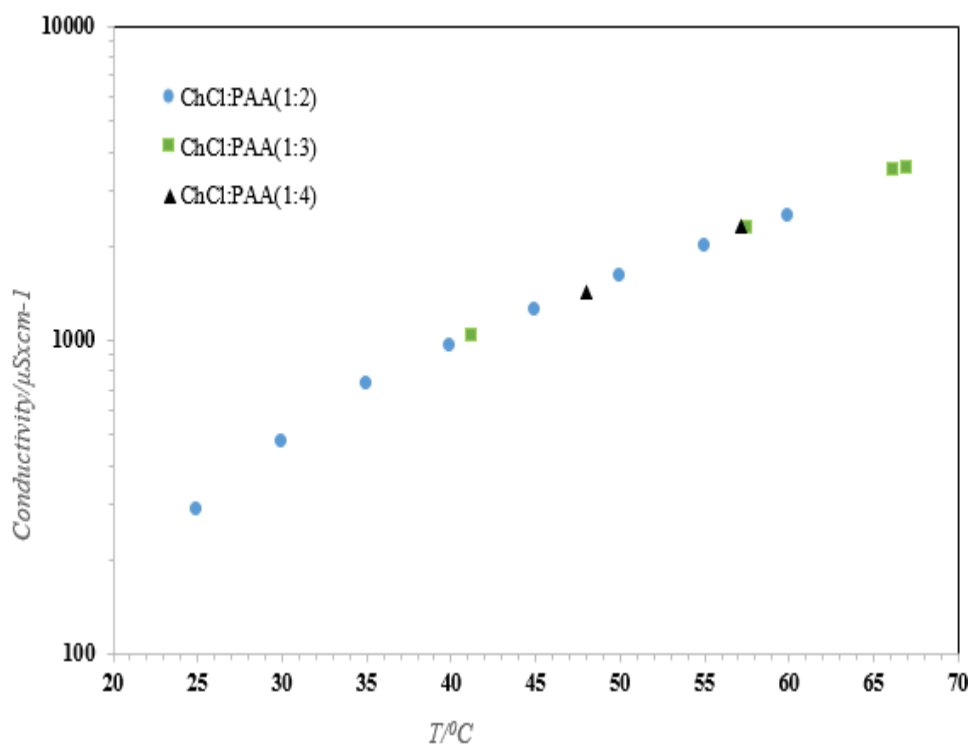


Figure 4.6. Conductivity plot for ChCl/PAA DES (1:2, 1:3 and 1:4) at temperature range of 298.15 K to 340.15 K.

## 4.5 Density

This measurement was performed, since density is considered as one of the most important thermophysical properties where this data can be used for simulation and modeling purposes. Densities of prepared DESs 1:2, 1:3 and 1:4 molar ratios measured at 293.15, 308.15 and 323.15 K respectively up to temperature of 363.15 K. Densities of ChCl/PAA based DESs (1:2, 1:3 and

1:4) appear to be 1.144, 1.138 and 1.127 g cm<sup>-3</sup> at temperature 298.15 K, 303.15 K and 323.15 K respectively. At temperature 298.15 K Abbott et al<sup>78</sup> and Leron et al<sup>77</sup> studied the density of ChCl/urea DES system at ratio of 1:2 and it's appear to be 1.1979 and 1.20 g cm<sup>-3</sup> where it is close to density of ChCL/PAA DES system at the same ratio. Density of malonic acid reported by Zhang et al<sup>74</sup> at temperature 303.15 was 1.0063 g cm<sup>-3</sup>.

All the densities at mentioned temperatures for ChCl/PAA DES system is shown in figure 4.7 , the densities sharply and linearly decrease by increasing the temperature where the same trend was absorbed for ChCl/Lev based DES<sup>16</sup>. Figure 4.7 shows an interesting comparison between DESs, where the density for the molar ratio of 1:3 and 1:2 are very close to each other while the other ratio 1:4 noticed to be away from the others, which means that with 1:3 and 1:2 molar ratios the interaction between the molecules are similar to each other than 1:4 molar ratio. Moreover, figure 4.7 shows results for other published stuiedid that they investigated the density over rang of temperatures where it shows that densities of this work are realistic.

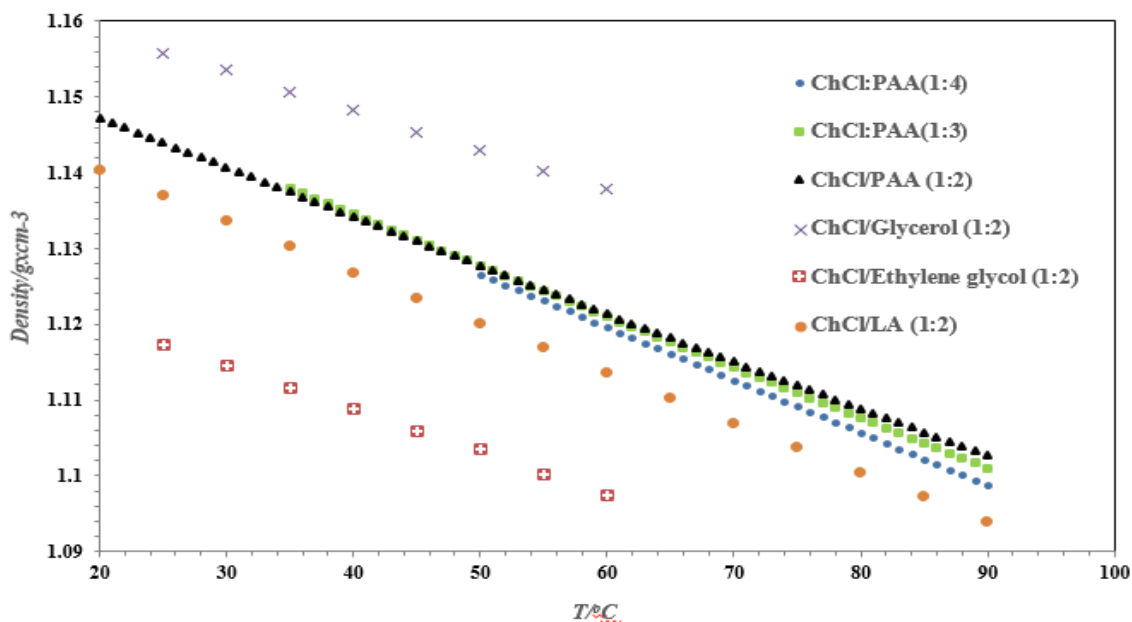


Figure 4.7. Density of ChCl:PAA system with ratio of 1:2,1:3,1:4 and ChCl/Glycerol and Ethylene glycol.

## 4.6 CO<sub>2</sub> Solubility of DES

The solubility of CO<sub>2</sub>/N<sub>2</sub> was investigated using magnetic suspension based MSA, details producer of using this device mentioned in the appendix. The solubility was measured at given temperature and pressure, then the amount of absorbed CO<sub>2</sub> and N<sub>2</sub> was calculated. The experiment was carried using accurate data from MS device where it was able to measure high temperature and pressure with accuracy of +/-0.5 K and 0.1% respectively. The values of in-situ density for CO<sub>2</sub> also was measured, since it is required for calculating the absorbed amount of CO<sub>2</sub>. The temperature and pressure selection of the solubility experiments are selected to suit more on the post combustion CO<sub>2</sub> capture conditions. However, the selected isotherms for the solubility experiments are lower than the classical post-combustion CO<sub>2</sub> capture conditions, simply by

considering heat integration and optimization is implemented in order to recover the waste heat in the process, thus leaving the CO<sub>2</sub> stream at lower temperatures.

ChCl/PAA based DESs with three different molar ratios (1:2, 1:3 and 1:4) were used to test the solubility of CO<sub>2</sub> and N<sub>2</sub>. The solubility of these two gases (CO<sub>2</sub>/N<sub>2</sub>) with prepared DESs were measured up to pressure of 30 bars at different intervals and at three different isotherms. At the first observation of figures 4.8 and 4.9 it's notice that by increasing the gas pressure the solubility of CO<sub>2</sub> and N<sub>2</sub> gas increase, while figure 4.10 shows that the solubility decrease with increasing the temperature of DESs.

Regards to the first molar ratio (1:2) of ChCl/PAA DES, it's found that at 30 bars it absorbed 2.12, 2.10 and 1.99 mmol/g of CO<sub>2</sub>, and 3.50, 3.30 and 3.1 mmol /g of N<sub>2</sub> at temperature 298.15, 308.15 and 318.15 K, respectively. While the DES with molar ratio of 1:3 absorbed 3.35, 3.22 and 3.05 mmol/g of CO<sub>2</sub> where it absorbs 3.20, 3.17 and 3.07 mmol/g of N<sub>2</sub> at temperature 308.15, 318.15, and 328.15 K respectively. ChCl/PAA with 1:4 molar ratio absorbed 2.50, 1.76 and 1.75 mmol/ g of CO<sub>2</sub> while for N<sub>2</sub> gas its absorbed 3.11, 1.84 and 1.80 mmol/g at temperature 323.15, 329.15 and 339.15 K respectively. It is obvious from the results that this DESs absorbed higher N<sub>2</sub> gas than the CO<sub>2</sub> where it gives an unusual but at the same time interesting outcome where it is useful for gas selectivity, since the solubility of CO<sub>2</sub> in ILs is higher than N<sub>2</sub> or other gases <sup>142</sup>.

The only comparison that can be done is between ChCl/PAA 1:2 and ChCh/PAA 1:3, where it found that at temperature 308.15 and 318 .15 K the adsorption capacity of CO<sub>2</sub> and N<sub>2</sub> is higher at molar ratio of 1:3 than 1:2. Furthermore, it's noticed that for ChCl/PAA 1:3 and 1:4 at temperature 328.15 and 329.15 K respectively (only one degree kelvin is difference) there is sharp

difference in the solubility of CO<sub>2</sub> and N<sub>2</sub>. From the results, it can conclude that the intake efficiency of CO<sub>2</sub> with this system as follow:

- ChCl/PAA at molar ratio of 1:3 > molar ratio of 1:2.
- At temperature 325.15 K molar ratio of 1:3 > 1:4 molar ratio at 329.15 K.

These results can be compared with other published DES system where some of them mentioned in section 2 (table 2.7). In section 2 three different DES with molar ratios of 1:2 are shown in table 2.7. These systems are: ChCl/urea<sup>132</sup>, ChCl/ethylene glycol<sup>133</sup> and ChCl/LA<sup>16</sup>. ChCl/urea system absorbed 3.559 mmol/g of CO<sub>2</sub> at 303.15 K and 60 bar, while ChCl/ethylene glycol absorbed 3.1265 mmol/g of CO<sub>2</sub> at 303.15 K and 58.63 bars, however the last system (ChCl/LA) at 308.15 K and 30 bar absorbed 2.100 mmol/g of CO<sub>2</sub>. These results can be compared with 1:2 molar ratio at temperature of 308.15 K and pressure of 30 bars where the DES 1:2 that reported in this work absorbed 2.10 mmol/g of CO<sub>2</sub> where it is similar to ChCl/LV system. Moreover, the reported systems in this work (1:2, 1:3 and 1:4) at 30 bars and different isotherms absorbed more CO<sub>2</sub> than 1-ethyl-3-methylimidazolium tetrafluoroborate [EMIM][BF<sub>4</sub>]<sup>143</sup> based ionic liquid where [EMIM][BF<sub>4</sub>] absorbed 1.5999 mmol/g of CO<sub>2</sub> at 298.15 K and 41.55 bars. Furthermore, the DES (1:2) at 298.15 K and 30 bars absorbed more CO<sub>2</sub> than 1-methoxyethyl-3-methylimidazolium hexafluoroborate ([EOMmim][PF<sub>6</sub>])<sup>144</sup> at the same temperature and 27.88 bars where [EOMmim][PF<sub>6</sub>] absorbed 1.7575 mol/kg of CO<sub>2</sub>. The same observation was noticed with 1:3 molar ratio of reported DES where it absorbed 2.50 mmol/g of CO<sub>2</sub> at 323.15 K and 30 bars, while [EOMmim][PF<sub>6</sub>] absorbed 1.1243 mol/kg of CO<sub>2</sub> at the same temperature and pressure of 28.71 bars.

In compared this system with amine based it's found that DES (1:4) at 323.5 K and 4.94 bar absorbed 0.306 mmol/g of CO<sub>2</sub> while fatty amine polyoxyethylene ethers (FAPEs)<sup>145</sup> at the

same conditions ( $T=323.15$  K and 4.94 bars) absorbed 0.174 mol/kg of  $\text{CO}_2$ . Furthermore, at pressure 4.94 bars and temperature of 308.15 K, DES absorbed 0.536 mmol/g of  $\text{CO}_2$  whereas the FAPEs at higher pressure and temperature ( $T=313$  K and  $P=5.069$  bars) absorbed 0.224 mol/kg. DES (1:3) system at maximum pressure of 30 bars and 308.15 K absorbed 3.35 mmol/g of  $\text{CO}_2$ , while solid amine sorbent, consisting of poly (ethylenimine) (PEI) <sup>146</sup> absorbed 2.8 mol/kg of  $\text{CO}_2$  at 353.15 K and partial pressures more than 10kPa (0.1 bar). Moreover, in compared with the most known amine in industry MEA, DES (1:3) at 30 bars and 308 K absorbed 3.35 mmol/g  $\text{CO}_2$  while MEA at 24 bar and 313 K absorbed 2.66 mmol/g  $\text{CO}_2$  <sup>147</sup>. The above-mentioned comparison are summarized in table 4.3

It is important to mention here that sorption hysteresis was also checked by conducting absorption / desorption cycle during conducting gas solubility experiments. Neither hysteresis nor chemisorption was observed during the sorption measurements and this is shown in figures 4.8 and 4.9 where we start with 0 pressure and 0 absorption and we got back to the same point of 0 pressure and 0 absorption., also the weight measurements provided the same path during both absorption and desorption cycles. in this work, we are going to high pressure to be able to compete with current -state -of the art amine solvents. High pressure also means energy and this is something to benchmark, this is something to consider economic visibility point of view. Moreover, every experiment was measured at mentioned temperatures for three times and there was no notable degradation or absorption activity loss observed of DESs.

On the other hand, the kinetics of the absorption on DES system (chcl/PAA) has been investigated. Figure 4.11 shows the amount of absorbed  $\text{CO}_2$  in DES system with time at both low and high pressures. At 1 bar pressures average of 7 minutes were required reaching the equilibrium



for a fully saturated DES solution. Whereas at 30 bars, 8 minutes passed to reach the equilibrium conditions.

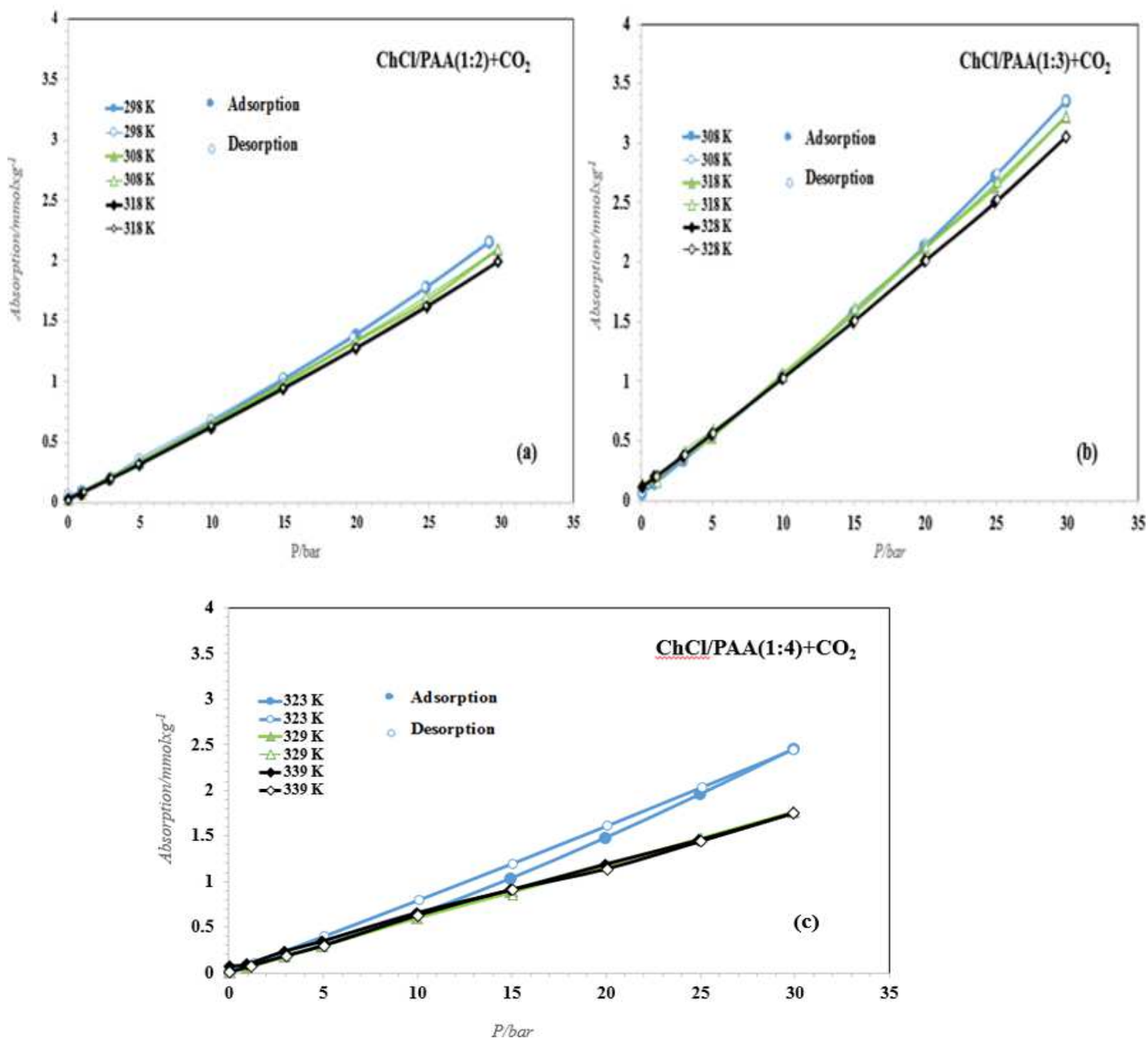


Figure 4.8. CO<sub>2</sub> solubility of ChCl/PAA DESs (a) 1:2 (b) 1:3 and (c) 1:4 molar ratio.

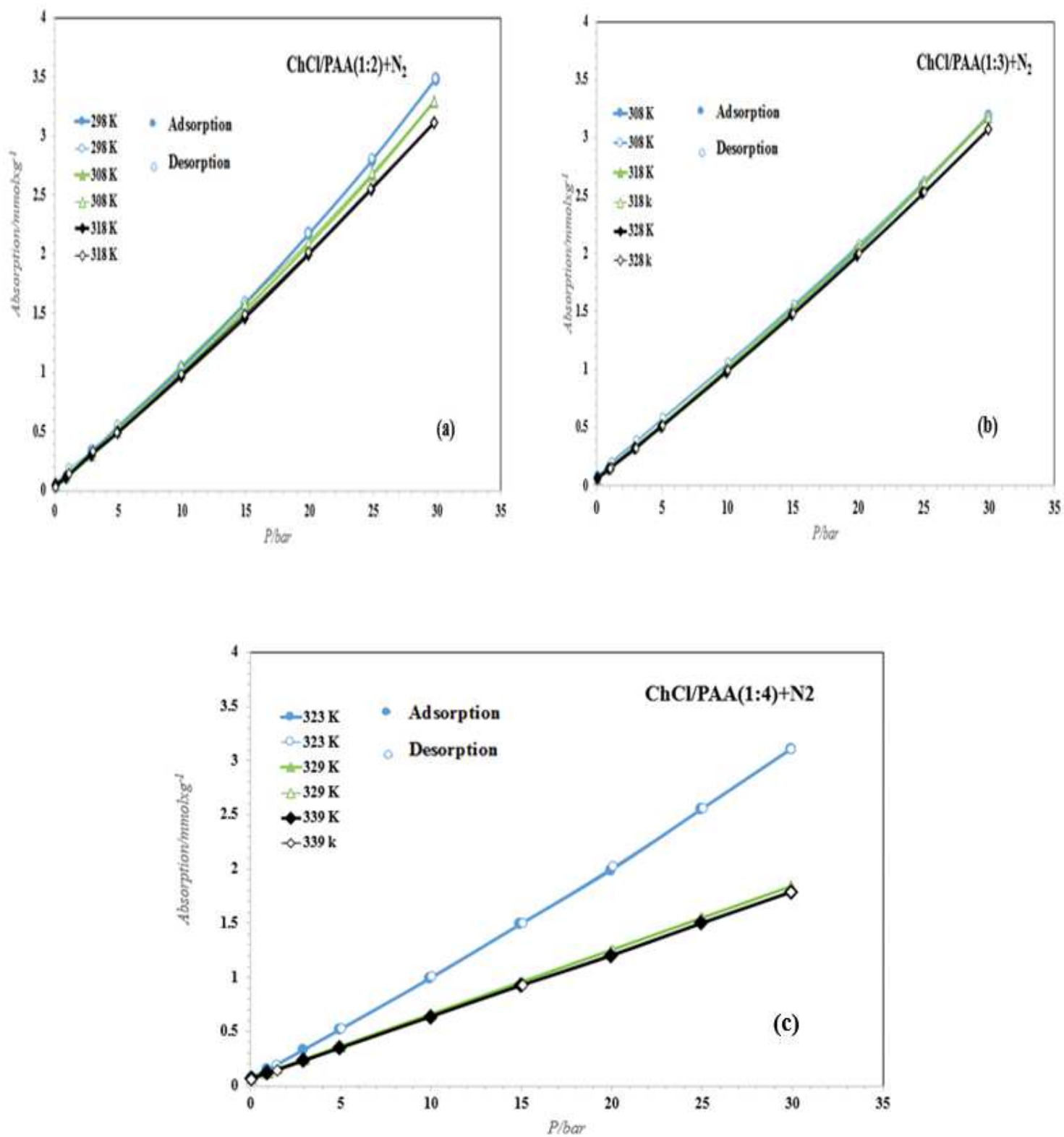


Figure 4.9.  $N_2$  solubility of ChCl/PAA DESs (a) 1:2 (b) 1:3 (c) 1:4 molar ratio.

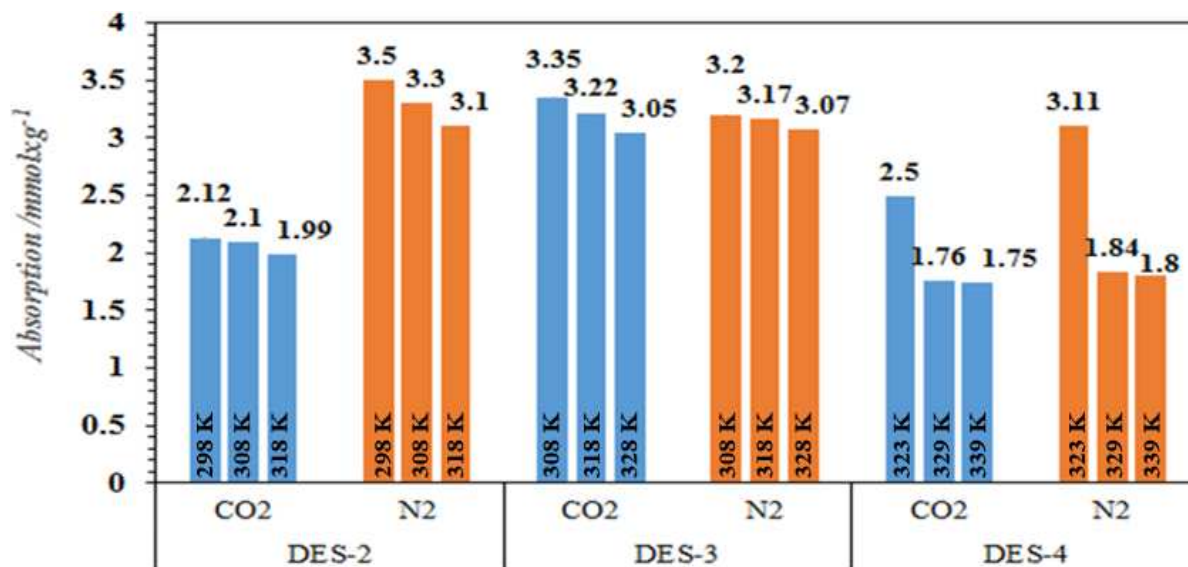


Figure 4.10. Column chart represent the absorption for the 3-different systems DES-2 (1:2), DES-3 (1:3), DES-4 (1:4).

Below table (Table 4.3) summarized all the comparison that mentioned in above for DES, IL and amine systems

Table 4.3. Solubility of CO<sub>2</sub> in different systems.

System	Solvents	Molar ratio	Absorbent	Solubility (mmol/g)	T/P (k/b)	Ref.
DES	ChCl/PAA	1:2	CO <sub>2</sub>	2.12	298.15/30	-
	ChCl/PAA	1:3		3.35	308.15/30	-
	ChCl/PAA	1:4		2.50	323.15/30	-
	ChCl/urea	1:2		3.559	303.15/60	132
	ChCl/ethylene glycol	1:2		3.1265	303.15/58.63	133
	ChCl/ LA	1:2		2.100	298.15/30	131
IL	[EMIM][BF <sub>4</sub> ]	-		1.5999	298.15/41.55	143
	[EOMmim][PF <sub>6</sub> ]	-		1.7575	298.15/27.88	144
amine	PEI	-		2.8	353.15/0.1	146
	MEA	-		2.66	313.15/24	147

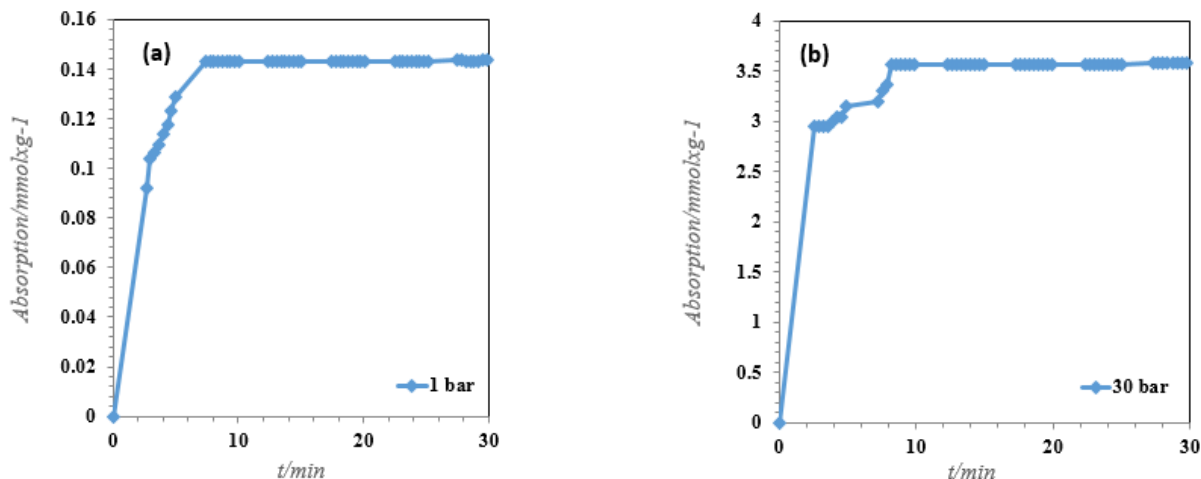


Figure 4.11. Isobaric CO<sub>2</sub> solubility in ChCl/PAA kinetics: (a) 1 bar and (b) 30 bar.

## 4.7 Contact Angle

In order to be able to characterize the degree of wettability or adhesion of liquid on solid surface, measurement of contact angle become an important tool. When the liquid sample become in contact with the solid surface this gives an angel and the wetting ability of the sample appear due to that. The interaction of intermolecular among the phases determine the contact angle, where the high wettability indicate that the contact angle is small and when the wettability is high that mean the contact angle is large. Numerous of studies<sup>148,149,150</sup> have been done on the contact angle of ILs, in order to investigate the wetting ability of ILs on different solid materials. ILs have low contact angle when it became in contact polar surface due to hydrogen bonding acceptability, therefore non-polar surface will lead to higher contact angle.

In this work, only ChCl/PAA with 1:2 molar ratio was measured, since measuring the other two ratios is not possible, because they are not at liquid state during the measurements. The ChCl/PAA 1:2 was studied on brass, carbon steel, stainless steel and on copper surfaces at temperature 293.15 K and the results is shown in figure 4.12. The results showed that the contact

angle of DES (1:2) at different solid surface is lower than  $90^{\circ}$  ( $36 < \theta < 56$ ), which means high wettability and the surface consider as hydrophilic, and the liquid can separate on large area of the surface. In comparing these results with ionic liquid that mentioned in section 2.17 it seems that they have nearly similar results where the contact angles of the ionic liquids were also lower than  $90^{\circ}$  ( $9 < \theta < 43$ ), however DES has higher contact angles then the ionic liquids. Furthermore, in the same section the contact angles of membranes with different concentration of amine based mentioned, where in this study Lv et al. state that the contact angles of all the membranes were above  $90^{\circ}$  ( $90 < \theta < 126.1$ ), therefore each one of studied membranes have hydrophobic surface. Consequently, contact angles of DES that reported in this work fall in between where it can be considered as moderate. Table 4.3 summarized the contact angles for the mentioned systems (DES, IL and membrane).

Table 4.4. Contact angles for DES, membrane and IL systems.

System	Contact angle	Contact angles range	Ref
DES	$< 90^{\circ}$	$36 < \theta < 56$	
IL	$< 90^{\circ}$	$9 < \theta < 43$	92
Membrane	$> 90^{\circ}$	$90 < \theta < 126.1$	91,94

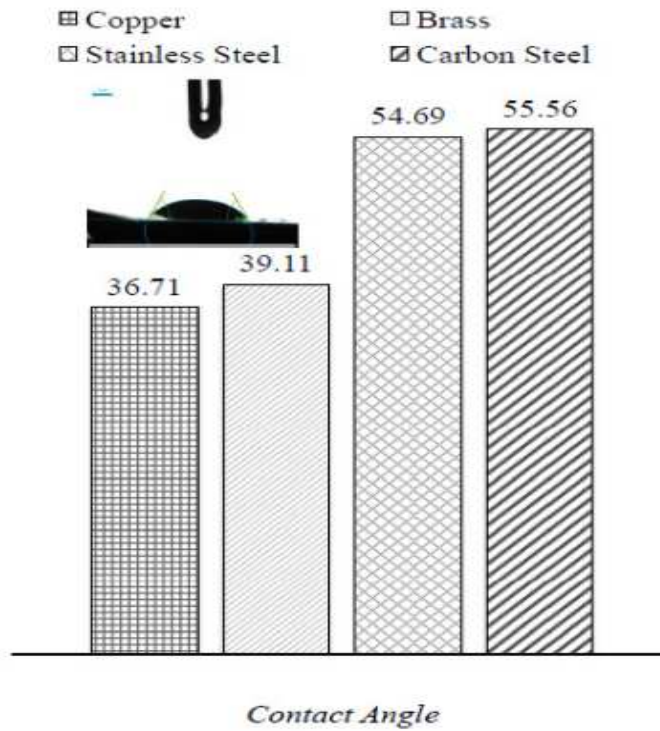


Figure 4.12. Contact Angles of ChCl/PAA (1:2) at different surfaces

## **5 . CONCLUSION AND FUTURE WORK**

### **5.1 Conclusions**

New and different technologies are needed in order to be able to face the problems related to the environment that cause due to processes design, and it should be environmentally friendly method. For the last 50 years, the main concern that motivated the researchers to develop process with zero emission was the globe warming. Therefore, decreasing the amount of CO<sub>2</sub> that emitted to the atmosphere turn into a hot topic for the scientist, because the main reason for greenhouse phenomenon is CO<sub>2</sub>. Capturing the CO<sub>2</sub> from the flue gas in post-combustion method that used by industry or removing this gas (CO<sub>2</sub>) from the natural gas become a significant problem, because CO<sub>2</sub> has large volume and also has low concentration. For the capturing purpose, amine- base absorbent such as DEA, MEA and MDEA are used. However, beside their good advantages they show same drawbacks such as operation cost, degradation and solvent regeneration. Thus, several processes have been suggested like membrane processes, solid adsorption and liquid absorption. Even though these processes were succeeded in industrial processes but the main problems with them are corrosion and energy consumption. Consequently, to solve mentioned problem a new family of IL has been proposed as promising green technology named DES.

The main idea behind this work was to studied characterization of ChCl/PAA based DESs system from the macroscopic viewpoints and check its capability to capture CO<sub>2</sub>. This study intensively focused on finding the physical properties of prepared DESs, as well as the solubility of CO<sub>2</sub> at different range of pressure where the main point of this experimental study was the temperature conditions.

The promising features of prepared DESs have been noticed for gas absorption capacity between two ratios of DES and as well as gas selectivity between CO<sub>2</sub> and N<sub>2</sub>. The amount of CO<sub>2</sub> that absorbed by ChCl/PAA 1:2 and 1:3 DESs at temperature 308.15 K and 30 bar pressure was 2.1 mmol/g and 3.35 mmol/g, at the same conditions these systems absorbed 3.30mmol/g and 3.20 mmol/g N<sub>2</sub> gas respectively. Unfortunately, because of experimental limitation, so with DES 1:4 no comprising can be done for gas (CO<sub>2</sub> or N<sub>2</sub>) solubility at the same temperature. However, the reported systems of DES showed higher CO<sub>2</sub> absorption than [EOMmim][PF<sub>6</sub>] and [EOMmim][PF<sub>6</sub>] ionic liquid based. In comparing with amine based the DES (1:4) at 323.5 K and 4.94 bars absorbed 0.306 mmol/g of CO<sub>2</sub>, while fatty amine polyoxyethylene ethers (FAPEs) at the same conditions (T=323.15 K and 4.94 bars) absorbed 0.174 mol/kg of CO<sub>2</sub>. Moreover, in compared with the most known amine in industry MEA, DES (1:3) at 30 bars and 308 K absorbed 3.35 mmol/g CO<sub>2</sub> while MEA at 24 bars and 313 K absorbed 2.66 mmol/g CO<sub>2</sub><sup>147</sup>

Furthermore, to check the stability of ChCl/PAA DESs system the absorption experiments repeated 4 times for each ratio and the same results were obtained in each time, in other words the sample can be used 4 times and it will give the same adsorption. When a gas dissolves in system like ionic liquid, conformational rearrangements of the ions takes place due this change polar as well as non-polar cavity formed. Thus, polar cavities favor dissolution of CO<sub>2</sub>, whereas nonpolar cavities accommodate both CO<sub>2</sub> and nonpolar gases. From this perspective, it is highly possible that ChCl/PAA system favors more to accommodate N<sub>2</sub> molecules.

Moreover, the corrosivity study shows that with CO<sub>2</sub> saturated DES the corrosion rate of ChCl/PAA 1:2, 1:3 and 1:4 is 0.044, 0.267, and 0.916 mm/yr respectively, while for CO<sub>2</sub> saturated MEA system the corrosion rate was 0.54 mm/yr.



The process of CO<sub>2</sub> absorption is characterized by a very minor volume expansion, confirming the ability of the fluid to rearrange its structuring without weakening hydrogen bond acceptor – hydrogen bond donor intermolecular interactions. The CO<sub>2</sub> capturing mechanism, which was studied in this work, can be characterized by a two steps process in which the development of water, CO<sub>2</sub> and nitrogen layers is the main step. It is quite possible that adsorbed water layers in the inner regions of the solvent – gas interface is could slow the CO<sub>2</sub> diffusion toward bulk liquid regions in the solvent, and should be considered in the design of CO<sub>2</sub> capturing operations using the studied DES.

## 5.2 Future Work

In a journey to find new sorts of green solvents, scientists come with ILs and DESs. ILs was the first invention and because of their low melting point also low vapour pressure under ambient conditions they become very popular. Nevertheless, the idea that these solvents are green is not true because several of ILs are toxic to the human and environmental. Therefore the next class of ILs are DESs ; DES and IL solvents share many solvation properties<sup>60</sup>. Moreover, DESs have others advantages such as; non-toxic, biodegradable, does not react with water and low flammability. Consequently, with all this benefits DESs can be considers as environmental-friendly solvents, however they have some limitation where most of DESs are solid at room temperature.

In order to solve the synthetic problem and to increase the candidates for ILs and DES and extend their applications, scientists find natural products such as organic acids<sup>151</sup>, amino acids<sup>152</sup>,<sup>153</sup>, sugars ,choline<sup>151</sup> and urea. In fact the natural products are plentiful and ideal source of DES and IL because of their massive chemical diversity, biodegradable properties, pharmaceutically acceptable toxicity profile and sustainability<sup>45</sup>. Therefor the natural deep eutectic solvent (NADES)

proposed as alternative, where it appear as a new generation of IL. Basically, the new solvent is a mixture of inexpensive and easily available components that is non-toxic ammonium salts and naturally-derived uncharged HBD.NADESs have many benefits that respect the environmental such as easily available components, inexpensive, easy to prepare, sustainability and low toxicity profile. Moreover, NADESs have perfect physicochemical properties including negligible volatility, even at temperature below 273.15 K they have liquid state, modifiable viscosity, a wide polar range and a high degree of solubilisation strength for different compounds. These solvents have several possible structures and for different object they can redesign physicochemical properties, thus they can consider as designer solvents<sup>154</sup>. Yuntao Dai et al<sup>45</sup> characterized and check the solubility for 100 different combination of NADESs some of this combination are shown in table 5.1.

Moreover, the utilization of DES towards the acid gas removal for gas streams that includes sulphur compounds (e.g. H<sub>2</sub>S or mercaptans) shall also be studied since the hydrogen bonding development will be superior with Sulphur containing gas streams and hydrogen bond acceptors in DES or NADES solvents. On the other hand, the utilization of DES systems might allow the process facilities to adopt these low volatile physical solvents with no or minimum process retrofitting requirements for already existing acid gas removal systems consist of absorber and regeneration columns. For this purpose, a thorough study on process system analysis and process simulations needs to be carried out with process simulator software (e.g. ASPEN/HYSYS) in order to be able to benchmark the DESs against the current state of the art physical (or chemical) solvents.

Table 5.1. Different combinations of DESs from natural products<sup>45</sup>.

Components		Molar ratio
Component 1	Component 2	
ChCl	Lactic acid	1:1
	Malonic acid	1:1
	Maleic acid	1:1, 2:1
	Citric acid	1:1, 2:1
	Aconitic acid	1:1
	Raffinose	11:2
	Sucrose	2:1
Betaine	d-(+)-Trehalose	4:1
	dl-Malic acid	1:1
	Citric acid	1:1
Citric acid	Raffinose	3:1
	d-Sorbitol	1:1
	Ribitol	1:1

## 6 . REFERENCES

1. Lu, M.; Han, G.; Jiang, Y.; Zhang, X.; Deng, D.; Ai, N., Solubilities of carbon dioxide in the eutectic mixture of levulinic acid (or furfuryl alcohol) and choline chloride. *The Journal of Chemical Thermodynamics* **2015**, *88*, 72-77.
2. Lindstad, H.; Asbjørnslett, B. E.; Strømman, A. H., Reductions in greenhouse gas emissions and cost by shipping at lower speeds. *Energy Policy* **2011**, *39* (6), 3456-3464.
3. Kysely, J.; Picek, J.; Beranová, R., Estimating extremes in climate change simulations using the peaks-over-threshold method with a non-stationary threshold. *Global and Planetary Change* **2010**, *72* (1–2), 55-68.
4. Sari, R.; Soytaş, U., Are global warming and economic growth compatible? Evidence from five OPEC countries? *Applied Energy* **2009**, *86* (10), 1887-1893.
5. Adetutu, M. O., Energy efficiency and capital-energy substitutability: Evidence from four OPEC countries. *Applied Energy* **2014**, *119*, 363-370.
6. Chiroma, H.; Abdul-kareem, S.; Khan, A.; Nawi, N. M.; Gital, A. Y. u.; Shuib, L.; Abubakar, A. I.; Rahman, M. Z.; Herawan, T., Global Warming: Predicting OPEC Carbon Dioxide Emissions from Petroleum Consumption Using Neural Network and Hybrid Cuckoo Search Algorithm. *PLoS ONE* **2015**, *10* (8), 1-21.
7. The largest producers of CO<sub>2</sub> emissions worldwide in 2015, based on their share of global CO<sub>2</sub> emissions. <https://www.statista.com/statistics/271748/the-largest-emitters-of-co2-in-the-world/> (accessed October,10,2016).
8. Fernández-Amador, O.; Francois, J. F.; Tomberger, P., Carbon dioxide emissions and international trade at the turn of the millennium. *Ecological Economics* **2016**, *125*, 14-26.

9. Jessop, P. G., Greenhouse Gas Carbon Dioxide Mitigation (Book Review). *Journal of the American Chemical Society* **2001**, *123* (29), 7197.
10. García, G.; Aparicio, S.; Ullah, R.; Atilhan, M., Deep Eutectic Solvents: Physicochemical Properties and Gas Separation Applications. *Energy & Fuels* **2015**, *29* (4), 2616-2644.
11. Bhogeswara, R. K.; Sexton, R. S.; Hignite, M., Predicting CO<sub>2</sub> Emissions: A Neural Network Approach. *Insights to a Changing World Journal* **2011**, (2), 58-88.
12. Pires, J. C. M.; Martins, F. G.; Alvim-Ferraz, M. C. M.; Simões, M., Recent developments on carbon capture and storage: An overview. *Chemical Engineering Research and Design* **2011**, *89* (9), 1446-1460.
13. Ali, E.; Hadj-Kali, M. K.; Mulyono, S.; Alnashef, I., Analysis of operating conditions for CO<sub>2</sub> capturing process using deep eutectic solvents. *International Journal of Greenhouse Gas Control* **2016**, *47*, 342-350.
14. Hanne, M. K.; Gary, T. R., Effects of the Temperature Bulge in CO<sub>2</sub> Absorption from Flue Gas by Aqueous Monoethanolamine. *Industrial & Engineering Chemistry Research* **2008**, *47* (3), 867-875.
15. Zhang, Y.; Ji, X.; Xie, Y.; Lu, X., Screening of conventional ionic liquids for carbon dioxide capture and separation. *Applied Energy* **2016**, *162*, 1160-1170.
16. Ullah, R.; Atilhan, M.; Anaya, B.; Khraisheh, M.; Garcia, G.; ElKhattat, A.; Tariq, M.; Aparicio, S., A detailed study of cholinium chloride and levulinic acid deep eutectic solvent system for CO<sub>2</sub> capture via experimental and molecular simulation approaches. *Physical Chemistry Chemical Physics* **2015**, *17* (32), 20941-20960.
17. Lee, S.-Y.; Park, S.-J., A review on solid adsorbents for carbon dioxide capture. *Journal of Industrial and Engineering Chemistry* **2015**, *23*, 1-11.

18. Kanniche, M.; Gros-Bonnivard, R.; Jaud, P.; Valle-Marcos, J.; Amann, J.-M.; Bouallou, C., Pre-combustion, post-combustion and oxy-combustion in thermal power plant for CO<sub>2</sub> capture. *Applied Thermal Engineering* **2010**, *30* (1), 53-62.
19. Sumida, K.; Rogow, D. L.; Mason, J. A.; McDonald, T. M.; Bloch, E. D.; Herm, Z. R.; Bae, T.-H.; Long, J. R., Carbon Dioxide Capture in Metal–Organic Frameworks. *Chemical Reviews* **2012**, *112* (2), 724-781.
20. MacDowell, N.; Florin, N.; Buchard, A.; Hallett, J.; Galindo, A.; Jackson, G.; Adjiman, C. S.; Williams, C. K.; Shah, N.; Fennell, P., An overview of CO<sub>2</sub> capture technologies. *Energy & Environmental Science* **2010**, *3* (11), 1645-1669.
21. Tan, Y.; Nookuea, W.; Li, H.; Thorin, E.; Yan, J., Property impacts on Carbon Capture and Storage (CCS) processes: A review. *Energy Conversion and Management* **2016**, *118*, 204-222.
22. Mondal, M. K.; Balsora, H. K.; Varshney, P., Progress and trends in CO<sub>2</sub> capture/separation technologies: A review. *Energy* **2012**, *46* (1), 431-441.
23. Meisen, A.; Shuai, X., Research and development issues in CO<sub>2</sub> capture. *Energy Conversion and Management* **1997**, *38*, Supplement, S37-S42.
24. Brunetti, A.; Scura, F.; Barbieri, G.; Drioli, E., Membrane technologies for CO<sub>2</sub> separation. *Journal of Membrane Science* **2010**, *359* (1–2), 115-125.
25. Wong, S. Module 2 CO<sub>2</sub> capture: Post combustion flue gas separation. <https://hub.globalccsinstitute.com/publications/building-capacity-co2-capture-and-storage-apec-region-training-manual-policy-makers-and-practitioners/module-2-co2-capture-post-combustion-flue-gas-separation> (accessed October .28.2016).
26. Olajire, A. A., CO<sub>2</sub> capture and separation technologies for end-of-pipe applications – A review. *Energy* **2010**, *35* (6), 2610-2628.

27. Kaithwas, A.; Prasad, M.; Kulshreshtha, A.; Verma, S., Industrial wastes derived solid adsorbents for CO<sub>2</sub> capture: A mini review. *Chemical Engineering Research & Design: Transactions of the Institution of Chemical Engineers Part A* **2012**, *90* (10), 1632-1641.
28. Samanta, A.; Zhao, A.; Shimizu, G. K. H.; Sarkar, P.; Gupta, R., Post-Combustion CO<sub>2</sub> Capture Using Solid Sorbents: A Review. *Industrial & Engineering Chemistry Research* **2012**, *51* (4), 1438-1463.
29. Siriwardane, R. V.; Shen, M.-S.; Fisher, E. P.; Poston, J. A. Adsorption of CO<sub>2</sub> on Molecular Sieves and Activated Carbon 2001, p. 279–284.
30. Clarke, D.; Heron, B.; Gabbutt, C.; Hepworth, J.; Partington, S.; Corns, S., Molecular structure of the activated carbon. <invention-title lang="EN" load-source="patent-office" mxw-id="PT58831295">INTENSE COLOURING PHOTOCHROMIC 2H-NAPHTHO[1, -. b. P. A. H. P. i. -t., Ed. Oct 1, 1998.
31. Davidson, R. M., 6 - Advanced adsorption processes and technology for carbon dioxide (CO<sub>2</sub>) capture in power plants A2 - Maroto-Valer, M. Mercedes. In *Developments and Innovation in Carbon Dioxide (CO<sub>2</sub>) Capture and Storage Technology*, Woodhead Publishing: 2010; Vol. 1, pp 183-202.
32. Siriwardane, R. V.; Shen, M.-S.; Fisher, E. P. Adsorption of CO<sub>2</sub>, N<sub>2</sub>, and O<sub>2</sub> on Natural Zeolites 2003, p. pp 571–576.
33. Siriwardane, R. V.; Shen, M.-S.; Fisher, E. P.; Losch, J., Adsorption of CO<sub>2</sub> on Zeolites at Moderate Temperatures. *Energy & Fuels* **2005**, *19* (3), 1153-1159.
34. Water Purification. <http://highschoolnanoscience.cnsi.ucla.edu/waterFilt>.

35. Millward, A. R.; Yaghi, O. M., Metal–Organic Frameworks with Exceptionally High Capacity for Storage of Carbon Dioxide at Room Temperature. *Journal of the American Chemical Society* **2005**, *127* (51), 17998-17999.
36. Yaghi, O. M.; O'Keeffe, M.; Ockwig, N. W.; Chae, H. K.; Eddaoudi, M.; Kim, J., Reticular synthesis and the design of new materials. *Nature* **2003**, *423* (6941), 705-714.
37. Styring, P., Chapter 2 - Carbon Dioxide Capture Agents and Processes. In *Carbon Dioxide Utilisation*, Armstrong, P. S. A. Q., Ed. Elsevier: Amsterdam, 2015; pp 19-32.
38. Hwang, G. S.; Stowe, H. M.; Paek, E.; Manogaran, D., Reaction mechanisms of aqueous monoethanolamine with carbon dioxide: a combined quantum chemical and molecular dynamics study. *Physical Chemistry Chemical Physics* **2015**, *17* (2), 831-839.
39. Ma'mun, S.; Svendsen, H. F.; Hoff, K. A.; Juliussen, O., Selection of new absorbents for carbon dioxide capture. *Energy Conversion and Management* **2007**, *48* (1), 251-258.
40. Bucklin, R. W., DGA - A WORKHORSE FOR GAS SWEETENING. *OIL GAS J* **1982**, *V* 80 (N 45), 204, 208-210.
41. Dixon, T.; Yamaji, K.; Dubois, L.; Thomas, D., GHGT-11 Proceedings of the 11th International Conference on Greenhouse Gas Control Technologies, 18-22 November 2012, Kyoto, Japan Postcombustion CO<sub>2</sub> Capture by Chemical Absorption: Screening of Aqueous Amine(s)-based solvents. *Energy Procedia* **2013**, *37*, 1648-1657.
42. Chowdhury, F. A.; Yamada, H.; Higashii, T.; Goto, K.; Onoda, M., CO<sub>2</sub> Capture by Tertiary Amine Absorbents: A Performance Comparison Study. *Industrial & Engineering Chemistry Research* **2013**, *52* (24), 8323-8331.



43. Hornbostel, M. D.; Bao, J.; Krishnan, G.; Nagar, A.; Jayaweera, I.; Kobayashi, T.; Sanjurjo, A.; Sweeney, J.; Carruthers, D.; Petruska, M. A.; Dubois, L., Characteristics of an advanced carbon sorbent for CO<sub>2</sub> capture. *Carbon* **2013**, *56*, 77-85.
44. Figueroa, J. D.; Fout, T.; Plasynski, S.; McIlvried, H.; Srivastava, R. D., Advances in CO<sub>2</sub> capture technology—The U.S. Department of Energy's Carbon Sequestration Program. *International Journal of Greenhouse Gas Control* **2008**, *2* (1), 9-20.
45. Dai, Y.; van Spronsen, J.; Witkamp, G.-J.; Verpoorte, R.; Choi, Y. H., Natural deep eutectic solvents as new potential media for green technology. *Analytica Chimica Acta* **2013**, *766*, 61-68.
46. Wasserscheid, P.; Welton, T., Ionic Liquids in Synthesis. **Die Deutsche Bibliothek** Die Deutsche Bibliothek: Germany, 2003.
47. Smith, E. L.; Abbott, A. P.; Ryder, K. S., Deep Eutectic Solvents (DESs) and Their Applications. *Chemical Reviews* **2014**, *114* (21), 11060-11082.
48. Supasitmongkol, S.; Styring, P., High CO<sub>2</sub> solubility in ionic liquids and a tetraalkylammonium-based poly(ionic liquid). *Energy & Environmental Science* **2010**, *3* (12), 1961-1972.
49. Aschenbrenner, O.; Supasitmongkol, S.; Taylor, M.; Styring, P., Measurement of vapour pressures of ionic liquids and other low vapour pressure solvents. *Green Chemistry* **2009**, *11* (8), 1217-1221.
50. Zhang, Q.; De Oliveira Vigier, K.; Royer, S.; Jerome, F., Deep eutectic solvents: syntheses, properties and applications. *Chemical Society Reviews* **2012**, *41* (21), 7108-7146.
51. El-Ela, A. Corrosion Behaviour of Carbon Steel in Absorption Based CO<sub>2</sub> Capture Plant, MSc Thesis, Qatar University, **2014**.

52. Krzemień, A.; Więckol-Ryk, A.; Smoliński, A.; Koterak, A.; Więclaw-Solny, L., Assessing the risk of corrosion in amine-based CO<sub>2</sub> capture process. *Journal of Loss Prevention in the Process Industries* **2016**, *43*, 189-197.
53. Kohl, A.; Nielsen, R., *Gas Purification*. Gulf publishing company: United States of America, 1997.
54. Ropital, F.; Chauvin, Y.; Jones, T., *Corrosion and degradation of metallic materials : understanding of the phenomena and applications in petroleum and process industries*. Paris : Editions Technip, 2010: 2010.
55. Veawab, A.; Tontiwachwuthikul, P.; Chakma, A., Corrosion Behavior of Carbon Steel in the CO<sub>2</sub> Absorption Process Using Aqueous Amine Solutions. *Industrial & Engineering Chemistry Research* **1999**, *38* (10), 3917-3924.
56. Kittel, J.; Idem, R.; Gelowitz, D.; Tontiwachwuthikul, P.; Parrain, G.; Bonneau, A., Corrosion in MEA units for CO<sub>2</sub> capture: Pilot plant studies. *Energy Procedia* **2009**, *1* (1), 791-797.
57. Gerus, B. R. D., Detection and Mitigation of Weight Loss Corrosion in Sour Gas Gathering Systems. SPE Symposium on Sour Gas and Crude, 11-12 November, Tyler, Texas, *Society of Petroleum Engineers* **1974**
58. Chiemela, A. N.; Robert, J. L., Electrochemistry in Deep Eutectic Solvents. *Journal of Physical Chemistry B* **2007**, *111* (46), 13271-13277.
59. Liu, L.; Kong, Y.; Xu, H.; Li, J. P.; Dong, J. X.; Lin, Z., Ionothermal synthesis of a three-dimensional zinc phosphate with DFT topology using unstable deep-eutectic solvent as template-delivery agent. *Microporous and Mesoporous Materials* **2008**, *115* (3), 624-628.

60. Shahbaz, K.; Mjalli, F. S.; Hashim, M. A.; AlNashef, I. M., Prediction of deep eutectic solvents densities at different temperatures. *Thermochimica Acta* **2011**, *515* (1–2), 67-72.
61. Shahbaz, K.; Mjalli, F. S.; Hashim, M. A.; AlNashef, I. M., Eutectic solvents for the removal of residual palm oil-based biodiesel catalyst. *Separation and Purification Technology* **2011**, *81* (2), 216-222.
62. Cojocar, P.; Magagnin, L.; Gomez, E.; Vallés, E., Using deep eutectic solvents to electrodeposit CoSm films and nanowires. *Materials Letters* **2011**, *65* (23–24), 3597-3600.
63. Jhong, H.-R.; Wong, D. S.-H.; Wan, C.-C.; Wang, Y.-Y.; Wei, T.-C., A novel deep eutectic solvent-based ionic liquid used as electrolyte for dye-sensitized solar cells. *Electrochemistry Communications* **2009**, *11* (1), 209-211.
64. Morrison, H. G.; Sun, C. C.; Neervannan, S., Characterization of thermal behavior of deep eutectic solvents and their potential as drug solubilization vehicles. *International Journal of Pharmaceutics* **2009**, *378* (1–2), 136-139.
65. Abbott, A. P.; Boothby, D.; Capper, G.; Davies, D. L.; Rasheed, R. K., Deep Eutectic Solvents Formed between Choline Chloride and Carboxylic Acids: Versatile Alternatives to Ionic Liquids. *Journal of the American Chemical Society* **2004**, *126* (29), 9142-9147.
66. Wen Cheng, S.; David Shan Hill, W.; Meng Hui, L., Effect of Water on Solubility of Carbon Dioxide in (Aminomethanamide + 2-Hydroxy-N,N,N-trimethylethanaminium Chloride). *Journal of Chemical & Engineering Data* **2009**, *54* (6), 1951-1955.
67. Abbott, A. P.; Capper, G.; Davies, D. L.; Munro, H. L.; Rasheed, R. K.; Tambyrajah, V., Preparation of novel, moisture-stable, Lewis-acidic ionic liquids containing quaternary ammonium salts with functional side chains. *Chemical Communications* **2001**, (19), 2010-2011.

68. Abbott, A. P.; Capper, G.; Davies, D. L.; Rasheed, R. K.; Tambyrajah, V., Novel solvent properties of choline chloride/urea mixtures. *Chemical Communications* **2003**, (1), 70-71.
69. Aronu, U. E.; Hessen, E. T.; Haug-Warberg, T.; Hoff, K. A.; Svendsen, H. F., Vapor–liquid equilibrium in amino acid salt system: Experiments and modeling. *Chemical Engineering Science* **2011**, *66* (10), 2191-2198.
70. Portugal, A. F.; Sousa, J. M.; Magalhães, F. D.; Mendes, A., Solubility of carbon dioxide in aqueous solutions of amino acid salts. *Chemical Engineering Science* **2009**, *64* (9), 1993-2002.
71. Wei, C.-C.; Puxty, G.; Feron, P., Amino acid salts for CO<sub>2</sub> capture at flue gas temperatures. *Chemical Engineering Science* **2014**, *107*, 218-226.
72. Shen, S.; Yang, Y.-n.; Wang, Y.; Ren, S.; Han, J.; Chen, A., CO<sub>2</sub> absorption into aqueous potassium salts of lysine and proline: Density, viscosity and solubility of CO<sub>2</sub>. *Fluid Phase Equilibria* **2015**, *399*, 40-49.
73. Liu, Y.-T.; Chen, Y.-A.; Xing, Y.-J., Synthesis and characterization of novel ternary deep eutectic solvents. *Chinese Chemical Letters* **2014**, *25* (1), 104-106.
74. Zhang, Y.; Ji, X.; Lu, X., Chapter 3 - Choline-Based Deep Eutectic Solvents for Mitigating Carbon Dioxide Emissions A2 - Shi, Fan. In *Novel Materials for Carbon Dioxide Mitigation Technology*, Morreale, B., Ed. Elsevier: Amsterdam, 2015; pp 87-116.
75. D'Agostino, C.; Harris, R. C.; Abbott, A. P.; Gladden, L. F.; Mantle, M. D., Molecular motion and ion diffusion in choline chloride based deep eutectic solvents studied by <sup>1</sup>H pulsed field gradient NMR spectroscopy. *Phys Chem Chem Phys* **2011**, *13* (48), 21383-91.
76. Mjalli, F. S.; Abdel Jabbar, N. M., Acoustic investigation of choline chloride based ionic liquids analogs. *Fluid Phase Equilibria* **2014**, *381*, 71-76.

77. Leron, R. B.; Li, M.-H., High-pressure density measurements for choline chloride: Urea deep eutectic solvent and its aqueous mixtures at  $T = (298.15 \text{ to } 323.15) \text{ K}$  and up to 50 MPa. *The Journal of Chemical Thermodynamics* **2012**, *54*, 293-301.
78. Abbott, A. P.; Ahmed, E. I.; Harris, R. C.; Ryder, K. S., Evaluating water miscible deep eutectic solvents (DESs) and ionic liquids as potential lubricants. *Green Chemistry* **2014**, *16* (9), 4156-4161.
79. Abbott, A. P.; Capper, G.; Gray, S., Design of improved deep eutectic solvents using hole theory. *Chemphyschem* **2006**, *7* (4), 803-6.
80. Yadav, A.; Pandey, S., Densities and Viscosities of (Choline Chloride + Urea) Deep Eutectic Solvent and Its Aqueous Mixtures in the Temperature Range 293.15 K to 363.15 K. *Journal of Chemical & Engineering Data* **2014**, *59* (7), 2221-2229.
81. Shahbaz, K.; Baroutian, S.; Mjalli, F. S.; Hashim, M. A.; AlNashef, I. M., Densities of ammonium and phosphonium based deep eutectic solvents: Prediction using artificial intelligence and group contribution techniques. *Thermochimica Acta* **2012**, *527*, 59-66.
82. Zhang, Q.; De Oliveira Vigier, K.; Royer, S. b.; Jérôme, F. o., Deep eutectic solvents: syntheses, properties and applications. *Chemical Society Reviews* **2012**, *41* (21), 7108-7146.
83. D'Agostino, C.; Harris, R. C.; Abbott, A. P.; Gladden, L. F.; Mantle, M. D., Molecular motion and ion diffusion in choline chloride based deep eutectic solvents studied by  $^1\text{H}$  pulsed field gradient NMR spectroscopy. *Physical Chemistry Chemical Physics* **2011**, *13* (48), 21383-21391.
84. Yadav, A.; Trivedi, S.; Rai, R.; Pandey, S., Densities and dynamic viscosities of (choline chloride + glycerol) deep eutectic solvent and its aqueous mixtures in the temperature range (283.15–363.15) K. *Fluid Phase Equilibria* **2014**, *367*, 135-142.

85. Florindo, C.; Oliveira, F. S.; Rebelo, L. P. N.; Fernandes, A. M.; Marrucho, I. M., Insights into the Synthesis and Properties of Deep Eutectic Solvents Based on Cholinium Chloride and Carboxylic Acids. *ACS Sustainable Chemistry & Engineering* **2014**, *2* (10), 2416-2425.
86. Guo, W.; Hou, Y.; Ren, S.; Tian, S.; Wu, W., Formation of Deep Eutectic Solvents by Phenols and Choline Chloride and Their Physical Properties. *Journal of Chemical & Engineering Data* **2013**, *58* (4), 866-872.
87. Hou, Y.; Gu, Y.; Zhang, S.; Yang, F.; Ding, H.; Shan, Y., Novel binary eutectic mixtures based on imidazole. *Journal of Molecular Liquids* **2008**, *143* (2-3), 154-159.
88. Andrew, P. A.; Robert, C. H.; Karl, S. R., Application of Hole Theory to Define Ionic Liquids by their Transport Properties†. *Journal of Physical Chemistry B* **2007**, *111* (18), 4910-4913.
89. Abbott, A. P.; Harris, R. C.; Ryder, K. S.; D'Agostino, C.; Gladden, L. F.; Mantle, M. D., Glycerol eutectics as sustainable solvent systems. *Green Chemistry* **2011**, *13* (1), 82-90.
90. Sedev, R., Surface tension, interfacial tension and contact angles of ionic liquids. *Current Opinion in Colloid & Interface Science* **2011**, *16* (4), 310-316.
91. Lv, Y.; Yu, X.; Tu, S.-T.; Yan, J.; Dahlquist, E., Wetting of polypropylene hollow fiber membrane contactors. *Journal of Membrane Science* **2010**, *362* (1-2), 444-452.
92. Blanco, D.; Viesca, J. L.; Mallada, M. T.; Ramajo, B.; González, R.; Battez, A. H., Wettability and corrosion of [NTf<sub>2</sub>] anion-based ionic liquids on steel and PVD (TiN, CrN, ZrN) coatings. *Surface and Coatings Technology* **2016**, *302*, 13-21.
93. Tang, H.; Zhang, Y.; Wang, F.; Zhang, H.; Guo, Y., Long-Term Stability of Polytetrafluoroethylene (PTFE) Hollow Fiber Membranes for CO<sub>2</sub> Capture. *Energy & Fuels* **2016**, *30* (1), 492-503.

94. Porcheron, F.; Drozd, S., Hollow fiber membrane contactor transient experiments for the characterization of gas/liquid thermodynamics and mass transfer properties. *Chemical Engineering Science* **2009**, *64* (2), 265-275.
95. Rafat, A.; Atilhan, M.; Kahraman, R., Corrosion Behavior of Carbon Steel in CO<sub>2</sub> Saturated Amine and Imidazolium-, Ammonium-, and Phosphonium-Based Ionic Liquid Solutions. *Industrial & Engineering Chemistry Research* **2016**, *55* (2), 446-454.
96. Gunasekaran, P.; Veawab, A.; Aroonwilas, A., Corrosivity of Single and Blended Amines in CO<sub>2</sub> Capture Process. *Energy Procedia* **2013**, *37*, 2094-2099.
97. Jeremy, D. Economic Evaluation of Leading Technology Options for Sequestration of Carbon Dioxide, MSc Thesis, Massachusetts Institute of Technology, 1976.
98. Aparicio, S.; Atilhan, M., Computational Study of Hexamethylguanidinium Lactate Ionic Liquid: A Candidate for Natural Gas Sweetening. *Energy & Fuels* **2010**, *24* (9), 4989-5001.
99. Bates, E. D.; Mayton, R. D.; Ntai, I.; Davis, J. H., Jr., CO<sub>2</sub> capture by a task-specific ionic liquid. *J Am Chem Soc* **2002**, *124* (6), 926-7.
100. Anthony, J. L.; Aki, S. N.; Maginn, E. J.; Brennecke, J. F., Feasibility of using ILs for carbon dioxide capture. *Int. J. Environ. Technol. Manage* **2004**.
101. Pennline, H. W.; Luebke, D. R.; Jones, K. L.; Myers, C. R.; Morsi, B. I.; Heintz, Y. J.; Ilconich, J. B., Progress in carbon dioxide capture and separation research for gasification-based power generation point sources. *Fuel Processing Technology* **2008**, *89* (9), 897-907.
102. Jason, E. B.; Trevor, K. C.; Christopher, J. G.; Dean, C.; Alexia, F.; Douglas, L. G.; Richard, D. N., Guide to CO<sub>2</sub> Separations in Imidazolium-Based Room-Temperature Ionic Liquids. *Industrial & Engineering Chemistry Research* **2009**, *48* (6), 2739-2751.

103. Cassity, C. G.; Mirjafari, A.; Mobarrez, N.; Strickland, K. J.; O'Brien, R. A.; Davis, J. H., Ionic liquids of superior thermal stability. *Chemical Communications* **2013**, *49* (69), 7590-7592.
104. Cadena, C.; Anthony, J. L.; Shah, J. K.; Morrow, T. I.; Brennecke, J. F.; Maginn, E. J., Why Is CO<sub>2</sub> So Soluble in Imidazolium-Based Ionic Liquids? *Journal of the American Chemical Society* **2004**, *126* (16), 5300-5308.
105. Jason, E. B.; Christopher, J. G.; Sonja, L.; Trevor, K. C.; Alexia, F.; Douglas, L. G.; Richard, D. N., Enhanced CO<sub>2</sub> Separation Selectivity in Oligo(ethylene glycol) Functionalized Room-Temperature Ionic Liquids. *Industrial & Engineering Chemistry Research* **2007**, *46* (16), 5380-5386.
106. Jessica, L. A.; JaNeille, K. D.; Joan, F. B., Solubility of CO<sub>2</sub>, CH<sub>4</sub>, C<sub>2</sub>H<sub>6</sub>, C<sub>2</sub>H<sub>4</sub>, O<sub>2</sub>, and N<sub>2</sub> in 1-Hexyl-3-methylpyridinium Bis(trifluoromethylsulfonyl)imide: Comparison to Other Ionic Liquids. *Accounts of Chemical Research* **2007**, *40* (11), 1208-1216.
107. Baltus; R, E.; Culbertson; B, H.; Dai; S; Luo; H; DePaoli; D, W., Low-Pressure Solubility of Carbon Dioxide in Room-Temperature Ionic Liquids Measured with a Quartz Crystal Microbalance. *Journal of Physical Chemistry B* **2004**, *108* (2), 721-727.
108. Jacquemin, J.; Husson, P.; Majer, V.; Gomes, M. F. C., Low-pressure solubilities and thermodynamics of solvation of eight gases in 1-butyl-3-methylimidazolium hexafluorophosphate. *Fluid Phase Equilibria* **2006**, *240* (1), 87-95.
109. Zhang, X.; Huo, F.; Liu, Z.; Wang, W.; Shi, W.; Maginn, E. J., Absorption of CO<sub>2</sub> in the Ionic Liquid 1-n-Hexyl-3-methylimidazolium Tris(pentafluoroethyl)trifluorophosphate ([hmim][FEP]): A Molecular View by Computer Simulations. *The Journal of Physical Chemistry B* **2009**, *113* (21), 7591-7598.



110. Aki; S. N. V, K.; Mellein; B, R.; Saurer; E, M.; Brennecke; J, F., High-Pressure Phase Behavior of Carbon Dioxide with Imidazolium-Based Ionic Liquids. *Journal of Physical Chemistry B* **2004**, *108* (52), 20355-20365.
111. Mark, J. M.; Sudhir, N. V. K. A.; Jessica, L. A.; JaNeille, K. D.; Joan, F. B., Improving Carbon Dioxide Solubility in Ionic Liquids. *Journal of Physical Chemistry B* **2007**, *111* (30), 9001-9009.
112. Carvalho, P. J.; Coutinho, J. A. P., On the Nonideality of CO<sub>2</sub> Solutions in Ionic Liquids and Other Low Volatile Solvents. *The Journal of Physical Chemistry Letters* **2010**, *1* (4), 774-780.
113. Ramdin, M.; Amplianitis, A.; Bazhenov, S. V., A.Volkov, V; Vlught, T. d. L., T. W, Solubility of CO<sub>2</sub> and CH<sub>4</sub> in ionic liquids: ideal CO<sub>2</sub>/CH<sub>4</sub> selectivity. *Ind. Eng. Chem. Res* **2014**.
114. Francisco, M.; van den Bruinhorst, A.; Kroon, M. C., New natural and renewable low transition temperature mixtures (LTTMs): screening as solvents for lignocellulosic biomass processing. *Green Chemistry* **2012**, *14* (8), 2153-2157.
115. Ramdin, M.; de Loos, T. W.; Vlught, T. J. H., State-of-the-Art of CO<sub>2</sub>Capture with IonicLiquids. *Industrial & Engineering Chemistry Research* **2012**, *51* (24), 8149-8177.
116. Besnard, M.; Cabaco, M. I.; Chavez, F. V.; Pinaud, N.; Sebastiao, P. J.; Coutinho, J. A. P.; Danten, Y., On the spontaneous carboxylation of 1-butyl-3-methylimidazolium acetate by carbon dioxide. *Chemical Communications* **2012**, *48* (9), 1245-1247.
117. Gurau, G.; Rodriguez, H.; Kelley, S.; Janiczek, P., Demonstration of Chemisorption of Carbon Dioxide in 1,3-Dialkylimidazolium Acetate Ionic Liquids. *Angew.Chem.Int.Ed* **13 October 2011**, *50* (50), 12024–12026.

118. Gurau, G.; Rodríguez, H.; Kelley, S.; Janiczek, P.; Roland, K.; Rogers, R., Demonstration of Chemisorption of Carbon Dioxide in 1,3-Dialkylimidazolium Acetate Ionic Liquids. *Angewandte Chemie* **13 OCT 2011**, *50* (50), 12024-12026.
119. Kazarian, S. G.; Briscoe, B. J.; Welton, T., Combining ionic liquids and supercritical fluids: ATR-IR study of CO dissolved in two ionic liquids at high pressures. *Chemical Communications* **2000**, (20), 2047-2048.
120. Seo, S.; DeSilva, M. A.; Brennecke, J. F., Physical Properties and CO<sub>2</sub> Reaction Pathway of 1-Ethyl-3-Methylimidazolium Ionic Liquids with Aprotic Heterocyclic Anions. *The Journal of Physical Chemistry B* **2014**, *118* (51), 14870-14879.
121. Holloczki, O.; Gerhard, D.; Massone, K.; Szarvas, L.; Nemeth, B.; Veszpremi, T.; Nyulaszi, L., Carbenes in ionic liquids. *New Journal of Chemistry* **2010**, *34* (12), 3004-3009.
122. Cabaço, M. I.; Besnard, M.; Danten, Y.; Coutinho, J. A. P., Solubility of CO<sub>2</sub> in 1-Butyl-3-methyl-imidazolium-trifluoro Acetate Ionic Liquid Studied by Raman Spectroscopy and DFT Investigations. *The Journal of Physical Chemistry B* **2011**, *115* (13), 3538-3550.
123. Zhang, J.; Zhang, S.; Dong, K.; Zhang, Y.; Shen, Y.; Lv, X., Supported absorption of CO<sub>2</sub> by tetrabutylphosphonium amino acid ionic liquids. *Chemistry* **2006**, *12* (15), 4021-6.
124. Zhang, Y.; Zhang, S.; Lu, X.; Zhou, Q.; Fan, W.; Zhang, X., Dual Amino-Functionalised Phosphonium Ionic Liquids for CO<sub>2</sub> Capture. *Chemistry – A European Journal* **2009**, *15* (12), 3003–3011.
125. Gurkan, B. E.; de la Fuente, J. C.; Mindrup, E. M.; Ficke, L. E.; Goodrich, B. F.; Price, E. A.; Schneider, W. F.; Brennecke, J. F., Equimolar CO<sub>2</sub> Absorption by Anion-Functionalized Ionic Liquids. *Journal of the American Chemical Society* **2010**, *132* (7), 2116-2117.

126. Gurkan, B.; Goodrich, B. F.; Mindrup, E. M.; Ficke, L. E.; Massel, M.; Seo, S.; Senftle, T. P.; Wu, H.; Glaser, M. F.; Shah, J. K.; Maginn, E. J.; Brennecke, J. F.; Schneider, W. F., Molecular Design of High Capacity, Low Viscosity, Chemically Tunable Ionic Liquids for CO<sub>2</sub> Capture. *The Journal of Physical Chemistry Letters* **2010**, *1* (24), 3494-3499.
127. Francisco, M.; van den Bruinhorst, A.; Zubeir, L. F.; Peters, C. J.; Kroon, M. C., A new low transition temperature mixture (LTTM) formed by choline chloride + lactic acid: Characterization as solvent for CO<sub>2</sub> capture. *Fluid Phase Equilibria* **2013**, *340*, 77-84.
128. Shah, D.; Mjalli, F. S., Effect of water on the thermo-physical properties of Reline: An experimental and molecular simulation based approach. *Physical Chemistry Chemical Physics* **2014**, *16* (43), 23900-23907.
129. Leron, R. B.; Li, M.-H., High-pressure volumetric properties of choline chloride–ethylene glycol based deep eutectic solvent and its mixtures with water. *Thermochimica Acta* **2012**, *546*, 54-60.
130. Xiaoyong, L.; Minqiang, H.; Xiaoling, W.; Buxing, H.; Lizhuang, Z., Solubility of CO<sub>2</sub> in a Choline Chloride + Urea Eutectic Mixture. *Journal of Chemical & Engineering Data* **2008**, *53* (2), 548-550.
131. Atilhan, M.; Anaya, B.; Ullah, R.; Majeda, K.; Garcia, G.; Elkattat, M.; Tariq, M.; Aparicio, S. A detailed study of cholinium chloride and levulinic acid deep eutectic solvent system for CO<sub>2</sub> capture via experimental and molecular simulation approaches 2015.
132. Sze, L. L.; Pandey, S.; Ravula, S.; Pandey, S.; Zhao, H.; Baker, G. A.; Baker, S. N., Ternary deep eutectic solvents tasked for carbon dioxide capture. *ACS Sustainable Chem. Eng* **2014**.

133. Leron, R. B.; Caparanga, A.; Li, M.-H., Carbon dioxide solubility in a deep eutectic solvent based on choline chloride and urea at  $T = 303.15\text{--}343.15$  K and moderate pressures. *Journal of the Taiwan Institute of Chemical Engineers* **2013**, *44* (6), 879-885.
134. Chen, Y.; Ai, N.; Li, G.; Shan, H.; Cui, Y.; Deng, D., Solubilities of Carbon Dioxide in Eutectic Mixtures of Choline Chloride and Dihydric Alcohols. *Journal of Chemical & Engineering Data* **2014**, *59* (4), 1247-1253.
135. Leron, R. B.; Li, M.-H., Solubility of carbon dioxide in a choline chloride–ethylene glycol based deep eutectic solvent. *Thermochimica Acta* **2013**, *551*, 14-19.
136. KRÜSS drop analysis system. <https://www.kruss.de/products/contact-angle/dsa25/drop-shape-analyzer-dsa25/>.
137. Karadas, F.; Yavuz, C. T.; Zulfiqar, S.; Aparicio, S.; Stucky, G. D.; Atilhan, M., CO<sub>2</sub> adsorption studies on hydroxy metal carbonates  $M(\text{CO}_3)_x(\text{OH})_y$  ( $M = \text{Zn}, \text{Zn-Mg}, \text{Mg}, \text{Mg-Cu}, \text{Cu}, \text{Ni}, \text{and Pb}$ ) at high pressures up to 175 bar. *Langmuir* **2011**, *27* (17), 10642-7.
138. Badawi, H. M.; Förner, W., Analysis of the infrared and Raman spectra of phenylacetic acid and mandelic (2-hydroxy-2-phenylacetic) acid. *Spectrochimica Acta Part A: Molecular and Biomolecular Spectroscopy* **2011**, *78* (3), 1162-1167.
139. Perkins, S. L.; Painter, P.; Colina, C. M., Experimental and Computational Studies of Choline Chloride-Based Deep Eutectic Solvents. *Journal of Chemical & Engineering Data* **2014**, *59* (11), 3652-3662.
140. Tao, D.-J.; Cheng, Z.; Chen, F.-F.; Li, Z.-M.; Hu, N.; Chen, X.-S., Synthesis and Thermophysical Properties of Biocompatible Cholinium-Based Amino Acid Ionic Liquids. *Journal of Chemical & Engineering Data* **2013**, *58* (6), 1542-1548.

141. Cardellini, F.; Tiecco, M.; Germani, R.; Cardinali, G.; Corte, L.; Roscini, L.; Spreti, N., Novel zwitterionic deep eutectic solvents from trimethylglycine and carboxylic acids: characterization of their properties and their toxicity. *RSC Advances* **2014**, *4* (99), 55990-56002.
142. Zhigang, L.; Chengna, D.; Biaohua, C., Gas Solubility in Ionic Liquids. *Chemical Reviews* **2014**, *114* (2), 1289-1326.
143. *Ali*, E.; *Hadj-Kali*, M.; *Mulyono*, S.; *Alnashef*, I.; *Fakeeha*, A.; *Mjalli*, F.; *Hayyan*, A., Solubility of CO<sub>2</sub> in deep eutectic solvents: Experiments and modelling using the Peng–Robinson equation of state. *Elsevier* **2014**, *9*.
144. Zhou, L.; Shang, X.; Fan, J.; Wang, J., Solubility and selectivity of CO<sub>2</sub> in ether-functionalized imidazolium ionic liquids. *The Journal of Chemical Thermodynamics* **2016**, *103*, 292-298.
145. Deng, D.; Chen, Y.; Cui, Y.; Li, G.; Ai, N., Low pressure solubilities of CO<sub>2</sub> in five fatty amine polyoxyethylene ethers. *The Journal of Chemical Thermodynamics* **2014**, *72*, 89-93.
146. Ebner, A. D.; Gray, M. L.; Chisholm, N. G.; Black, Q. T.; Mumford, D. D.; Nicholson, M. A.; Ritter, J. A., Suitability of a Solid Amine Sorbent for CO<sub>2</sub> Capture by Pressure Swing Adsorption. *Industrial & Engineering Chemistry Research* **2011**, *50* (9), 5634-5641.
147. Cao, L. D.; Dong, H. F.; Zhang, X. P.; Zhang, S. J.; Zhao, Z. J.; Zeng, S. J.; Gao, J. B., Highly efficient carbon dioxide capture by a novel amine solvent containing multiple amino groups. *Journal of Chemical Technology and Biotechnology* **2015**, *90* (10), 1918-1926.
148. Lichao, G.; McCarthy, T. J., Ionic Liquids Are Useful Contact Angle Probe Fluids. *Journal of the American Chemical Society* **2007**, *129* (13), 3804-3805.

149. Restolho, J.; Mata, J. L.; Shimizu, K.; Canongia Lopes, J. N.; Saramago, B., Wetting Films of Two Ionic Liquids: [C8mim][BF<sub>4</sub>] and [C2OHmim][BF<sub>4</sub>]. *The Journal of Physical Chemistry C* **2011**, *115* (32), 16116-16123.
150. Restolho, J.; Mata, J. L.; Saramago, B., Choline based ionic liquids: Interfacial properties of RTILs with strong hydrogen bonding. *Fluid Phase Equilibria* **2012**, *322–323*, 142-147.
151. Abbott, A. P.; Boothby, D.; Capper, G.; Davies, D. L.; Rasheed, R. K., Deep Eutectic Solvents Formed between Choline Chloride and Carboxylic Acids: Versatile Alternatives to Ionic Liquids. *Journal of the American Chemical Society* **2004**, *126* (29), 9142-9147.
152. Fukumoto, K.; Yoshizawa, M.; Ohno, H., Room Temperature Ionic Liquids from 20 Natural Amino Acids. *Journal of the American Chemical Society* **2005**, *127* (8), 2398-2399.
153. Gore, S.; Baskaran, S.; Koenig, B., Efficient synthesis of 3,4-dihydropyrimidin-2-ones in low melting tartaric acid-urea mixtures. *Green Chemistry* **2011**, *13* (4), 1009-1013.
154. Radošević, K.; Ćurko, N.; Gaurina Srček, V.; Cvjetko Bubalo, M.; Tomašević, M.; Kovačević Ganić, K.; Radojčić Redovniković, I., Natural deep eutectic solvents as beneficial extractants for enhancement of plant extracts bioactivity. *LWT - Food Science and Technology* **2016**, *73*, 45-51.
155. Lösch, H. W., *Development and Design of New Magnetic Suspension Balances for Non-Contact Measurements of Vertical Forces*. VDI Verlag: Düsseldorf, 1987.
156. Patel, H. A.; Karadas, F.; Canlier, A.; Park, J.; Deniz, E.; Jung, Y.; Atilhan, M.; Yavuz, C. T., High capacity carbon dioxide adsorption by inexpensive covalent organic polymers. *Journal of Materials Chemistry* **2012**, *22* (17), 8431-8437.

## 7 . APPENDIX

### **Rubotherm® magnetic suspension**

For high pressure (up to 200 bar) CO<sub>2</sub>/N<sub>2</sub> sorption measurements, a Rubotherm® magnetic suspension sorption apparatus (figure 7.1 and 7.2) based on magnetic levitation was employed. The magnetic suspension balances make it possible to weigh the samples of interest in almost all environments including compressed gas at high pressures and high temperatures with a balance located at ambient conditions. The sample is located in the measuring cell and can be coupled specifically to the balance without a physical link. An electromagnet, which is attached to the bottom of the balance, lifts a so-called suspension permanent magnet assembly (PMA) that consists of a permanent magnet, sensor core and a measuring load basket (or cage). The electromagnet assembly (EMA), which is attached to the bottom of the weighing balance via hook connections, maintains a free suspension state of the PMA via an electronic control unit. This arrangement allows different vertical positions for the PMA based on the control action commands to the EMA. The first position is called the zero point (ZP) in which the suspension part suspends alone contactless and thus represents the unburdened balance. The second EMA point is called the measuring point (MP) in which the suspension part reaches to a higher vertical position and couples the sample to the balance and transmits the weight of the sample to the balance. This principle is illustrated in the figure 7.3.

For buoyancy calculations used in sorption measurements, in-situ density of the pressurized gas in the high-pressure cell is measured. Archimedes' principle is used for density measurements by utilizing a calibrated silicon sinker placed just above the sample basket in the pressure cell. The silicon sinker used in this apparatus had a volume of 4.4474 cm<sup>3</sup> measured at 20 °C with a 0.0015 cm<sup>3</sup> uncertainty and a density of 4508 kg/m<sup>3</sup> measured at 20 °C with a 4 kg/m<sup>3</sup> uncertainty.

Buoyancy force on a submerged object is famously explained by Archimedes' principle: "when a solid body (sinker) is immersed in a fluid, it displaces a volume of fluid the weight of which is equal to the buoyancy force exerted by the fluid on the sinker." Magnetic sorption apparatus is equipped with a sinker body, which enables the in-situ density measurements of the adsorbate gas based on Archimedes' hydrostatic buoyancy method via contactless magnetic levitation principles. In classical buoyancy based densimeters, a sphere or cylinder shaped sinker hangs from a commercial digital balance by a thin wire. The pressure and temperature of the fluid remains constant in the pressure cell using a temperature control mechanism. The sinker is submerged in the fluid, and the weight of the sinker is measured. According to the same Archimedes' principle, the density of the fluid can be calculated using equation 7.1:

$$\rho = \frac{m_v - m_a}{V_s(T, P)} \quad (7.1)$$



In Equation 7.1,  $m_v$  is the ‘true’ mass of the sinker measured in vacuum,  $m_a$  is the apparent mass of the sinker in the fluid that is charged in the pressure cell and  $V_s$  is the calibrated volume of the sinker, which is a function of temperature and pressure. When compared with the classical buoyancy densimeters, the novelty of the magnetic suspension coupling is that it uses non-physical-contact force transmission between the sinker in the pressurized cell and the weighing balance at atmospheric pressure, thus allowing a cell design that covers wide temperature and pressure ranges<sup>155</sup>.

In a typical sorption measurement, the weight of the adsorbent is measured initially under vacuum and that is followed by weight measurements of the adsorbent at each pressurized adsorbate gas condition. Meanwhile a titanium sinker with a calibrated volume is weighed continuously in a sequential order with the sorption measurements in order to obtain the density of the measuring fluid surrounding the sample as it is required for the buoyancy correction of the measured sorption values. The simultaneous measurement of sorption and density is especially needed if the buoyancy effects caused by the density of the adsorbate gas are large, i.e., high pressure or low temperature conditions. From thermodynamics point of view, density measurement in a binary gas mixture also offers the possibility of determining the concentration for the gas mixture without further analysis since the density is a function of the mixture composition.

Typical measurements start with placing an approximately 0.25 g of a sorbent sample within the sample holder after activating by degassing at 150 °C. Once the sample is in place, the system is taken under vacuum for 24 h at 65 °C. Carbon dioxide is then pressurized via a Teldyne Isco 260D fully automated gas booster and charged into the high-pressure cell. For each pressure point it takes about 45 minutes to reach equilibrium and once temperature and pressure equilibrium is reached, four different sets of measurements are taken for a period of 10 min each. During the 10 min measurement period pressure, temperature and weighing measurements are collected at every 30 sec along with the sinker weight measurements for in-situ density values of the absorbate gas. Some pressure points might require repetition, depending on the experimental stability. Consequently, the total duration of each experimental sorption measurement takes about 40 to 60 min. At the end of each pressure point, the system goes to the next automatically.

In this work, pressures up to 30 bar are used for maximum pressure and at the end of each isotherm, a hysteresis check is conducted by collecting desorption data as the system is depressurized. The temperature of the high-pressure cell is controlled by an automated external constant temperature circulator (Polyscience model 9512) via a platinum resistance thermometer (Jumo DMM 5017 Pt100) attached to the high-pressure cell body. The cell temperature is maintained within  $\pm 0.6$  °C accuracy. The automatic gas dosing system is used for controlling the pressure inside the high-pressure cell. The pressure control unit is a combination of shut valves, a special PID control instrument and precise pressure transducer, Paroscientific® Digiquartz 745-3

K with an accuracy of with an accuracy of 0.01 %. The schematic of the automatic gas dosing system is given in figure 7.4.

Adsorption data is analyzed and the amount of adsorbed gas on the sample is calculated by using equation 7.2:

$$W + W_{buoy,sample} + W_{buoy,sink} = m_{ads} + m_{sample} + m_{sink} \quad (7.2)$$

Where;

$W$  = Signal read by the instrument

$W_{buoy,sample} = V_{sample} * d_{gas}$  = Buoyancy correction due to the sample

$V_{sample}$  = Volume of the sample

$$V_{sample} = V_{total} - V_{pore}$$

$d_{gas}$  = Density of the gas

$W_{buoy,sink} = V_{sinker} * d_{gas}$  = Buoyancy correction due to the sinker

$V_{sinker}$  = Volume of the sinker

$m_{ads}$  = Surface excess mass of the CO<sub>2</sub>

$m_{sample}$  = Mass of the sample

$m_{sink}$  = Mass of the sinker

$d_{gas}$  is measured *in situ* and the mass of empty sinker is measured at several pressures of helium to determine the buoyancy caused by the sinker ( $W_{buoy,sinker}$ ). Volume of the sinker ( $V_{sinker}$ ) is calculated from the slope of weight vs. density plot obtained from this measurement. A blank measurement at vacuum is performed to determine the mass of the sinker ( $m_{sink}$ ). The buoyancy correction caused by the sample ( $W_{buoy,sample}$ ) is performed by calculating the volume of the sample ( $V_{sample}$ ), which is obtained by subtracting the pore volume of the sample measured by BET analysis ( $V_{pore}$ ) from the total volume of the sample ( $V_{total}$ ) calculated from the density of the material determined by tapping method. A typical screenshot from the sorption apparatus for vacuum measurement and adsorption test under pressure measurement is given in figure 7.5.

The single-sinker densitometer also operates based upon Archimedes' principle for the buoyancy force acting on a cylindrical sinker in the presence of a fluid. The density is calculated by measuring  $m_v$ , the 'true mass' of the sinker in vacuum,  $m_a$ , the 'apparent mass' of the sinker in the presence of fluid and  $v_s$ , the volume of the sinker calculated using equation 7.3:

$$\rho = \frac{m_v - m_a}{v_s} \quad (7.3)$$

The sinker volume appearing in above equation undergoes a change because of distortion of the sinker material at a temperature and pressure (T, P) other than the reference temperature and pressure ( $T_0, P_0$ ) at which the reference sinker volume,  $v_{s0}$ , is measured (equation 7.4).

$$v_s(T, P) = v_{s_0}(T_0, P_0) + v_{s_0}(T_0, P_0) \left[ 3 \frac{\Delta L}{L_0}(T) - 3 \frac{(P - P_0)}{E(T)} \{1 - 2\nu(T)\} \right] \quad (7.4)$$

where,  $\Delta L/L_0$  is the thermal expansion,  $E$  is the Young's modulus and  $\nu$  is the Poisson's ratio of the sinker material at a temperature,  $T$ . The thermal expansion was calculated using equation 7.5:

$$\frac{\Delta L}{L_0}(T) = \alpha(T - T_0) \quad (7.5)$$

where,  $\alpha$  is the thermal coefficient of expansion of the sinker material. For titanium,  $\alpha$  is calculated to be  $8.8 \times 10^{-6} \text{ K}^{-1}$  in the range (-80 to 260) °C. The reference sinker volume calibration, Rubotherm made the measurements at 20 °C and 990.4 mbar as  $4.4474 \text{ cm}^3$  with the uncertainty of  $0.0015 \text{ cm}^3$  in sinker volume <sup>156</sup>.

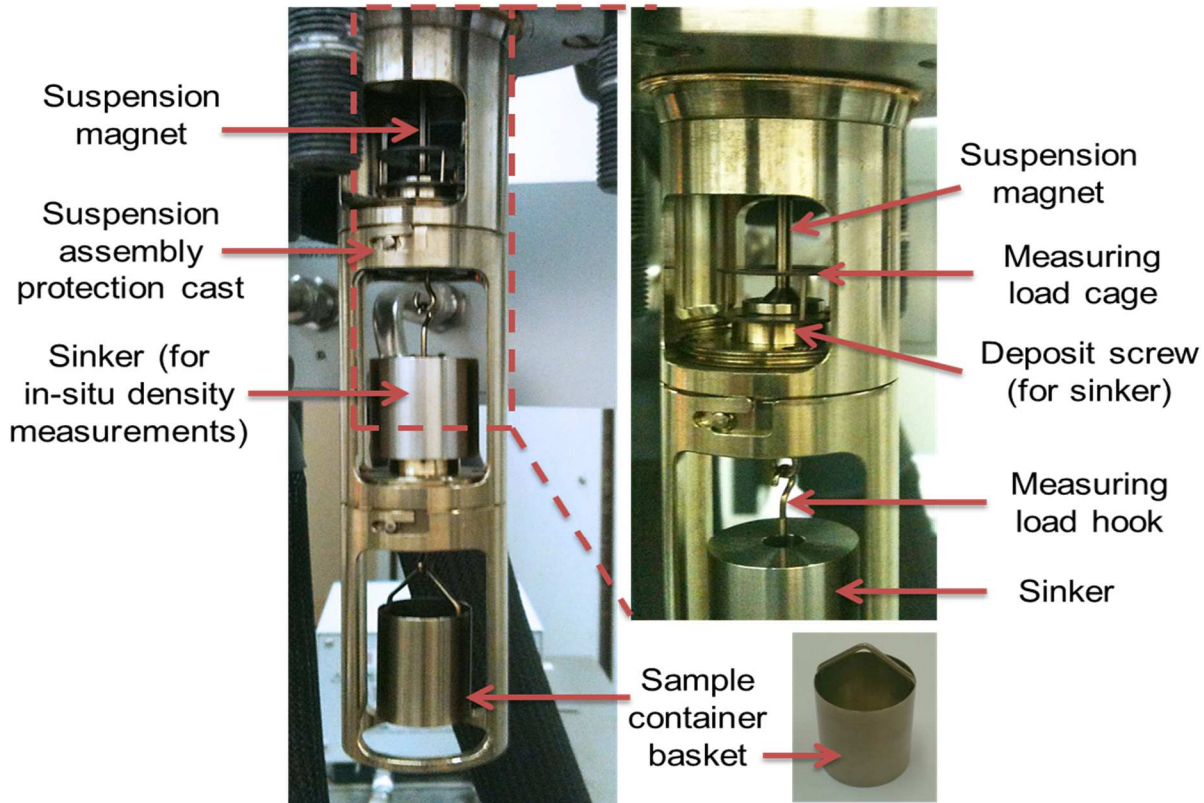


Figure 7.1. Rubotherm® Magnetic Suspension Balance (MSB). Photos of the magnetic suspension assembly and the sample container basket<sup>156</sup>.

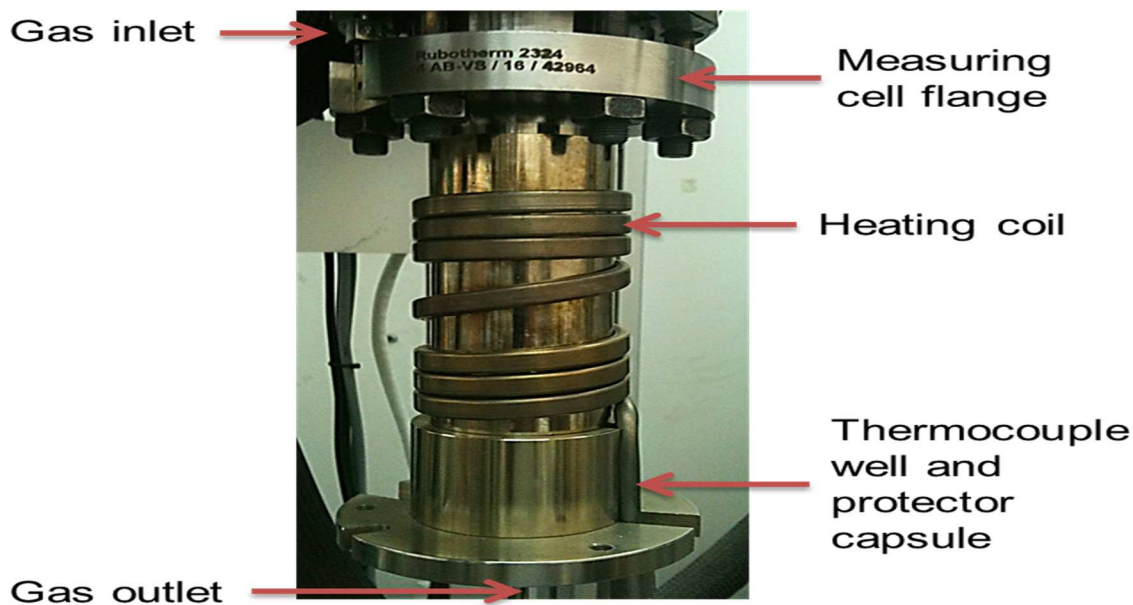


Figure 7.2. MSB overview. Photo of the measuring cell and the magnetic coupling housing<sup>156</sup>

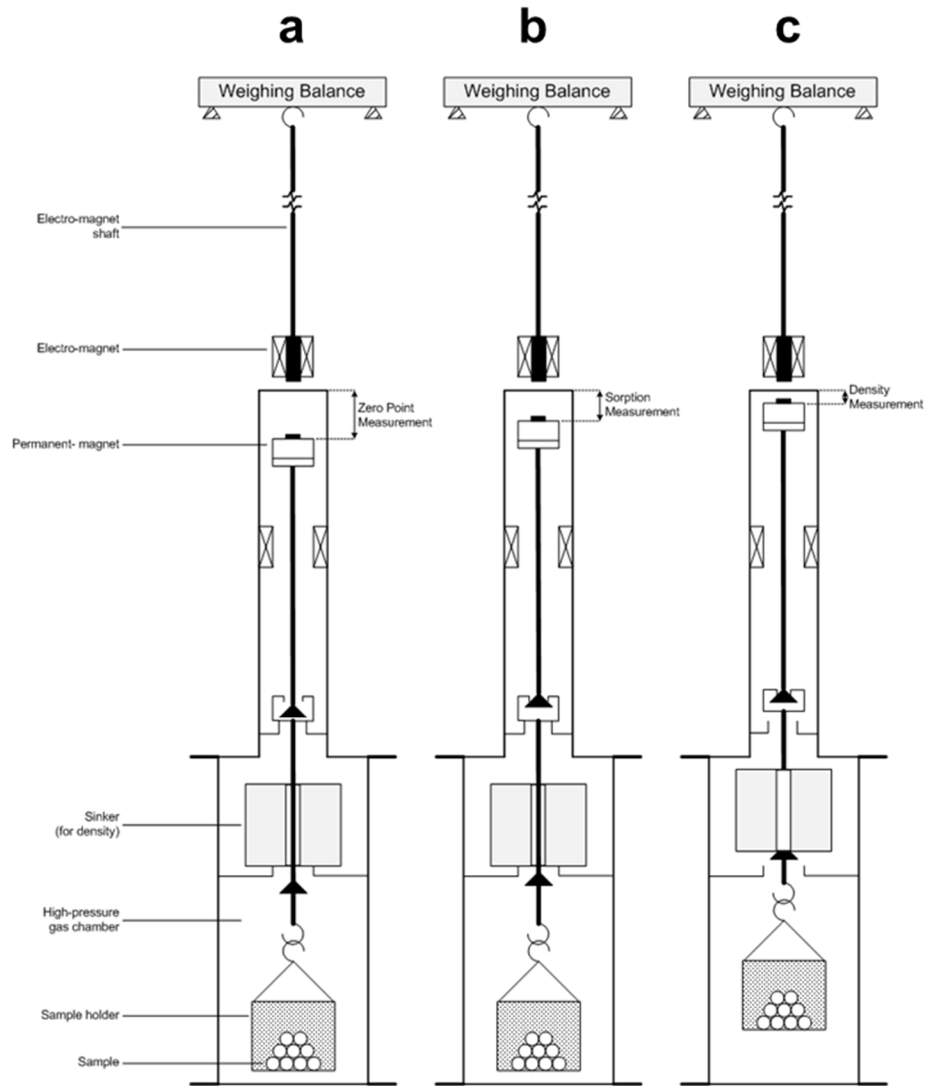


Figure 7.3. Schematics of magnetic suspension sorption apparatus operating principle. (a) sample loaded to measuring basket in high pressure cell; (b) Measurement point 1 (MP1) - magnetic coupling is on and mass of the sample is measured; (c) Measurement point 2 (MP2) – in-situ density of the adsorbed gas is measured<sup>156</sup>.

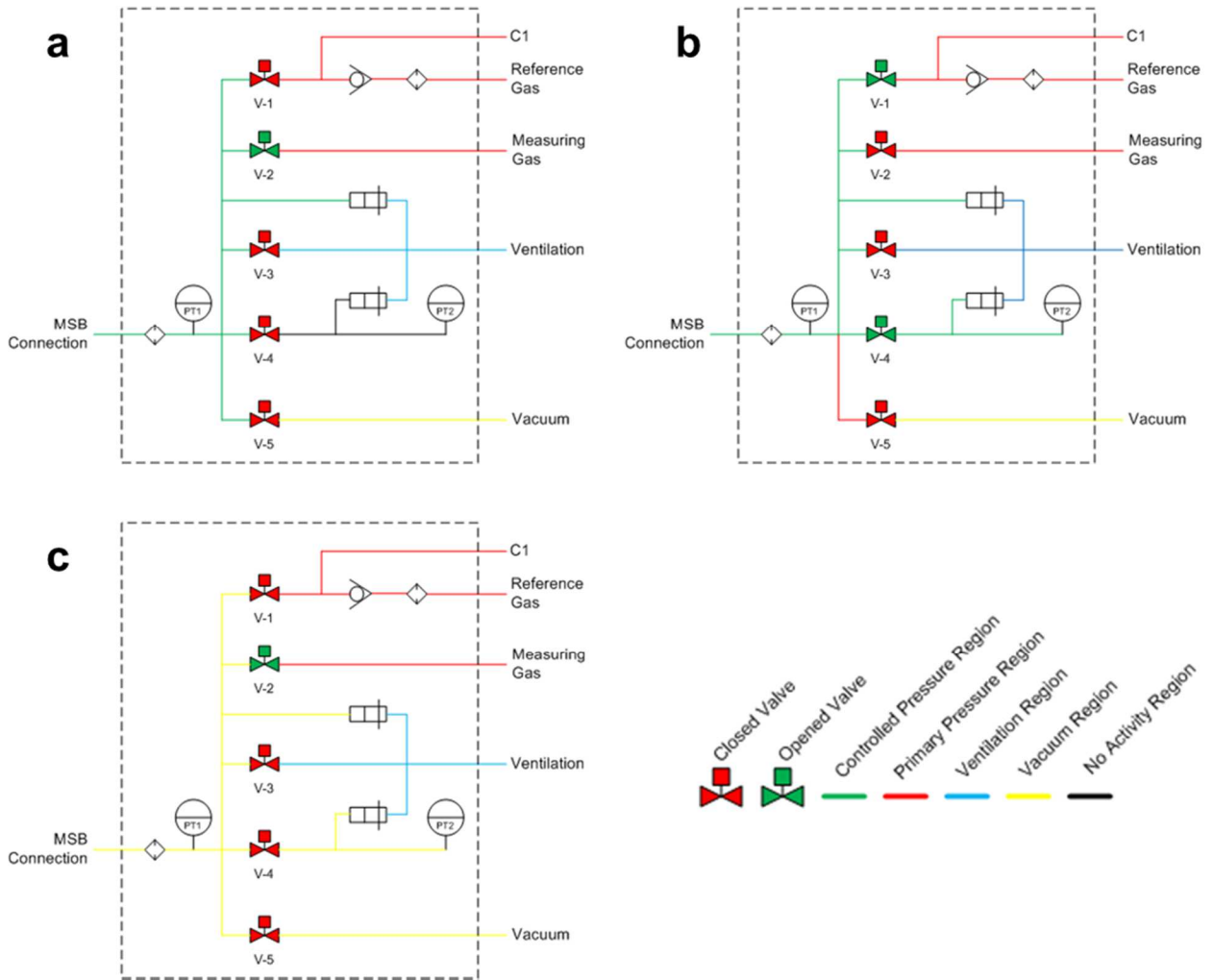


Figure 7.4. Schematics of the gas dosing manifold system under (a) CO<sub>2</sub> measurement; (b) reference gas (He) measurement; (c) vacuum measurement<sup>156</sup>.



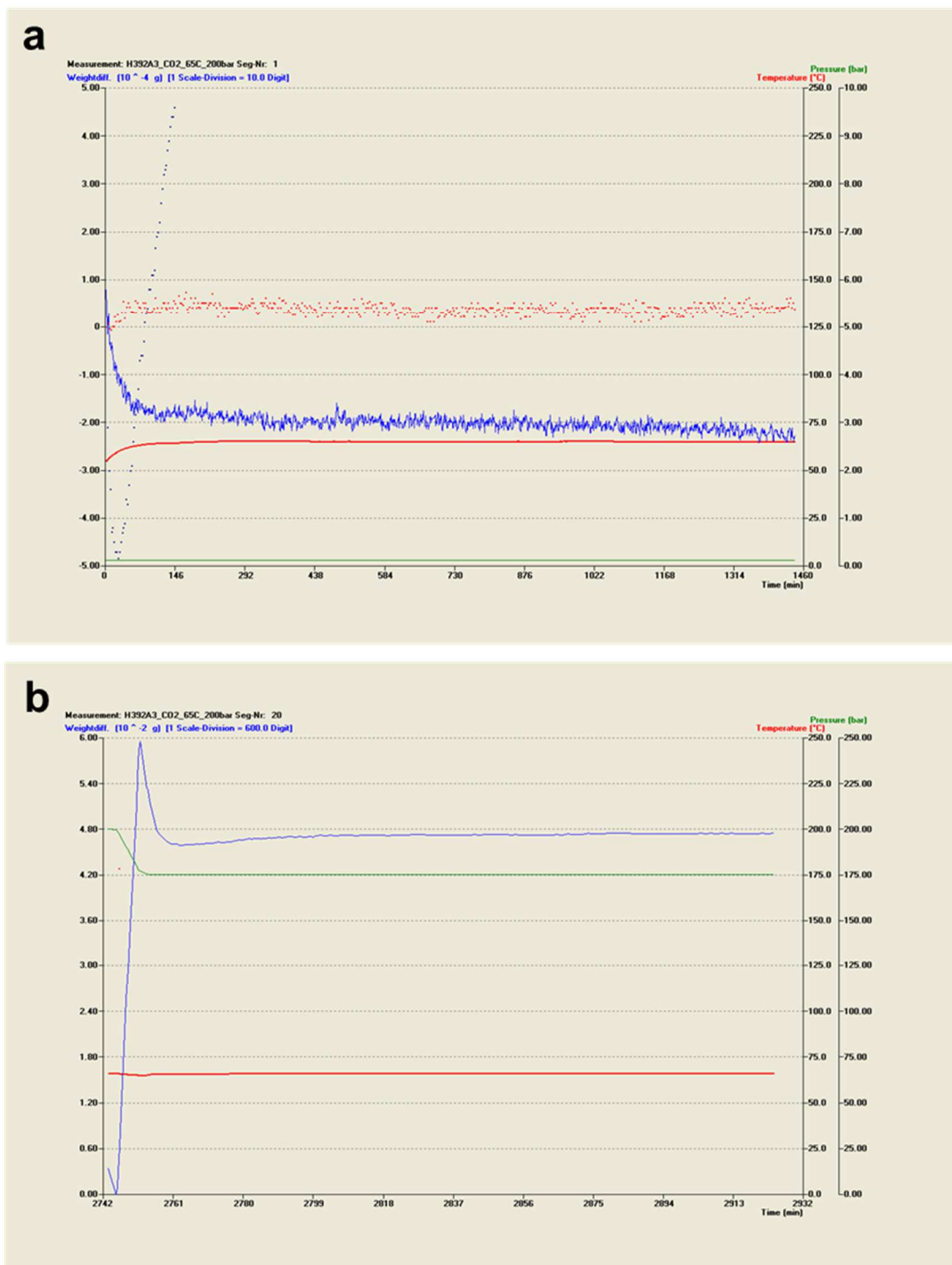


Figure 7.5 .Magnetic suspension sorption apparatus screenshots at, (a) vacuum and, (b) under pressure measurement <sup>156</sup>.